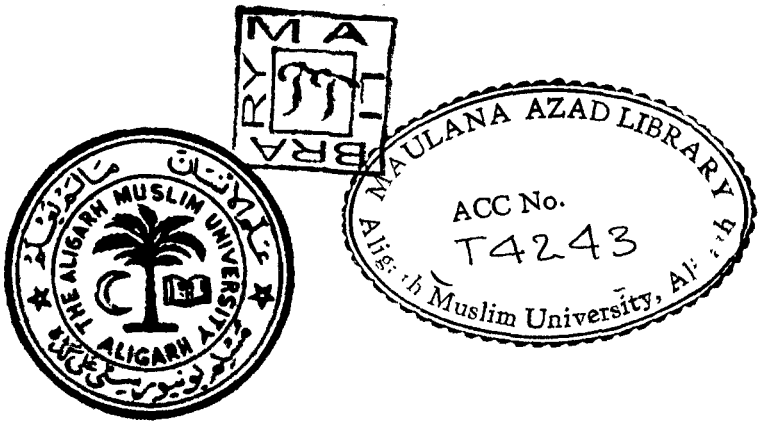

INSTANT - CONTROLLED SWITCHING AND APPLICATIONS

RESUME

OF THE THESIS SUBMITTED FOR THE DEGREE OF

Doctor of Philosophy

IN

ELECTRICAL ENGINEERING

BY

M. SYED JAMIL ASGHAR

DEPARTMENT OF ELECTRICAL ENGINEERING
ALIGARH MUSLIM UNIVERSITY
ALIGARH (INDIA)
1993

ABSTRACT

The switching transient in an AC circuit mainly depends upon the initial condition and the switching instant or the point on the voltage wave. In the work presented here, the equations of the current response with any initial condition is derived in the normalized form to obtain universal curves for peak transient current against switching instant for all types of AC circuits. For the first time, it is theoretically analyzed and experimentally verified that the switching current (peak) in any linear circuit can be pushed to its maximum level or constrained to its minimum level (equal to or close to steady-state value) simply by controlling the switching instant of the circuit. General equations and universal curves are also given to determine the extremum for all circuits. The maximum value of the switching current gives the correct value of the maximum possible switching transient current that may flow into the circuit.

Different types of instant-controlled switching circuits have been designed. Besides other applications, for the first time, they are used successfully to eliminate the switching inrush current in 1-phase as well as 3-phase transformers and reduce them considerably in induction motors.

Moreover these circuits are used in integral-cycle power control mode for resistive and inductive loads as well as in speed control applications of induction motors (1-phase as well

as 3-phase).

Basically this study is useful for the estimation and control of the transients in all electrical circuits and systems which are subject to repeated switching and where transient condition has got some significance.

Details of the work carried out and covered in this thesis are listed below:

(i) Derivation of equations for current response in all linear circuits with initial conditions in the normalized form.

(ii) Development of software to determine the critical conditions by optimization technique at which the transient current (peak) is at its extremum.

(iii) Development of software for the study and estimation of the transient current (peak) at different conditions.

(iv) Preparation of universal lookup graphs for peak transient current in all circuits at different initial conditions, power factors and switching instants.

(v) Development of a digital instant-controlled switching circuit for switching the circuit/device at any specific predetermined switching instant only.

(vi) Development of an analog instant-controlled switching circuit for accurate control of switching instant.

(vii) Development of a frequency invariant phase-angle and power-factor meter for measuring switching instant accurately.

(viii) Verification of the computerized investigation experimentally for different circuits at various predetermined switching instants.

(ix) Development of a master-controller circuit (MCC) based on instant-controlled switching (ICS) technique which, in addition to the above operations, successfully works as a controller circuit for converters/inverters (1-phase and 3-phase), choppers and integral-cycle power control in circuits and machines, and further as static distance relays.

(x) Application of the ICS technique for integral-cycle power control of resistive loads.

(xi) Application of the ICS technique for integral-cycle power control of inductive loads.

(xii) Application of the ICS technique for determination of switching current in machines (transformers)

(xiii) Application of the ICS technique for elimination of inrush current in 1-phase and 3-phase transformers.

(xiv) Application of the ICS technique for switching current control of 1-phase and 3-phase induction motors.

(xv) Application of the ICS technique for speed control of 1-phase and 3-phase induction motors.

INSTANT-CONTROLLED SWITCHING AND APPLICATIONS

Ph. D. THESIS

By

M. SYED JAMIL ASGHAR

DEPARTMENT OF ELECTRICAL ENGINEERING
ALIGARH MUSLIM UNIVERSITY
ALIGARH (INDIA)

1993

IQRA BISMI-RABBIKALLAZEE, KHALAQ.

KHALAQAL INSANA MIN-ALAQ.

IQRA WA RABBUKAL AKRAMULLAZEE,

ALLAMAL BIL'QALAM.

ALLAMAL INSANA MALAM YALAM.

(The first revelation of holy Kur'an. The last verse above is engraved in the university monogram)

Approximate translation:

Read: In the name of thy Lord the cherisher, Who created-
Created (and elevated) the man from (mere) clot.
Read: And thy Lord is most bounteous.
He taught (the man, conventionally) by the pen.
Taught the man (by revealing the knowledge)
that which he knew not.

Phone Nos. : { Public : 6910
University : 273

DEPARTMENT OF ELECTRICAL ENGINEERING
Z. H. COLLEGE OF ENGINEERING & TECHNOLOGY
ALIGARH MUSLIM UNIVERSITY, ALIGARH

Ref. No..... *Dated*.....

CERTIFICATE OF SUPERVISOR

This is to certify that the thesis entitled "**Instant-Controlled Switching and Applications**," submitted by Mr. **M. Syed Jamil Asghar**, Reader, Department of Electrical Engineering, Aligarh Muslim University, Aligarh, for the award of the degree of **Doctor of Philosophy (Ph. D.)**, is a record of the candidate's own work carried out under my supervision and not reported elsewhere for any degree or diploma, according to best of my knowledge.

Dated 10.12.1993

(Prof. M. Salman Beg)
Supervisor

ACKNOWLEDGMENTS

All praise is due to Almighty God Who is source of all knowledge which He reveals to man when He desires and peace be upon all the true messengers (prophets) sent by Him time to time to all peoples throughout the world, including Mohammed, the prophet of the last worldwide religion, for the guidance and success of the whole mankind here as well as in hereafter.

I sincerely acknowledge the help of all the people who directly or indirectly, in one way or the other, helped in my research work and during the process of writing this thesis.

I am very much indebted to my supervisor, Prof. M. Salman Beg, whose penetrating comments, constructive suggestions and expert advices during various stages of this work helped me immensely in conducting my research work smoothly. In his capacity as the Lab. superintendent, he very kindly arranged the procurement of equipments and materials required for my work from time to time.

I am sincerely thankful to Prof. K. P. Basu, Chairman, Department of Electrical Engg. and Prof. Prabhat Kumar for straightening up the simulation Lab. and for their sustained efforts for promotion of research work in the department.

I am also grateful to all my teachers and senior colleagues

of the department specially Prof. M. A. Jani, Prof. K. P. Basu, Prof. Mohibullah and Dr. Badrulhasan Khan who have worked in the field of switching transients and their work provided a sound base for this work.

I am also expressing my sincere thanks to Mr. Abdul Ghafoor, Foreman of the Department and one of the best technical personnel of this university, for his all-round cooperation and experienced suggestions.

Similarly the cooperation and help of Prof. S. K. Mukerji, Prof. Tariq Aziz (Dept. of Applied Maths.), Dr. Anees Ahmad (Dept. of Chemistry), Dr. Ali Ahmad (Dept. of Education), Dr. Shamim Ahmad (Dept. of Business Administration), Mr. Naseem Ahmad, Mr. Shamim Ahmad, Mr. Iftikhar Ahmad and Nanney Khan are also thankfully acknowledged.

Last but not least, I would like to express my deep gratitude to my elder sister (w/o Dr. S. Shamim Anwer, University Health Officer) for her motherly treatment that provided me a home away from home relieving me from all domestic problems and thus enabled me to concentrate fully on my research work.

At last,
it comes out,
from the core of the heart,
thanks God it is over.

(Jamil Asghar)

ABSTRACT

The switching transient in an AC circuit mainly depends upon the initial condition and the switching instant or the point on the voltage wave. In the work presented here, the equations of the current response with any initial condition is derived in the normalized form to obtain universal curves for peak transient current against switching instant for all types of AC circuits. For the first time, it is theoretically analyzed and experimentally verified that the switching current (peak) in any linear circuit can be pushed to its maximum level or constrained to its minimum level (equal to or close to steady-state value) simply by controlling the switching instant of the circuit. General equations and universal curves are also given to determine the extremum for all circuits. The maximum value of the switching current gives the correct value of the maximum possible switching transient current that may flow into the circuit.

Different types of instant-controlled switching circuits have been designed. Besides other applications, for the first time, they are used successfully to eliminate the switching inrush current in 1-phase as well as 3-phase transformers and reduce them considerably in induction motors.

Moreover these circuits are used in integral-cycle power control mode for resistive and inductive loads as well as in speed control applications of induction motors (1-phase as well

as 3-phase).

Basically this study is useful for the estimation and control of the transients in all electrical circuits and systems which are subject to repeated switching and where transient condition has got some significance.

Details of the work carried out and covered in this thesis are listed below:

(i) Derivation of equations for current response in all linear circuits with initial conditions in the normalized form.

(ii) Development of software to determine the critical conditions by optimization technique at which the transient current (peak) is at its extremum.

(iii) Development of software for the study and estimation of the transient current (peak) at different conditions.

(iv) Preparation of universal lookup graphs for peak transient current in all circuits at different initial conditions, power factors and switching instants.

(v) Development of a digital instant-controlled switching circuit for switching the circuit/device at any specific predetermined switching instant only.

(vi) Development of an analog instant-controlled switching circuit for accurate control of switching instant.

(vii) Development of a frequency invariant phase-angle and power-factor meter for measuring switching instant accurately.

(viii) Verification of the computerized investigation experimentally for different circuits at various predetermined switching instants.

(ix) Development of a master-controller circuit (MCC) based on instant-controlled switching (ICS) technique which, in addition to the above operations, successfully works as a controller circuit for converters/inverters (1-phase and 3-phase), choppers and integral-cycle power control in circuits and machines, and further as static distance relays.

(x) Application of the ICS technique for integral-cycle power control of resistive loads.

(xi) Application of the ICS technique for integral-cycle power control of inductive loads.

(xii) Application of the ICS technique for determination of switching current in machines (transformers).

(xiii) Application of the ICS technique for elimination of inrush current in 1-phase and 3-phase transformers.

(xiv) Application of the ICS technique for switching current control of 1-phase and 3-phase induction motors.

(xv) Application of the ICS technique for speed control of 1-phase and 3-phase induction motors.

LIST OF SYMBOLS/ABBREVIATIONS USED

SI	Switching instant (on the applied voltage wave).
PF	Power-factor.
FF	Flip-flop (Set-Reset).
ICS	**Instant-controlled switching.**
ICC	**Integral-cycle control.**
ZCI	Zero-crossing instant.
PZI	Positive zero-crossing instant.
PFC	Pulse-forming circuit.
PSC	Phase-shifting circuit.
PSD	Phase-sequence detector.
DBC	Driver and buffer circuit.
MCC	Master-controller circuit.
ZVS	Zero-voltage switching.
RFI	Radio-frequency interference.
PWM	Pulse width modulation.
θ	Angle of the applied voltage wave at the SI.
Z	Circuit impedance.
ϕ	Power-factor angle of impedance, Z, of the circuit.
Im	Study-state maximum current of the circuit.
Io	Current flowing in the circuit at the SI.
Ip	The peak current of circuit during the transient period before steady-state condition.
Ze	Damping-ratio (zeta) of circuit.
Xc	Capacitive reactance.
Xl	Inductive reactance.
Qo	Initial charge stored on capacitor before applying the input voltage.
Y	Ratio of the initial voltage before switching, Qo/C, to the maximum voltage on the capacitor, Im.Xc, at steady-state.
n	Ratio of the initial current, Io, at the SI to the maximum current at steady-state (Io/Im).
Va	Phase voltage (L-N) of phase A.
Vab	Line voltage of between phase A and B (L-L).
i_a	Phase current in phase A (winding).
Xm_1	Magnetizing reactance of primary winding.
Xm_{1a}	Magnetizing reactance of primary winding of phase A.
Xm_{1ab}	Mutual reactance of primary windings between A & B.

CONTENTS

1. GENERAL INTRODUCTION AND REVIEW

1.1 INTRODUCTION

The current in an inductor and the voltage across a capacitor cannot change instantaneously. Thus a change in an electric circuit results in transients before it acquires another steady-state condition. Although the transients persist only for a short while, the resulting high values of currents or voltages could be dangerous and as such cannot be ignored easily. Therefore the behavior of the circuit under transient condition demands a thorough study.

1.2 TRANSIENTS IN DC CIRCUITS

Transient response of the circuits when DC voltage (forcing function) is applied are well known [1,2,3]. The current, after the application of the DC voltage, increases or decreases exponentially in the RL and RC circuits respectively (Fig. 1.1). But the nature of the current response of such circuits (RL or RC) is same irrespective of the magnitudes of its circuit parameters (Appendix I). Even the presence of the initial current, Io, in RL circuit and the initial charge, Qo, on the capacitor in RC circuit, do not change the nature of response as shown in Fig. 1.2. Similarly the nature of the current response

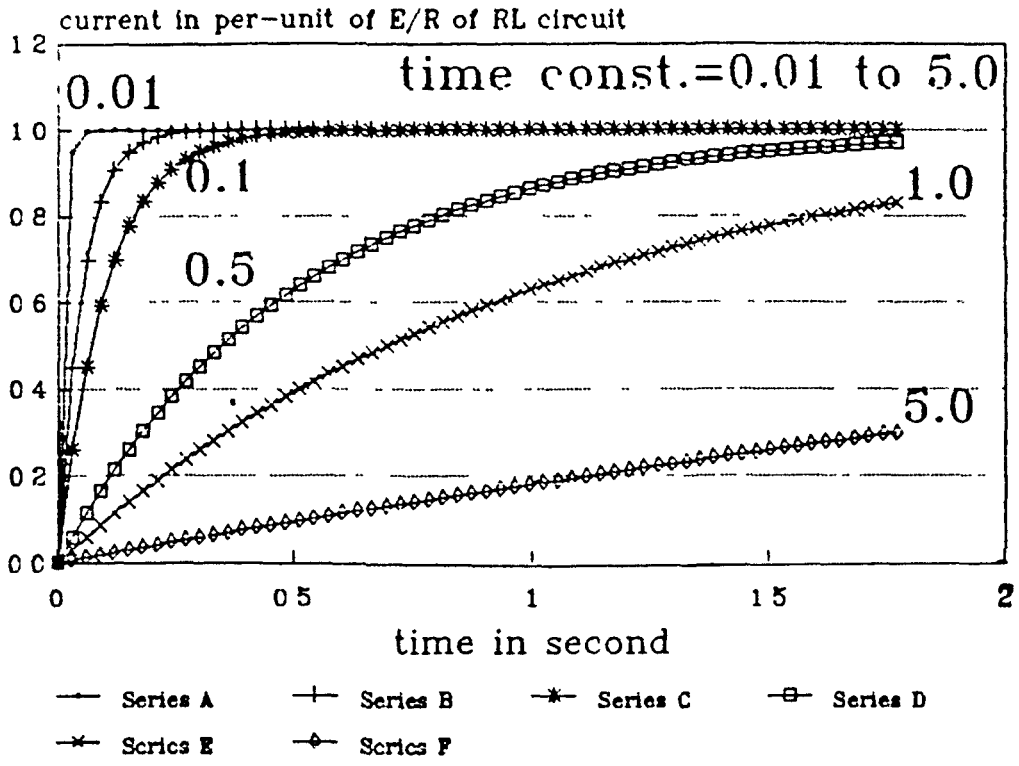

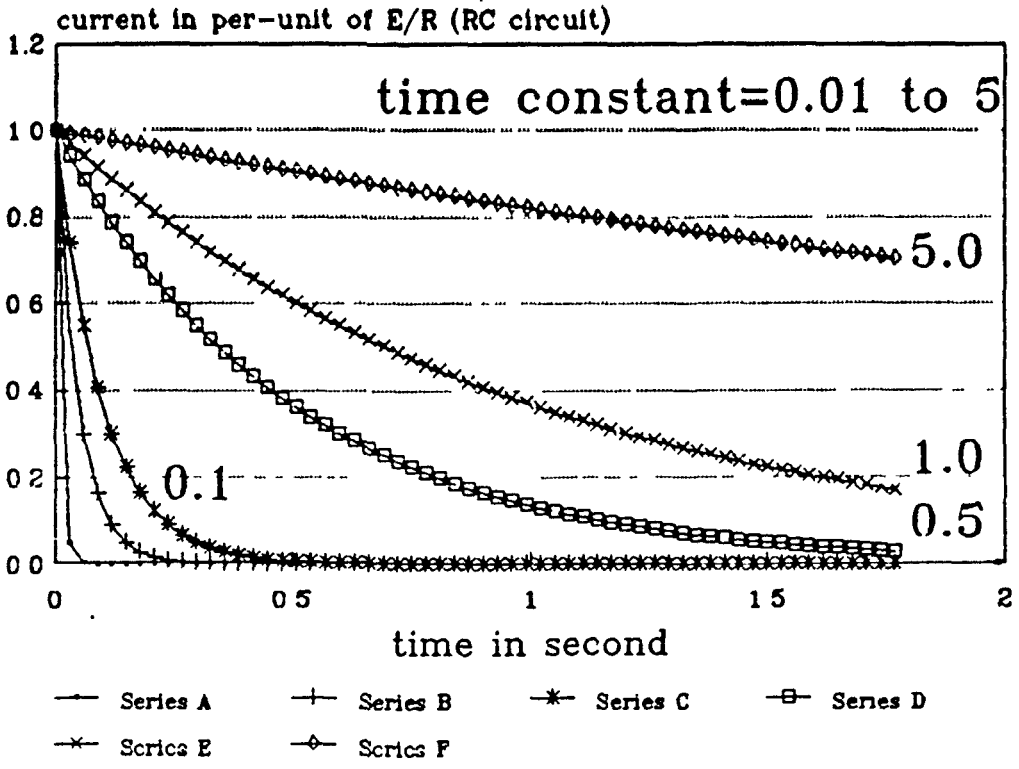

Fig. 1.1.Current response of RL and RC circuits under direct voltage input.

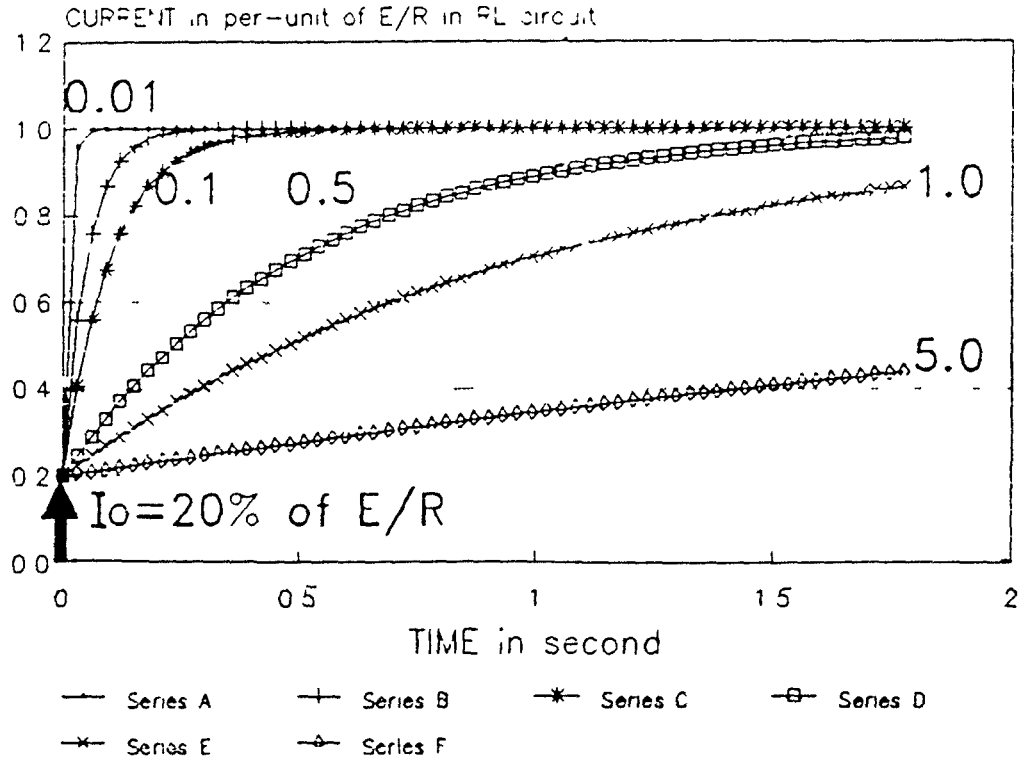

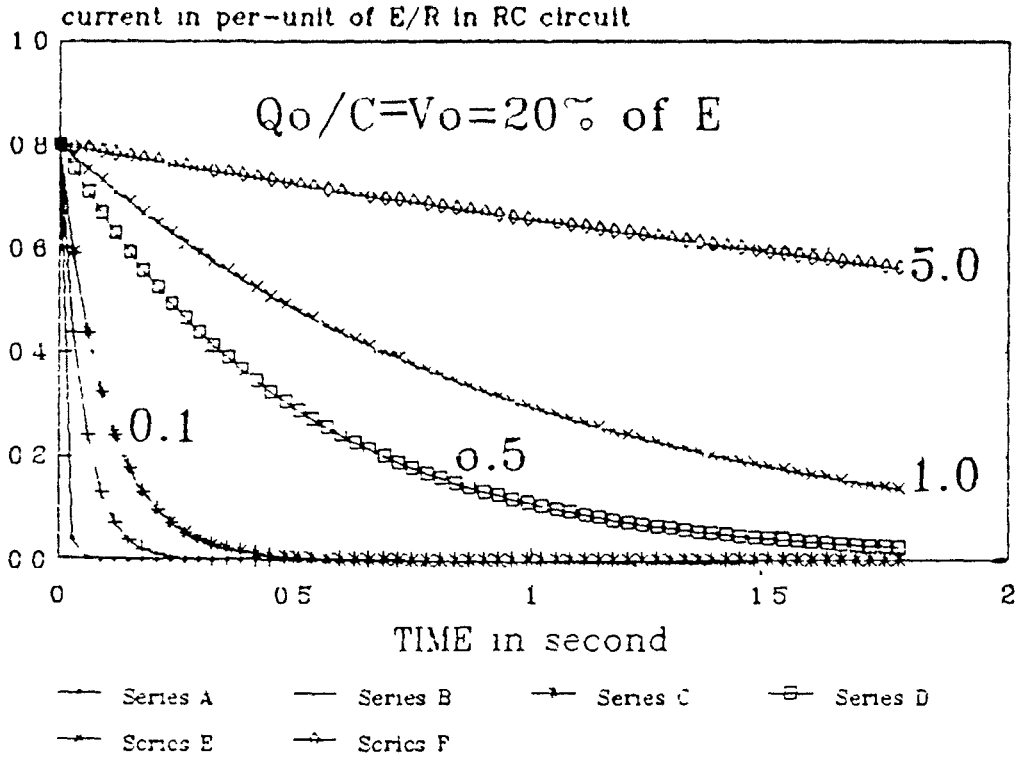

Fig. 1.2.Current response of RL and RC circuits under direct voltage input with initial condition.

and peak current (over shoot) in the RLC circuit depend upon the damping-ratio of the circuit. This is evident from the current response equation derived for RLC circuit with the initial condition (Appendix II). Fig. 1.3 shows clearly that the initial conditions simply affect the overall magnitude of the current while the nature of the response remains same.

1.3 TRANSIENTS IN AC CIRCUITS

In case of AC circuits, the nature of switching transients in RL circuit is well known. The effect of switching instant (the instant on the voltage wave when the circuit is closed) in RL circuit have appeared in the text books [1,2,3,4] and are well documented [5,6,7]. Digital and micro-processor based circuits have been reported for gradually reducing the switching transients in a 1-phase RL load working under integral-cycle control condition, by the feedback of the DC offset current [8,9].

In general, the current response depends upon the individual magnitudes of the circuit parameters, impedance of the circuit as well as the magnitude and the phasor position, θ, of the applied voltage at the switching instant (SI), in addition to the initial condition of the circuit. The variation of the SI or θ is limited within 0 to 2π, while the initial condition may vary up to any extent. The current response of a typical RLC circuit (under-damped, Ze=0.2, capacitive reactance), when switched at different SIs with zero and non-zero initial conditions, is shown in Fig. 1.4. It appears that the transients are unpredictable in nature

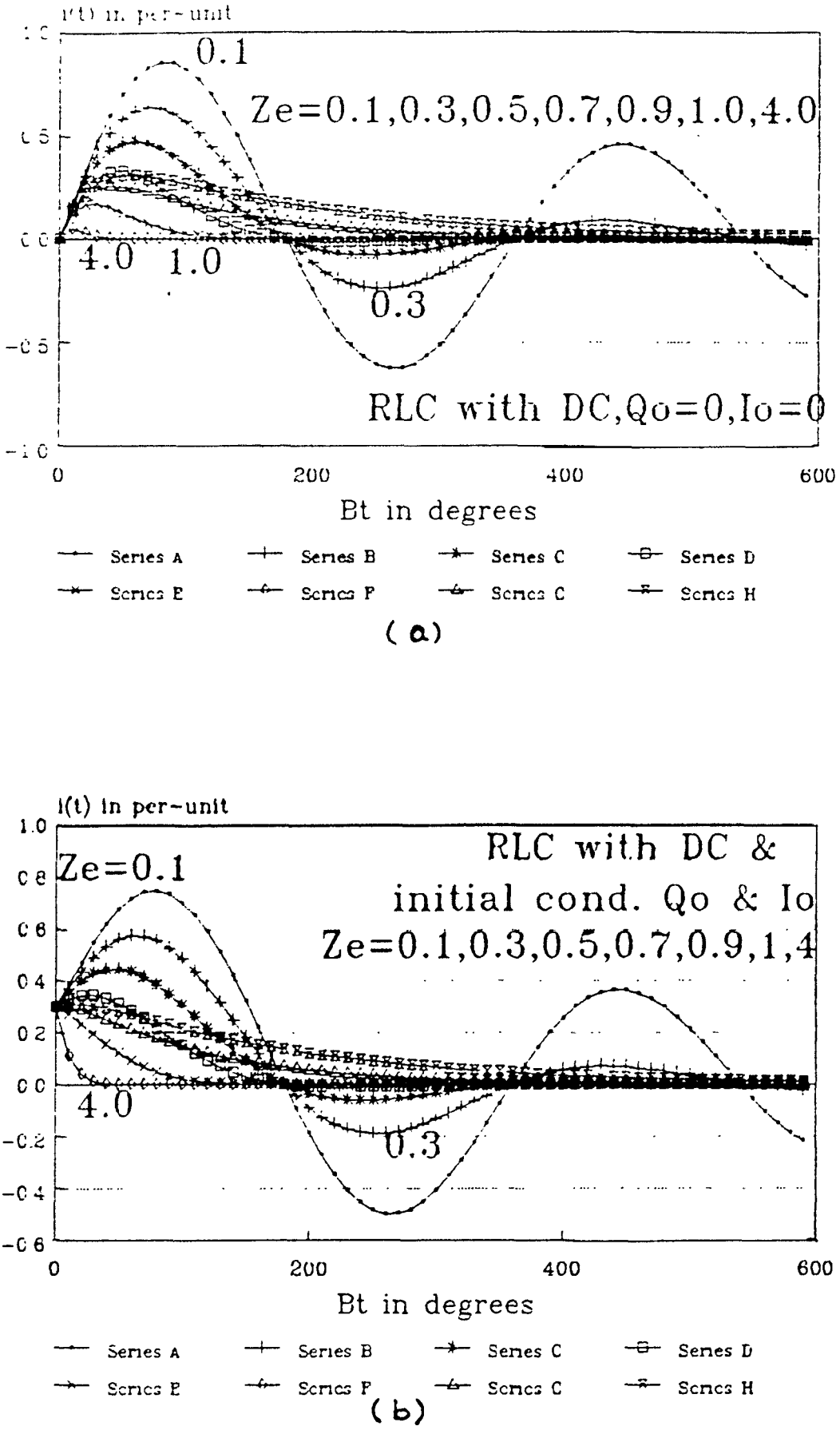

Fig. 1.3.Current response of RLC circuit under direct voltage input (a) with zero initial condition and (b) with initial condition.

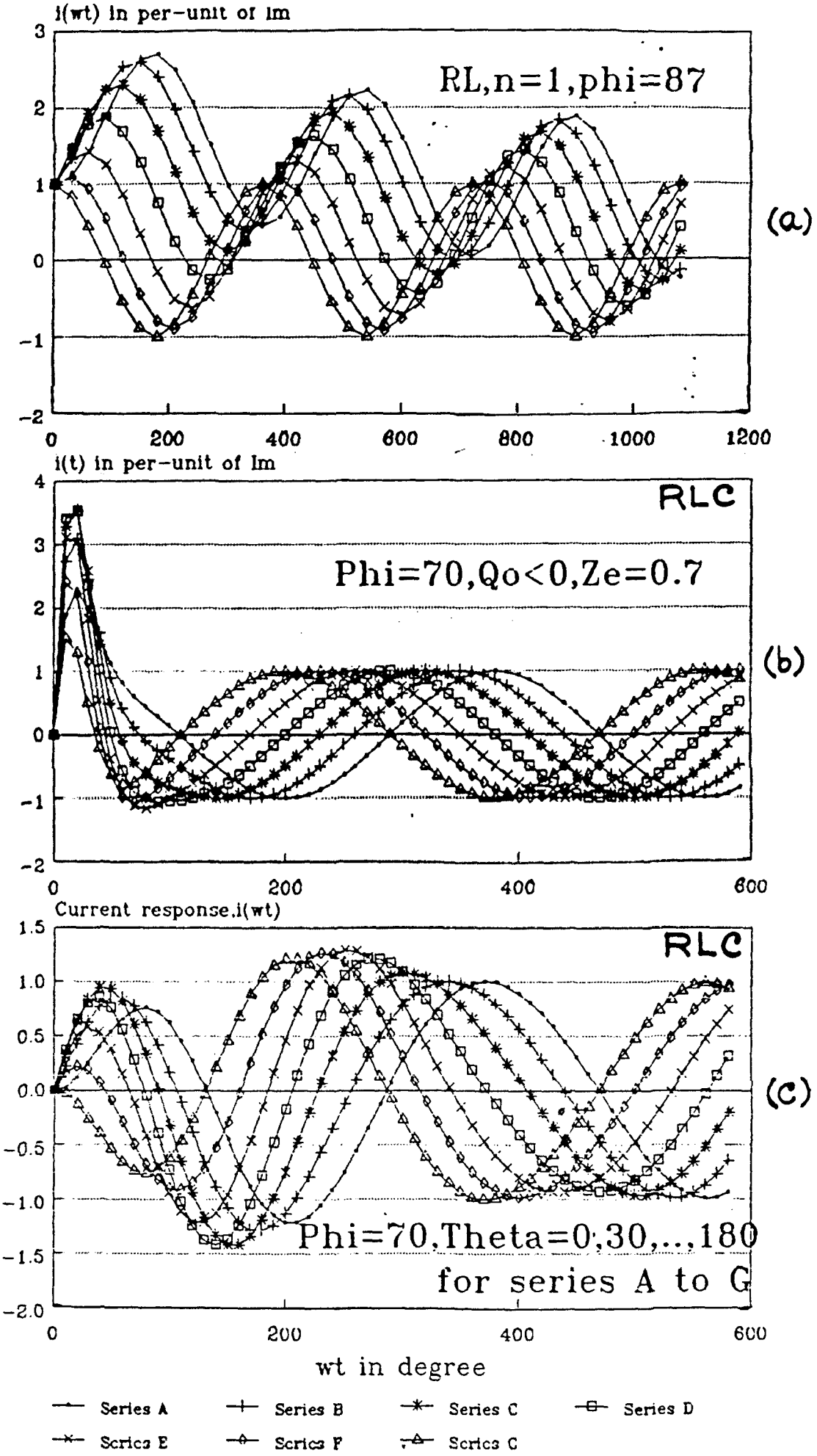

Fig. 1.4. Current response of (a) RL, (b) Capacitive RLC circuit and (c) inductive RLC circuits with AC input. Series A,B,C,D,E,F and G (curves) correspond to switching angle, θ=0°, 30°, 60°, 90°, 120°, 150° and 180° respectively.

and it is difficult to have a generalized and systematic knowledge of the transients in AC circuits taking into consideration all these factors together. Perhaps due to this complexity of the problem no significant work could be done earlier with generalized approach. The problem becomes more complicated in case of 3-phase AC circuits and machines.

1.4 STATEMENT OF PROBLEM

A complete analysis of all AC circuits i.e. RL, RC and RLC (capacitive and inductive; under-damped, over-damped & critically damped) with different initial conditions (Io & Qo), can give an overall picture of the transients of linear circuits which can be extended easily to the electrical linear and non-linear circuits and systems for controlling the switching transients as well as their performance. This study would be useful for estimation, elimination and control of the switching transients and performance of all AC (1-phase and 3-phase) circuits and machines.

After complete analysis of all AC circuits, this Knowledge could be successfully utilized for controlling the switching transient/inrush currents and performance of different circuits and machines (transformers and induction motors).

1.5 ORGANIZATION OF THESIS

Here the equations of the switching transient in the linear circuits are analyzed for the first time in the generalized form by introducing two factors for initial conditions to normalize

the response equations and to make the transients predictable for any circuit. It is found that there always exist a SI or θ, say θmax, for every circuit, at which the switching transient current (peak), Ip, is maximum. Similarly at a particular value of θ, say θmin, Ip is minimum. Thus transients become completely controllable and predictable and for this purpose **"instant-controlled switching circuits"** are developed which avoid random switching and enable the switching at the desired SI or θ.

Thus for over all study of the transients in linear circuits, response equations (including the initial conditions) are derived, simplified, normalized, software is developed, switching circuits are designed, circuit performance is recorded and their applications for controlling the switching currents and performance of different electrical machines (1-phase & 3-phase transformers and induction motors) and systems (resistive and inductive loads, static relays) are studied.

Chapter-2 deals with the computerized analysis of the circuit by optimization technique as well as by direct computation with the help of different software developed. From the computed values universal lookup curves/graphs are prepared for each type of linear circuit at different initial conditions. This is not only useful for controlling the transients but equally useful for estimation of the maximum possible transient current that could flow into a circuit.

Chapter-3 covers the details regarding the design, performance and utility of different instant-controlled switching (ICS) circuits. Different digital and analogue ICS circuits are

developed. Finally a versatile ICS circuit (master controller circuit) is developed which is capable to work in different control modes (controller for converters, choppers and integral-cycle power control) and to realize various other functions (static relays etc.).

Chapter-4 deals with the applications of the ICS circuits on transformers, induction motors and other systems. It is shown for the first time that the switching inrush current of 1-phase as well as 3-phase transformers in any mode of connection can be eliminated completely by using an ICS circuit. Similarly the switching currents of 1-phase as well as 3-phase induction motors are controlled/reduced significantly by controlling the SIs. Integral-cycle control (ICC) and ICS techniques are used together for zero-voltage switching of the resistive load as well as for ICC of inductive loads.

In **chapter-5**, conclusion is given and the scope of further possible work outlined. At the end, the details of different equations used, flow charts and computer programs etc. are given in the **appendices** to avoid lengthy detraction from the main theme in the text. List of the papers prepared and published from this thesis is also given.

2.SWITCHING TRANSIENT CURRENTS IN CIRCUITS (ANALYSIS & CONTROL)

2.1. INTRODUCTION

The switching transient current in AC circuits depends upon its impedance, individual magnitudes of circuit parameters as well as magnitude and the switching instant (SI) or the phasor position, θ, of the applied voltage at the instant of switching, in addition to the initial condition [1]. The transient period in the circuits and machines are, generally, of short duration. However, during these periods, sometimes, most serious operating problems are encountered. In most of the highly reactive or low power-factor (PF) circuits, often, the switching current (peak) is several times higher than the steady-state maximum current (Im). The doubling effect in the RL circuit is one of its examples. A complete knowledge of the transient behavior of all types of circuits is useful from the point of view of the maximum and minimum magnitude of the current response. The maximum switching current is the maximum instantaneous current that could flow into the circuit and it is also helpful in determination of the maximum possible voltage that could appear across each circuit element under the transient condition. The minimum switching current ensures that the transient current under a

certain condition is either zero or minimum and the system is safe from the dangerous transients. All types of linear series circuits are discussed here separately.

The switching transient response of RL, RC and RLC circuits can be easily determined using the expressions for their total current response. The exact condition at which the peak of the current response, Ip, is maximum or minimum (global), depends upon the SI on the voltage wave and also the initial condition, if any, of the circuit viz. the initial charge, Qo, stored on the capacitor and the initial current, Io, present in the circuit. For this purpose two switching arrangements employed are shown in Fig. 2.1 and 2.2. The variation of the SI or θ of the voltage is confined between 0 and 2π, while the initial condition of the circuit varies over wide range. This makes it difficult to foresee or predict the nature and magnitude of the transient current. A typical current response of RL circuit when switched at a particular value of θ is shown in Fig. 2.3. The effect of the SI or θ on the current response of RLC (under-damped) circuit with and without Qo is shown in Figures 2.4(a) and 2.4(b) respectively. These response clearly show the nature of the transients, variation of its magnitude, and Ip of the same circuit for different θ. The effect of θ in deciding the nature and magnitude of the transient can also be visualize from the well known equations for the total current response of linear series circuits [1].

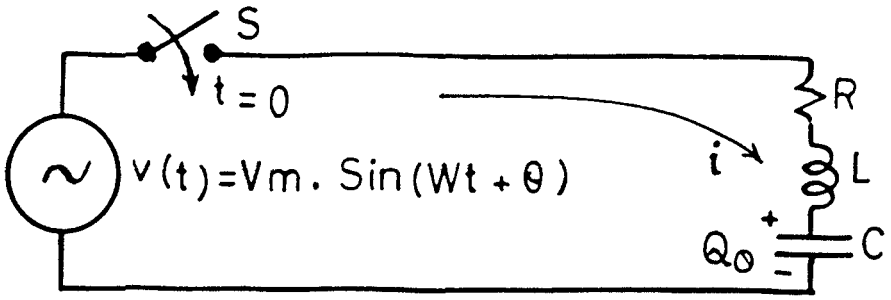

Fig. 2.1.Circuit arrangement for initial condition Qo.

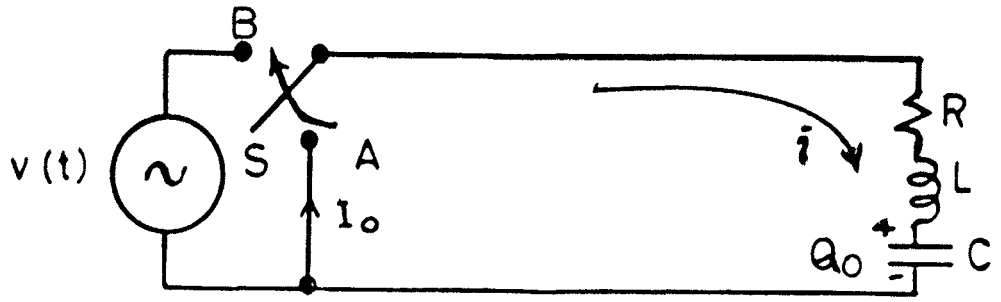

Fig. 2.2.Circuit arrangement for initial conditions Qo and Io.

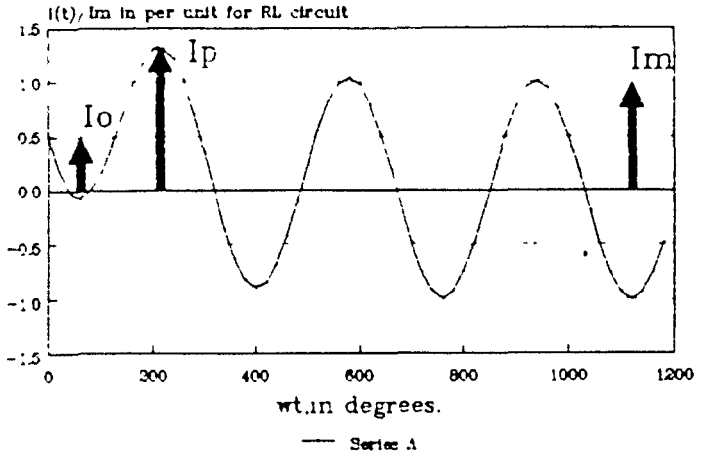

Fig. 2.3.A typical current response of an inductive circuit (RL) under alternating voltage input.

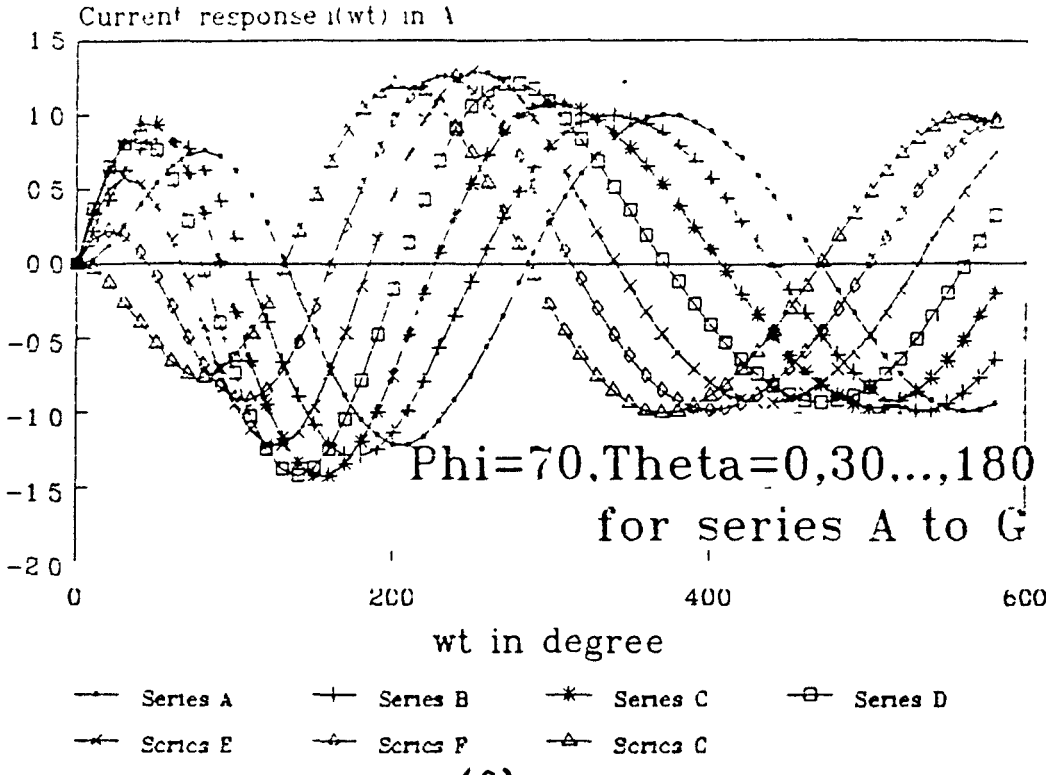

(a)

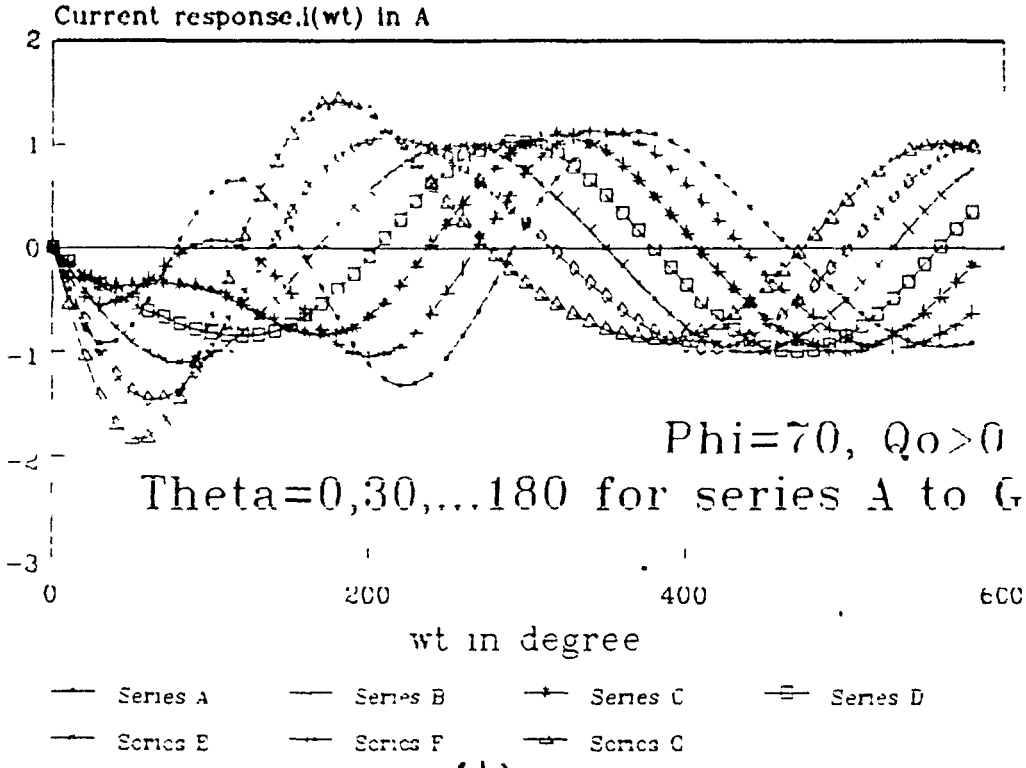

(b)

Fig. 2.4.Current response of an inductive (RLC) circuit under alternating voltage input with (a) zero initial condition and (b) with initial condition (Qo).

2.2 OPTIMIZATION OF TRANSIENT CURRENTS

To find out the exact condition in terms of θ, at which Ip for a circuit, with a particular initial condition, is maximum or minimum, classical optimization technique can be employed [10]. However, due to the presence of the exponential term, the first derivatives of the current cannot easily yield separate equations for " θ and t." Alternatively, simplest and most straight-forward method, although lengthy, is to compute the total current response i(θ,t) for each value of t while keeping θ constant (say θ=θ1) till the transient term vanishes i.e. the total current response becomes close to steady-state. Then the highest value of the current i(θ1,t) say I1p has to be compared with another highest value of current i(θ2,t) say I2p. In this way the largest value of Ip can be found while θ is varied from 0 to 2π. Thus θ=θmax, corresponding to the switching instant at which the maximum transient current (maximum of Ip's) flows in the circuit and θ=θmin, corresponding to the SI where transient is either zero or minimum (i.e. Ip is equal to Im or close to it) are evaluated.

2.2.1. Optimization by numerical methods

To cut short the above mentioned lengthy process the transient term (without the damping-factor), I_{tt}, can be optimized to give approximately the same results. Hence maximum and minimum values of Ip (global) can be easily found out in case of RL and RC circuits. But, it becomes difficult in case of the

RLC circuit to find out separate equations for θ and t from the first derivatives of I_{tt}, as the variables θ and t are not separable. Therefore, the classical method can not be applied as such. The derivatives of I_{tt} can thus be solved by numerical method to obtain the values of θ where possible maxima/minima of Ip exist.

Various numerical techniques can be applied to find the roots but the values of the roots obtained may be any stationary, local maximum/minimum or global maximum/minimum points. For example Newton-Raphson method, although fast enough, needs initial approximations for each root and therefore it can converge to a root amongst several roots that may not correspond to a global extremum. Similarly the bisection or false-position techniques suffer from the same drawback although the convergence is guaranteed in each method [11]. Therefore, to avoid local and false optima, classical and direct-search techniques together are used here for determination of the optimum transient current in RLC circuits. The equations of the first derivatives of I_{tt} can be used to find the roots by the direct-search method which correspond to the minimum, maximum or stationary points. At each root value of θ, current response has to be calculated again and its peak current Ip has to be picked up. Then global maximum and minimum values of Ip and corresponding θ (θmax and θmin) can be easily determined.

2.2.2. Derivation of equations

The total current response of different circuits with an initial condition (Qo only) is given in [1]. The applied

alternating voltage is Vm.sin(wt+θ) and the current response equations for the RL, RC, RLC over-damped (O/D), RLC critically damped (C/D)* and RLC under-damped (U/D) circuits respectively are given below:

$$i(t)=Im.\sin(wt+\theta-\phi)-Im.\sin(\theta-\phi).e^{-Rt/L}] \quad (2.1)$$

$$i(t)=Im.\sin(wt+\theta+\phi)-\tan\phi[wQo+Im.\cos(\theta-\phi)]e^{-t/RC} \quad (2.2)$$

$$i(t)=Im.\sin(wt+\theta-\phi)+[(Ed/bL)\sinh bt-Im.\sin(\theta-\phi)\cosh bt]e^{-at} \quad (2.3)$$

$$i(t)=Im.\sin(wt+\theta-\phi)+[(t.Ed/L)-Im.\sin(\theta-\phi)].e^{-at} \quad (2.4)$$

$$i(t)=Im.\sin(wt+\theta-\phi)+[(Ed/bL)\sin Bt-Im.\sin(\theta-\phi)\cos Bt].e^{-at} \quad (2.5)$$

where w, Z, Xl, Xc and ϕ are angular frequency of supply voltage, total impedance, inductive reactance (wL), capacitive reactance (1/wC) and PF angle of the circuit respectively and

$$a = R/2L,\ b = \sqrt{(R2-4L/C)}/2L,\ B = jb \quad \text{and}$$

$$Ed = Vm.\sin\theta-(Qo/C)-Xl.Im.\cos(\theta-\phi)-R.Im.\sin(\theta-\phi)/2 \quad (2.6)$$

The equations of the current response in all circuits (RL, RC and RLC) are derived for the condition when Qo and Io both are present in the circuit. Complete derivations for different

P.T.O.

* Kerchner & Corcoran in their book [1] have derived the current response equations for O/D and U/D cases only. However they have further suggested that the value of 'b' be made zero in the equation for O/D circuit, to get an equation for critically damped circuit (page 572, chapter XIV, reference 1). However this statement is **not true** because this results in the current response equation, either a 0/0 condition for an AC circuit or reduces the whole equation to zero in case of a DC circuit.

circuits are given in the Appendix II and the final equations are stated below for RL, RC and O/D, C/D and U/D circuits respectively.

$$i(t)=Im.\sin(wt+\theta-\phi)-[Im.\sin(\theta-\phi)-Io].e^{-Rt/L} \quad (2.7)$$

$$i(t)=Im.\sin(wt+\theta-\phi)-\tan\theta[wQo+Im.\cos(\theta+\phi)].e^{-t/RC} \quad (2.8)$$

$$i(t)=Im.\sin(wt+\theta-\phi)+[(Eo/bL)\sinh bt-\{Im.\sin(\theta-\phi)-Io\}\cosh bt]e^{-at} \quad (2.9)$$

$$i(t)=Im.\sin(wt+\theta-\phi)+[Eo.t/L-\{Im.Sin(\theta-\phi)-Io\}].e^{-at} \quad (2.10)$$

$$i(t)=Im.\sin(wt+\theta-\phi)+[(Eo/BL)\sin Bt-\{Im.\sin(\theta-\phi)-Io\}.\cos Bt]e^{-at} \quad (2.11)$$

where

$$Eo=Vm.\sin\theta-(Qo/C)-Xl.Im.\cos(\theta-\phi)-R\{Im.\sin(\theta-\phi)+Io\}/2 \quad (2.12)$$

From the above equations the conditions for the maxima and minima (θmax and θmin) of $|I_{tt}|$ can be easily found out.

2.2.3 Optimization condition for RL Circuits

It is evident from (2.7) that the transient term depends upon I_{tt}, therefore, the values of θ for which Ip is maximum or minimum, are given by

$$\theta max = -\pi/2+\phi \quad \text{for } Io \geq 0$$
$$= \pi/2+\phi \quad \text{for } Io \leq 0 \quad (2.13)$$

and $$\theta min = \sin^{-1}(Io/Im) + \phi \quad (2.14)$$

2.2.4 Optimization condition for RC Circuits

The values of θ for which Ip is maximum or minimum (as in the previous case) are given by

$$\theta max = -\phi \qquad \text{for } Qo \geq 0$$
$$= \pi - \phi \qquad \text{for } Qo \leq 0 \qquad (2.15)$$

and $\theta min = \cos^{-1}(-wQo/Im) - \phi$ (2.16)

2.2.5 Optimization condition for RLC Circuits

Here the classical method is used to find out the expressions which can be solved to get roots where the probable maxima/minima exist. Applying the classical technique i.e. putting

$$\delta I_{tt}/\delta t = 0 \qquad (2.17)$$

and $$\delta I_{tt}/\delta \theta = 0 \qquad (2.18)$$

For an O/D case, it is obtained from (2.9) and (2.17) that

$$(Eo/L).\cosh bt - b(Im.\sin(\theta-\phi) - Io)\sinh bt = 0 \qquad (2.19)$$

or $$\coth bt = (bL/Eo)(Im.\sin(\theta-\phi) - Io) \qquad (2.20)$$

Similarly from (2.9) and (2.18)

$$(Elo/bL)\sinh bt - Im.\cos(\theta-\phi).\cosh bt = 0 \qquad (2.21)$$

where

$$Elo = \delta Eo/\delta\theta = Vm.\cos\theta + Xl.Im.\sin(\theta-\phi) - R.Im.\cos(\theta-\phi)/2 \qquad (2.22)$$

Further from (2.21) and (2.20) a function $f(\theta)$ is obtained such that

$$f(\theta) \equiv Elo.Eo - (bL)2.Im.\cos(\theta-\phi).\{Im.Sin(\theta-\phi) - Io\} = 0 \qquad (2.23)$$

The expression $f(\theta)$ for U/D circuit is same as above except

that *b* has to be replaced by B, or *b* and B can be made equal to each other for the purpose of calculation as

$$b=\sqrt{|(R2-4L/C)|}/2L = B \qquad (2.24)$$

Now, for the C/D circuit, the whole transient term can be used to find f(θ) such that

$$t=[\{Im.\sin(\theta-\phi)-Io\}+1/a]L/Eo \qquad (2.25)$$

and $$f(\theta)=(E1o/Eo)\{Im.\sin(\theta-\phi)-Io\}+(E1o/aL)-Im.\cos(\theta-\phi) \qquad (2.26)$$

Now f(θ) can be calculated from θ=0 to 2π and it becomes zero for those values of the θ (say θ1, θ2,.... etc.) where roots exist i.e. where any maximum or minimum or stationary points exist. i(θ,t) has to be now calculated for these values of θ i.e. i(θ1,t), i(θ2,t),....., from t = 0 to the five time-periods of the circuit (t = 5t ≈ 5/a, as the transient term $I_{tt}.e^{-at}$ becomes 0.67% of the its initial value). Now I1p, I2p,..... corresponding to θ1, θ2,..... can be compared to find out the global maximum and global minimum values of the switching current (peak) and their corresponding switching angles θmax and θmin respectively.

2.2.6 Computation

Initially (2.23) or (2.26) can be used to determine the optimum conditions with respect to θ and then (2.9), (2.11) and (2.10) for calculation of Ip (global) for O/D and U/D or C/D circuits respectively. However, if value of R is slightly increased (say by 0.001%) then C/D circuit becomes an O/D circuit

(damping ratio, Ze = 1.00001). Now the C/D circuit can thus be analyzed as an O/D circuit as the transients in both the cases are non-oscillatory. The value of $f(\theta)$ changes its sign or becomes equal to zero (where the root lies) when the following condition is satisfied.

$$f1.fo \leq 0 \qquad (2.27)$$

where

$fo = f(\theta_n)$ at nth value of θ

$f1 = f(\theta_{n+1})$ at (n+1)th value of θ.

Since more accurate value of θ (with fraction of one degree) is normally not significant for practical purposes, the step of calculation for $f(\theta)$ is kept $\pi/180$ radian or one degree only (the exact value of the root may be found by any iterative method, if necessary). When the condition given in (2.23) or (2.26) is satisfied, then i(t) is calculated at each root value of θ where step-size taken is, wt=1.8° (200 times in each cycle of the applied voltage). Normally four roots are found for a particular RLC circuit as is evident from Fig. 2.5 The maximum value of $|i(t)|$ is picked up, which is nothing but Ip. At each root value ($\theta1$, $\theta2$,....) Ip's can be compared to find out the global maximum and global minimum values of Ip and hence corresponding θmax and θmin.

The flowchart and related computer programs are given in Appendix III. The program for (B) part of the flowchart, meant for C/D circuit, is same as for (A) part. However as discussed earlier C/D circuit can also be analyzed as a special case of O/D circuit. Programs were run to findout θmin and θmax for a

FIG. 2.5 Plot of function f(theta).

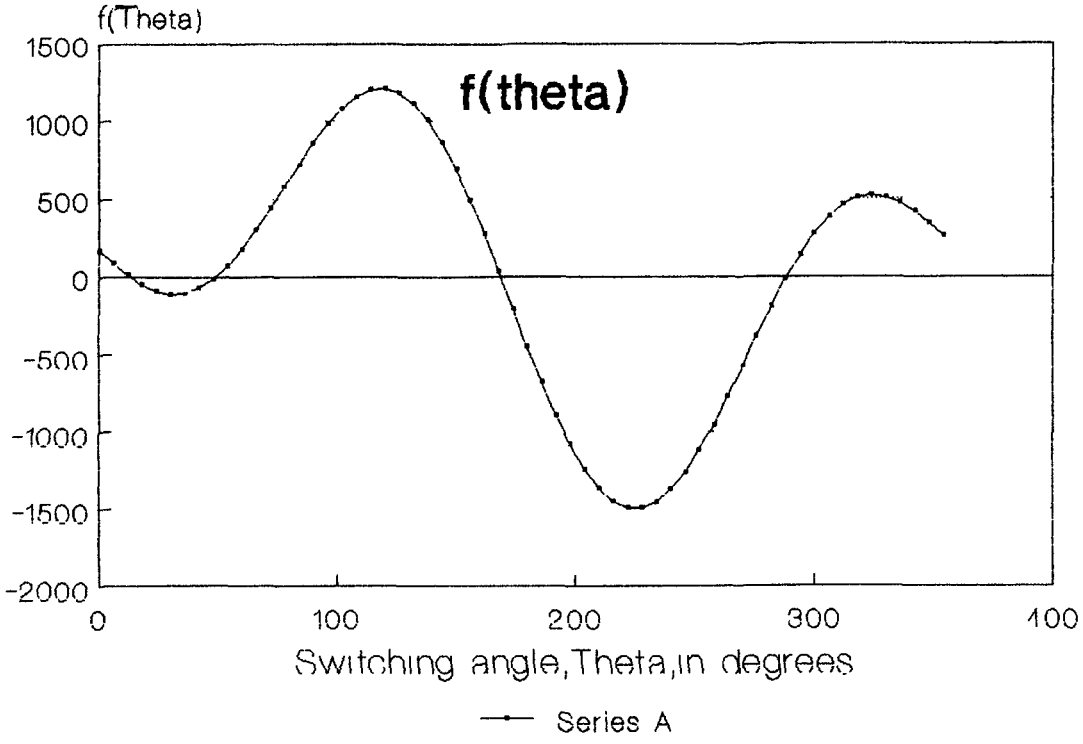

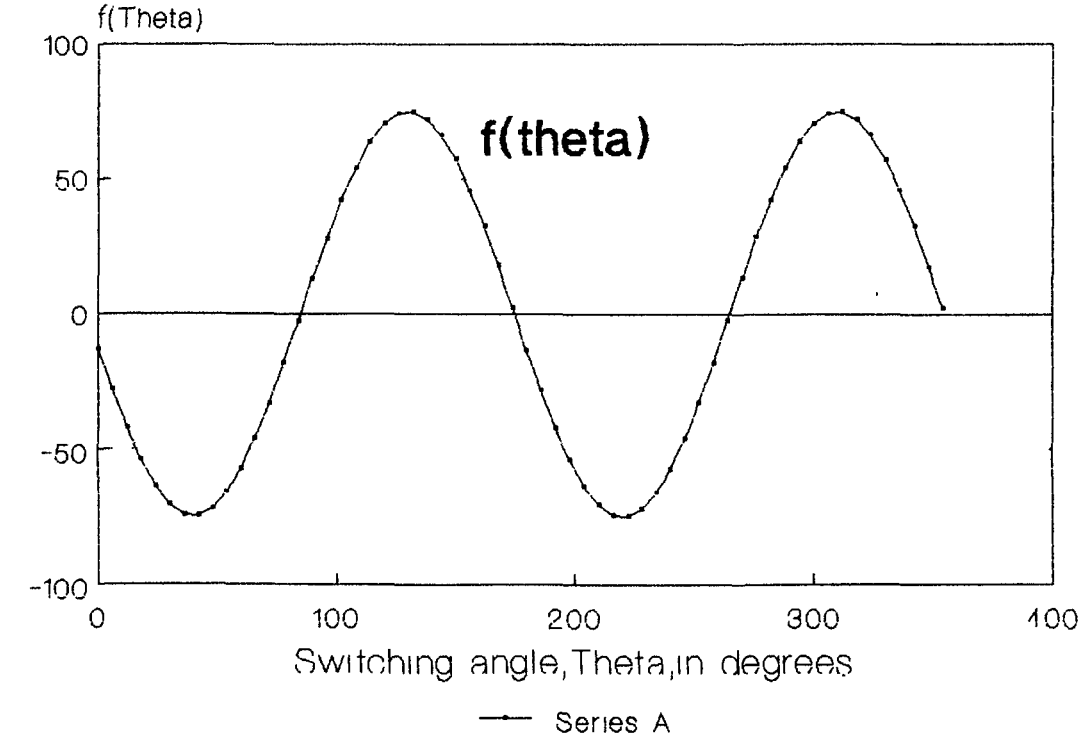

particular circuit.

2.3 GENERALISED APPROACH

The method of determination of Ip, as discussed in preceeding section, is an approximate one and each computation is confined to a particular circuit. However a thorough knowledge of the transient behavior of all circuits in the normalized form is always desirable.

2.3.1. Normalization of equations

The set of the five equations, (2.1) to (2.5), are modified to (2.28) to (2.32) below by defining the two terms "Y" and "n" such that the universal response (in term of per-unit of Im) for each case can be obtained easily.

$$i(wt)=Im.[\sin(wt+\theta-\phi)-\{\sin(\theta-\phi)-n\}.e^{-\cot\phi.wt}] \quad (2.28)$$

$$i(wt)=Im.[\sin(wt+\theta-\phi)-\tan\phi\{Y+\cos(\theta+\phi)\}.e^{-\tan\phi.wt}] \quad (2.29)$$

$$i(wt)=Im.[\sin(wt+\theta-\phi)+\{(Zo/bL)\sinh bt-(\sin(\theta-\phi)-n)\cosh bt\} e^{-(R/2Xl)wt}] \quad (2.30)$$

$$i(wt)=Im.[\sin(wt+\theta-\phi)+\{(Zo.t/L)-(\sin(\theta-\phi)-n)\}e^{-(R/2Xl)wt}] \quad (2.31)$$

$$i(wt)=Im.[\sin(wt+\theta-\phi)+\{(Zo/BL)\sin Bt-(\sin(\theta-\phi)-n)\cos Bt\} e^{-(R/2Xl)wt}] \quad (2.32)$$

where

Y = ratio of initial voltage (Qo/C) to the maximum voltage on capacitor at steady-state (Im.Xc),

n = ratio of Io to Im =Io/Im,

Zo = Eo/Im and therefore,

$$Eo = Ed+(Im.n.R)/2$$
$$= Vm.\sin\theta-(Qo/C)-Xl.Im.\cos(\theta-\phi)-R\{Im.\sin(\theta-\phi)-Io\}/2$$
$$= Im.[Z.\sin\theta-(Y.Xc)-Xl.\cos(\theta-\phi)-R\{\sin(\theta-\phi)-n\}/2] \quad (2.33)$$

Now the current response for every circuit, with any initial condition, can be found by using the above equations in the normalized form. Ip is then calculated by a software developed for calculation and comparison of i(wt) in the circuit. To normalize the magnitude of i(wt) or Ip, or to express them in terms of per-unit of Im, the impedance of the circuit is numerically taken equal to Vm. The current response, i(wt) is calculated for particular value of θ, ϕ, Y and n, at an interval of wt=1.8° and up to the five time-periods of the circuit i.e. till the transient term becomes 0.67% of its maximum value. Then the maximum value of |i(wt)| is picked up which is Ip at that θ (as discussed previously in the A-part of the flowchart). Several programs are developed for computation of current response as well as Ip in RL, RC and RLC circuits and some of them are given in Appendix III. Graphs are plotted for these Ip's at each θ for given Y and n of a particular circuit. The values of R, Xl and Xc are calculated for the particular value of Ze (in the RLC circuit). The graphs are plotted for Ip versus θ (from 0° to 360°) at eight PF. angles viz. ϕ=20°, 30°, 40°, 50°, 60°, 70°, 80° and 87.13° (R = 5% of Z) in each as shown in curves A to H. The maximum and minimum |Ip| indicate the maximum and minimum transient currents that could flow in the circuit at those conditions respectively.

In the following passages, firstly, all the circuits with the initial condition of Qo only and then for Qo as well as Io are discussed.

2.3.2 Analysis of circuits with Qo only (Io=0)

The current response is found similar in RL and in all types of RLC circuits where inductive reactance is larger than the capacitive reactance. Similarly the same behavior of the circuit is found in RC and in all types of RLC circuits where capacitive reactance is larger than inductive reactance. Therefore capacitive and inductive circuits are being discussed separately.

(a) Analysis of inductive circuits:

Let the circuit as shown in Fig. 2.1 be switched on by closing the switch "S" at the instant t=0, for all types of series circuits considered below:

(i) RL circuit: It is evident from equations (2.1) or (2.28) that the transient term vanishes, if switching is done at PF angle and hence

$$Ip=\text{Maximum of } |i(t)|=Im \quad \text{for } \theta=\theta min=\phi \text{ or } \pi+\phi \qquad (2.34)$$

Similarly a general condition for maximum transient in the RL circuit can also be found out. Fig. 2.6 shows the trend of Ip in RL circuit. Series A to H represents the curves of Ip for the impedance angles 20° to 87.13° respectively as mentioned above. Ip depends simultaneously upon the steady-state as well as the transient terms of equation (2.28).

(ii)RLC circuits: The current response of the RLC circuit depends upon the damping-ratio of the circuit [2]

FIG.2.6 Variation of Ip at different SIs for circuits of different PF (phi).

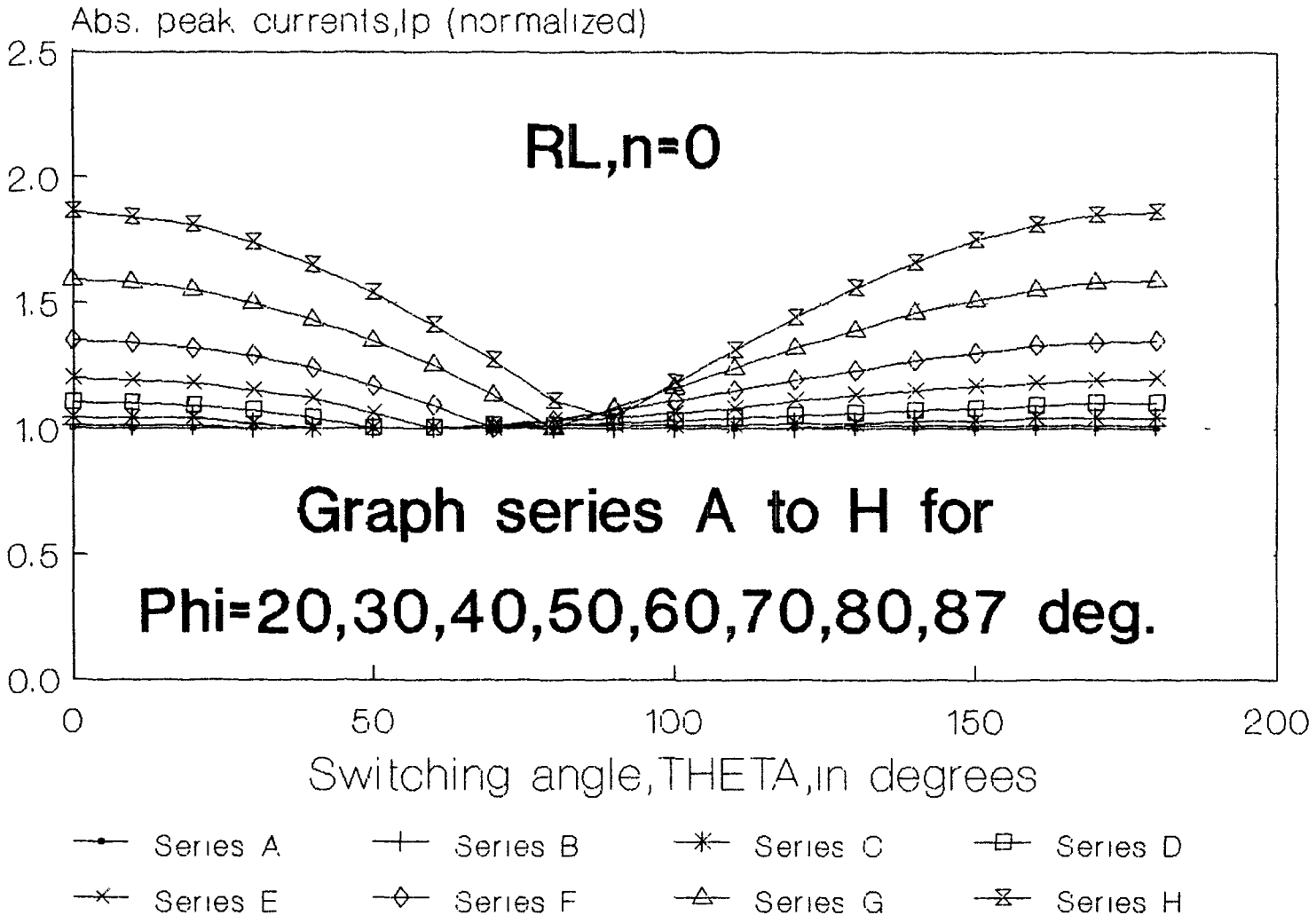

$$Ze = R/\{2\sqrt{(L/C)}\} = R/\{2\sqrt{(Xl.Xc)}\} \qquad (2.35)$$

The computation of the current becomes independent of source frequency, w. Therefore, for a particular value of Ò, the actual values of circuit parameters R, L and C are not required in above equations. For an inductive RLC circuit the values of Xl and Xc as derived in Appendix IV are given by

$$Xl=[\sqrt{\{X2+(R/Ze)2\}}+X]/2 \quad \text{and}$$

$$Xc=Xl-X \qquad (2.36)$$

Similarly for a capacitive circuit

$$Xc=[\sqrt{\{X2+(R/Ze)2\}}+X]/2 \quad \text{and}$$

$$Xl=Xc-X \qquad (2.37)$$

The current response of the circuit is found in the generalized form. Thus the actual values of w, Qo, Io and Im are not required. Ip is calculated for different values of Y (1, 0.75, 0.5, .25 and 0) for each value of Ze = 1.2, 1.4, 2, 2.8 and 3. The current response of C/D circuit is found similar to O/D circuit as both are non-oscillatory. Therefore, the C/D case is considered as a special case of O/D circuit (Ze= 1.00001).

Fig. 2.7 shows the variation of Ip in the whole range of θ with different values of Y for O/D (Ze =1.4) circuit. It is evident from the graphs that the transient dies completely when the switching is done at a particular value of θ. The variations of Ip for $Y \leq 0$ is found to be similar as for $Y \geq 0$ except that it is displaced by 180° or π radian. Similarly, for all cases of $Y \leq 0$, θmin and θmax are found displaced by an angle of 180° as shown in Fig. 2.7(b). Henceforth, conditions for θmin and θmax are given

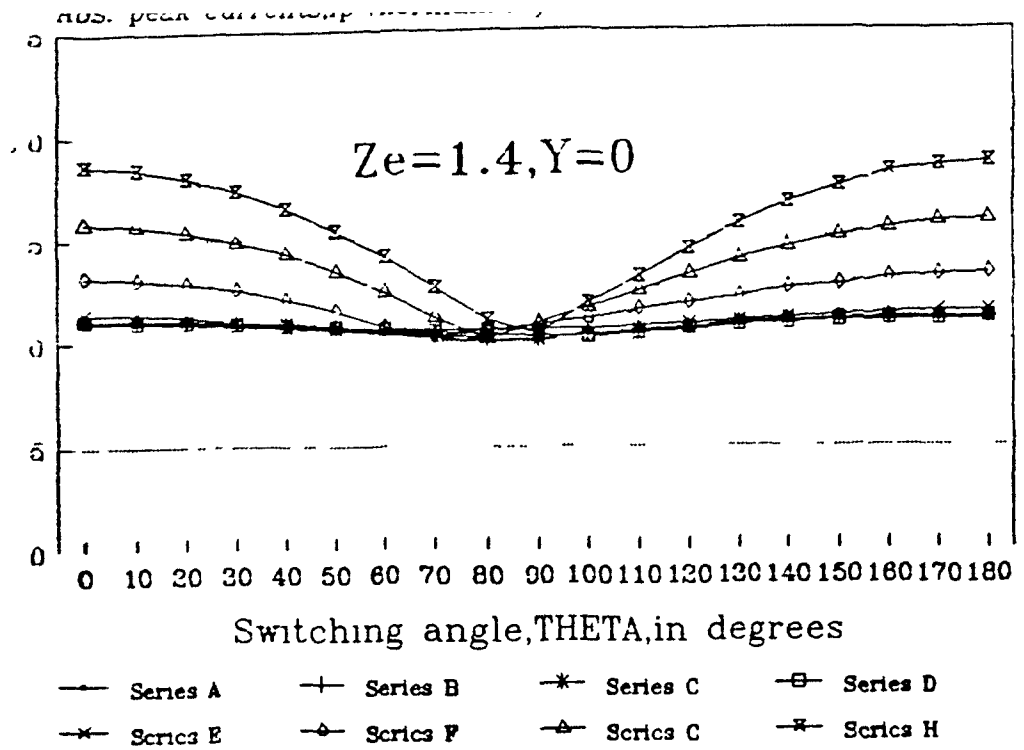

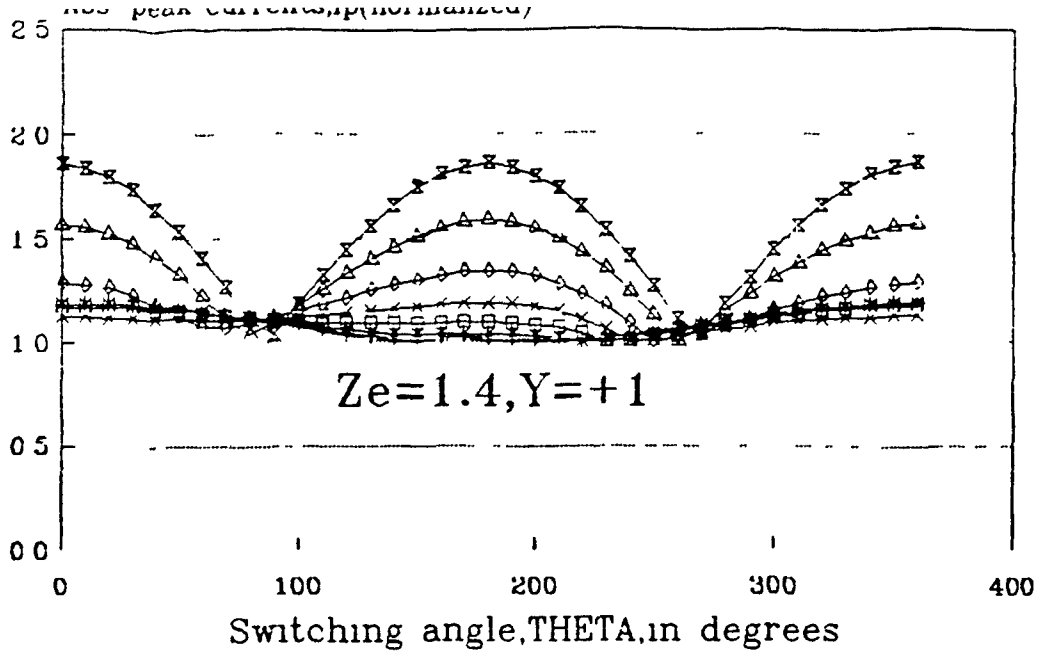

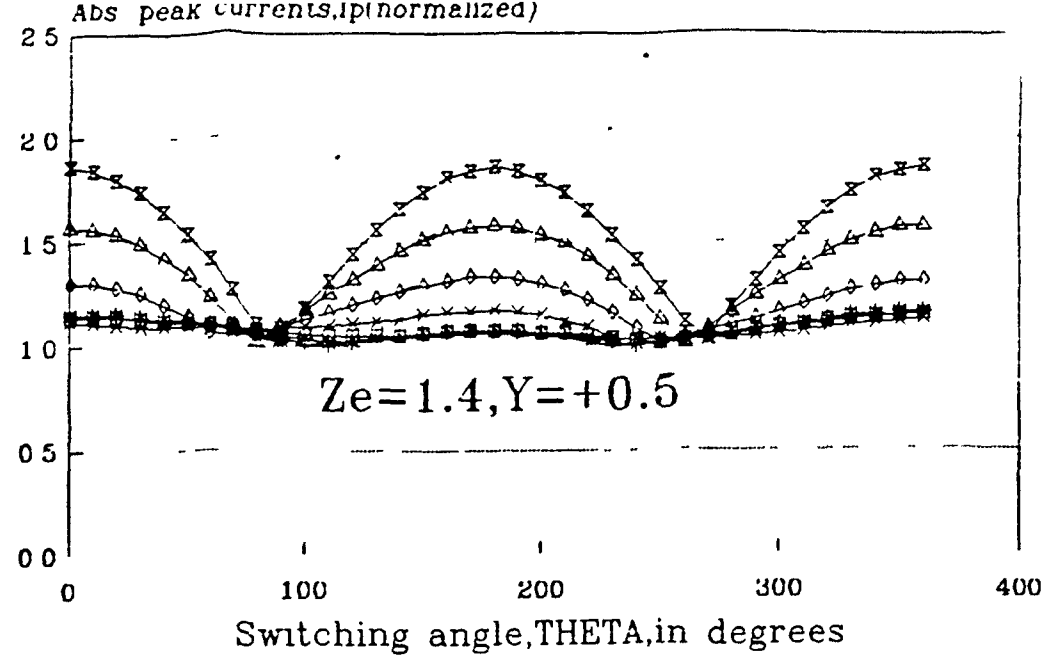

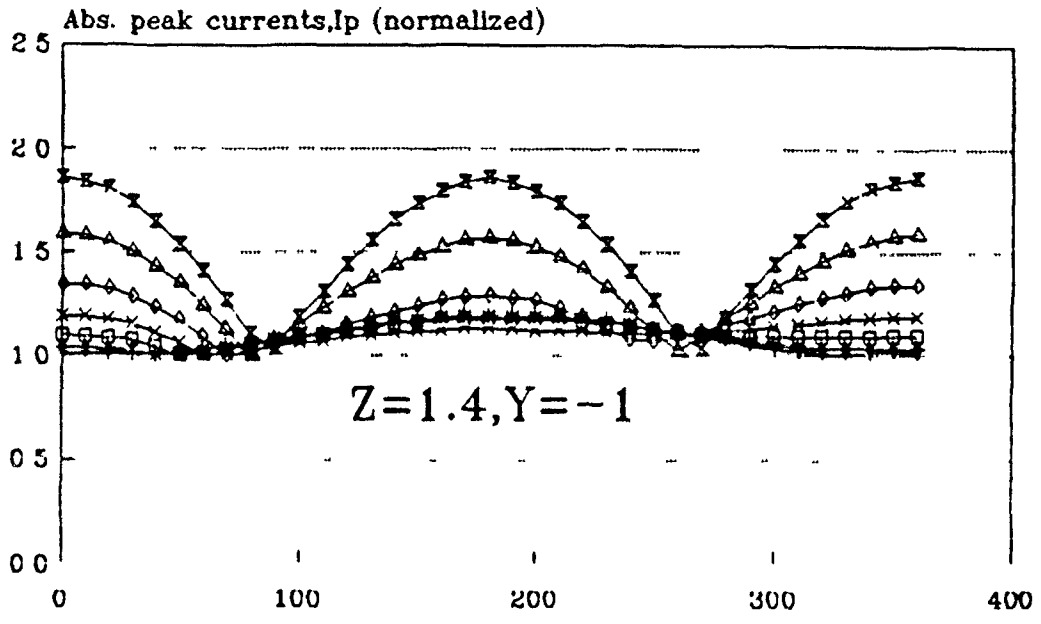

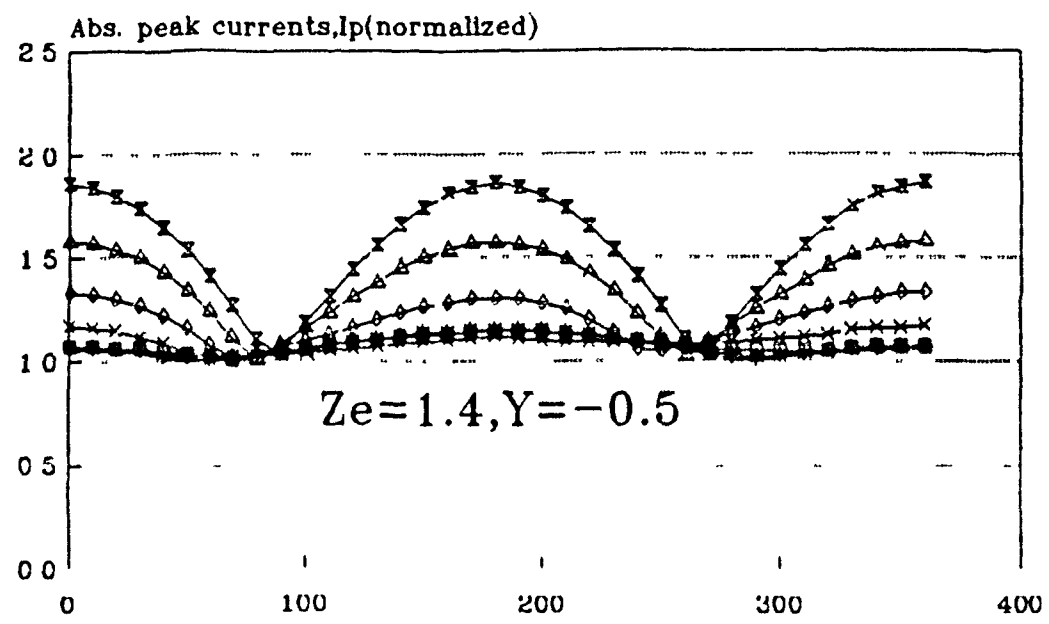

Fig. 2.7. Ip for over-damped (inductive) circuits for different Y (Io=0).

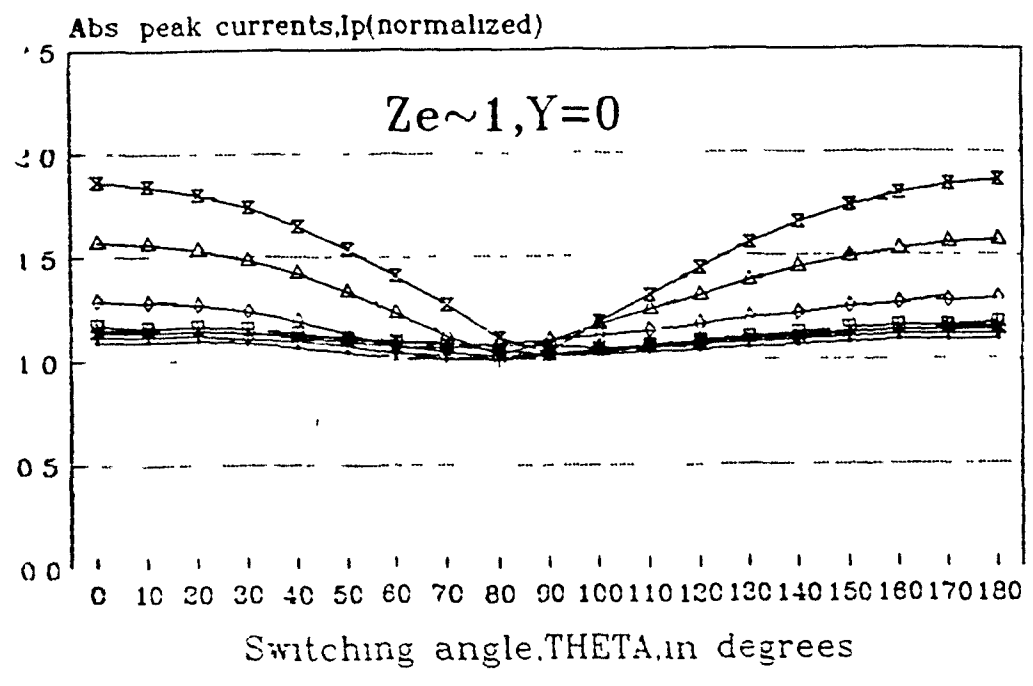

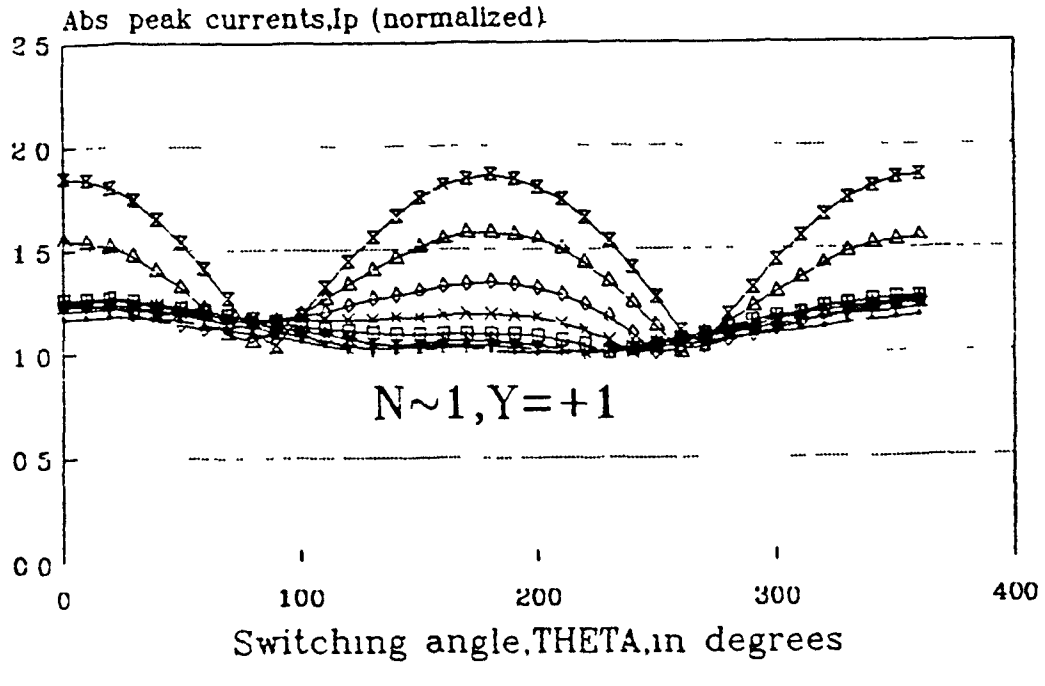

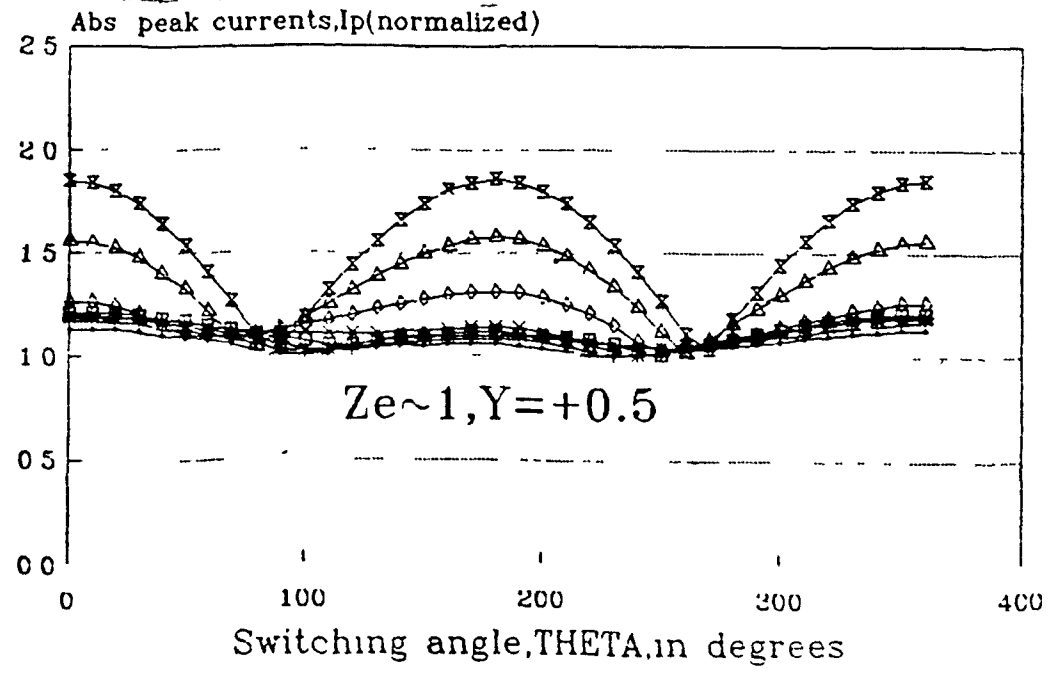

Fig. 2.8. Ip for critically-damped circuits for different Y.

for $Y \geq 0$ only. Fig. 2.8 shows the variation of Ip for different values of Y in C/D circuits.

The result obtained for U/D circuits are found similar to that for O/D circuits. Fig. 2.9 shows the variation of Ip for Ze=0.7 and 0.2 in the whole range of θ with and without stored charge on capacitor. θmax and θmin are found same in case of an O/D circuit. The variation pattern of Ip is found same for all values of Ze. However the minimum level of Ip is larger for lower value of Ze which is shown in Fig.2.10.

(b) Analysis of capacitive circuits:

The variation of Ip for $Y \leq 0$ is found same as in case of $Y \geq 0$ except that it is displaced by 180° (as discussed in previous section). Therefore θmin and θmax (for $Y \leq 0$) are also shifted by 180°. The conditions for minimum and maximum transient in the circuit at $Y \geq 0$ are given below. Different types of these circuits are separately discussed.

(i) RC circuit: Fig.2.11 shows the variation of Ip in the RC circuit for the whole range of θ, with and without stored charge on capacitor.

(ii) RLC circuits: Similarly the calculations are done for Ze=1.2, 1.4, 2, 2.8, and 3 for an O/D circuit. Figures 2.12 and 2.13 show the variation of Ip for O/D (Ze=1.4) and C/D circuits respectively as in previous cases. The condition of maximum Ip is found to be same as in RC circuit. The error as compared to the actual values of θmax and θmin is found maximum in C/D circuits. In general, the error can be reduced by reducing θmax merely by

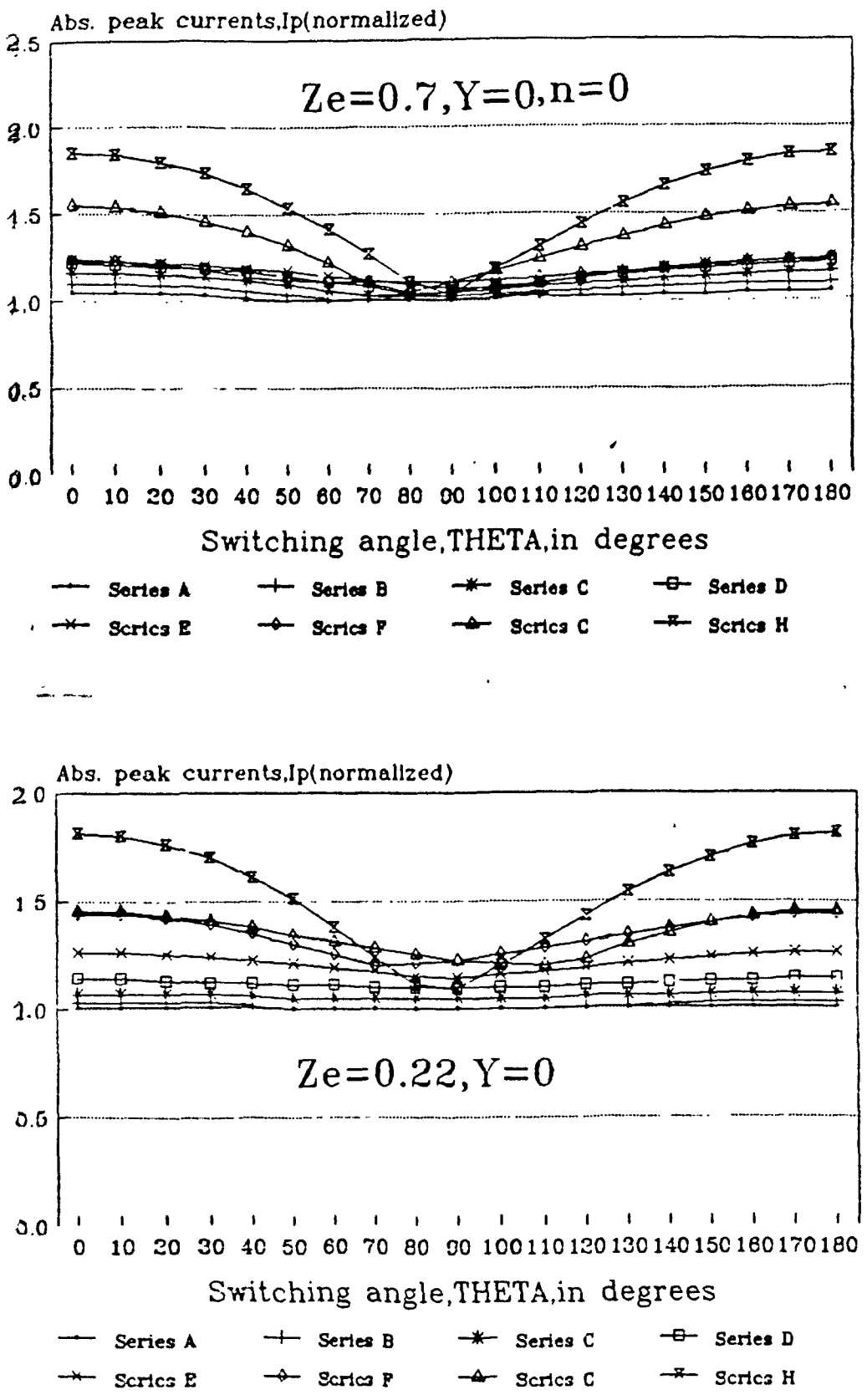

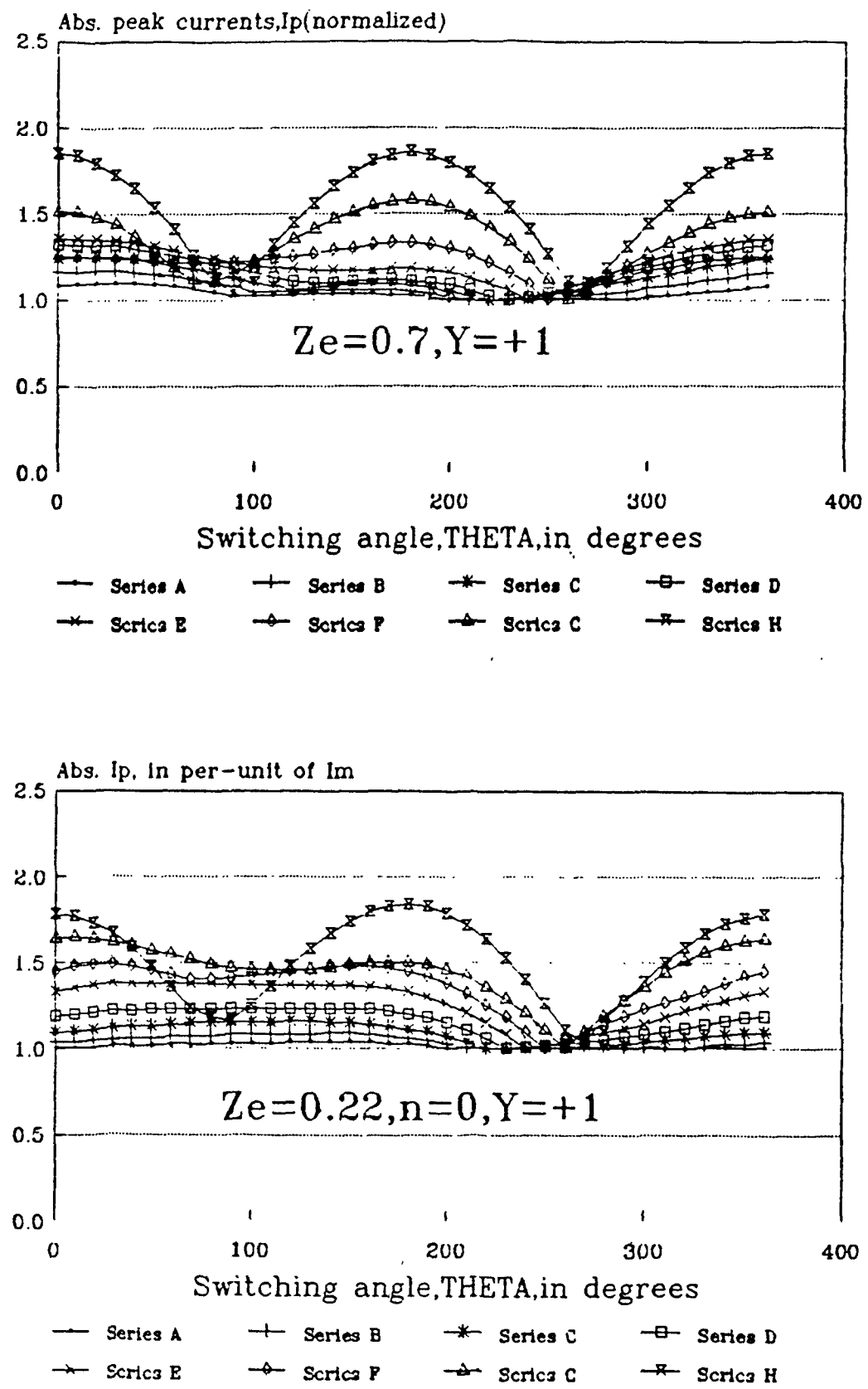

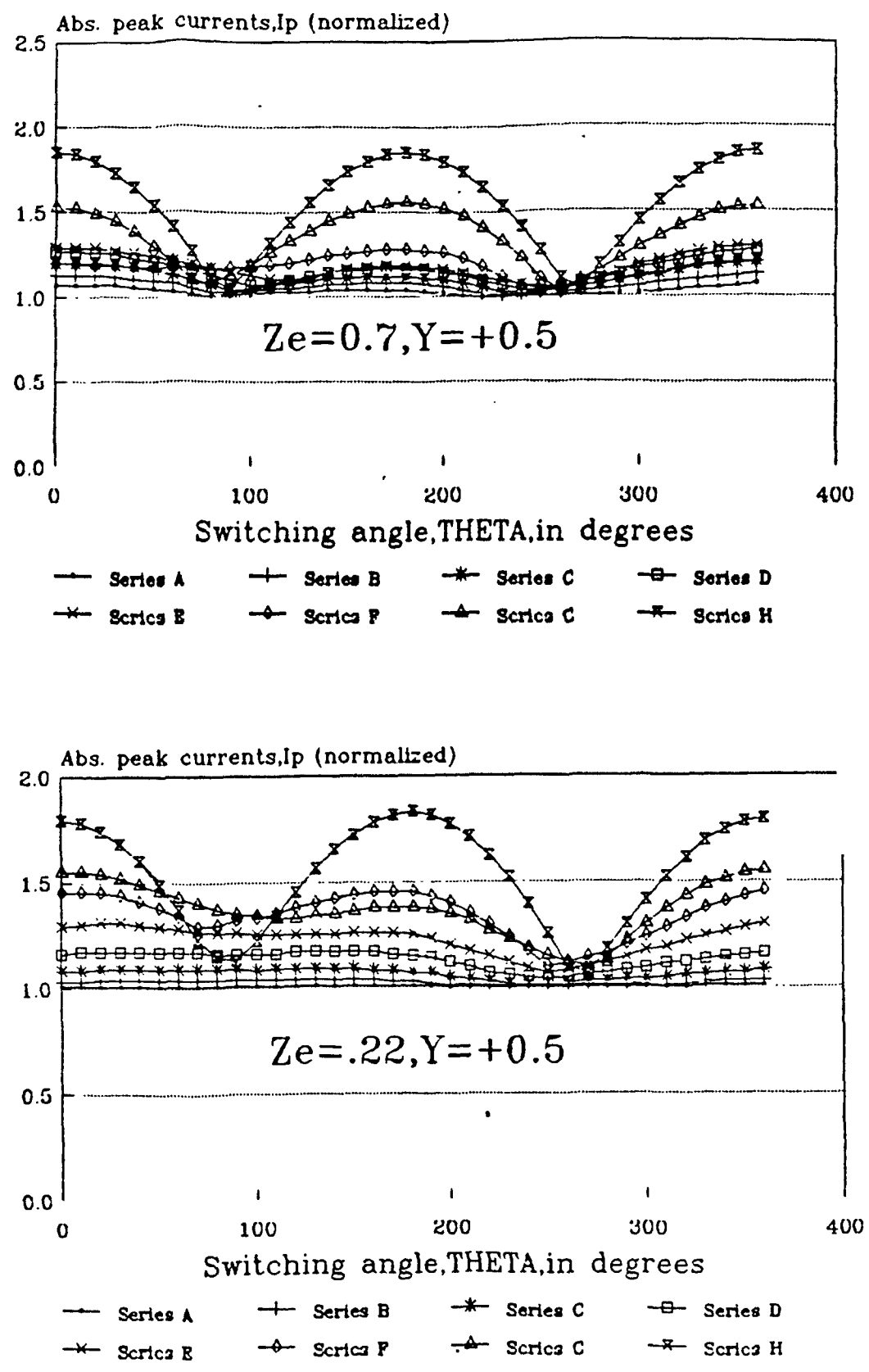

Fig. 2.9. Ip for under-damped circuits for different Y.

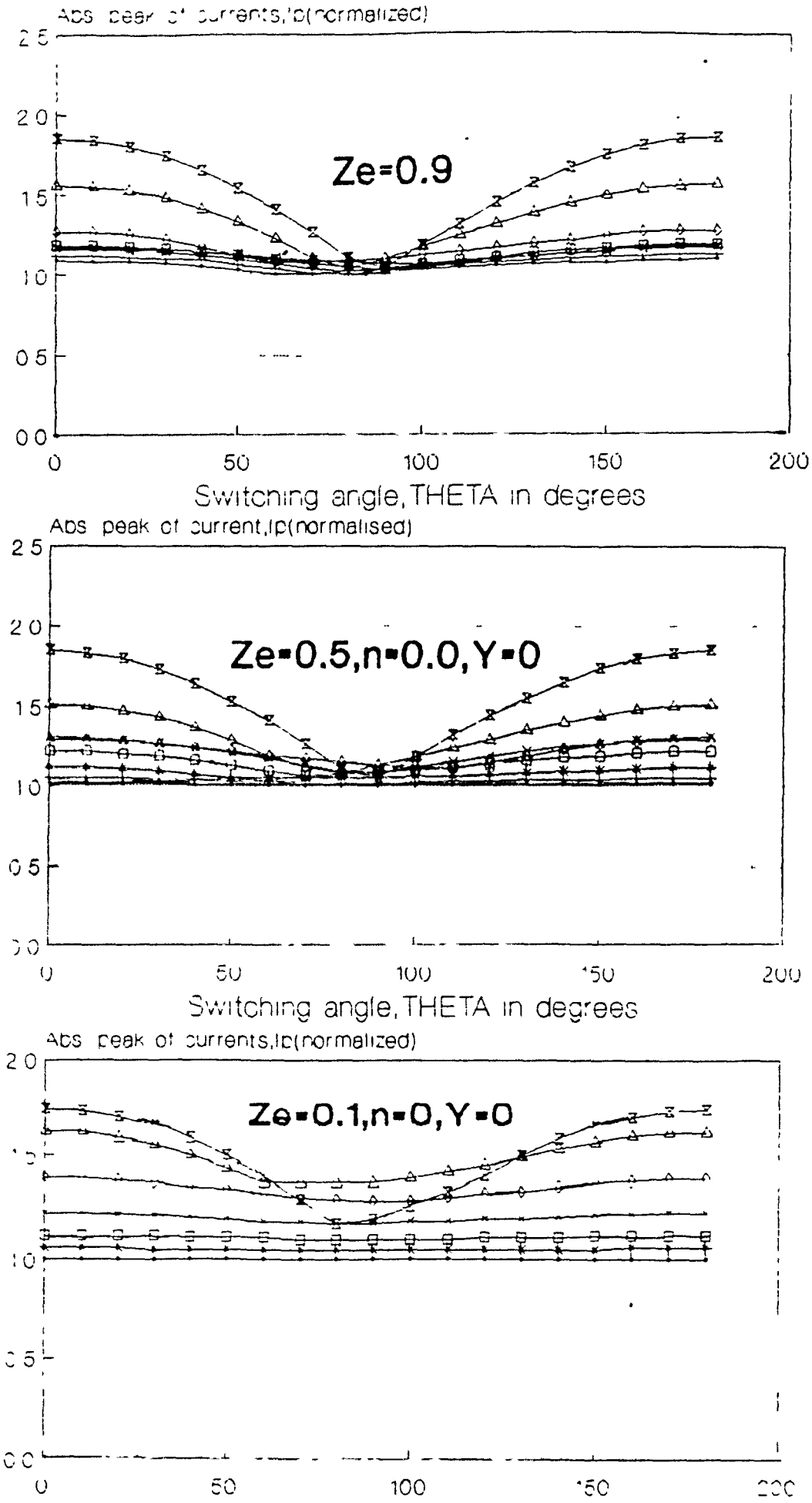

Fig. 2.10. Effect of Ze on Ip(minimum).

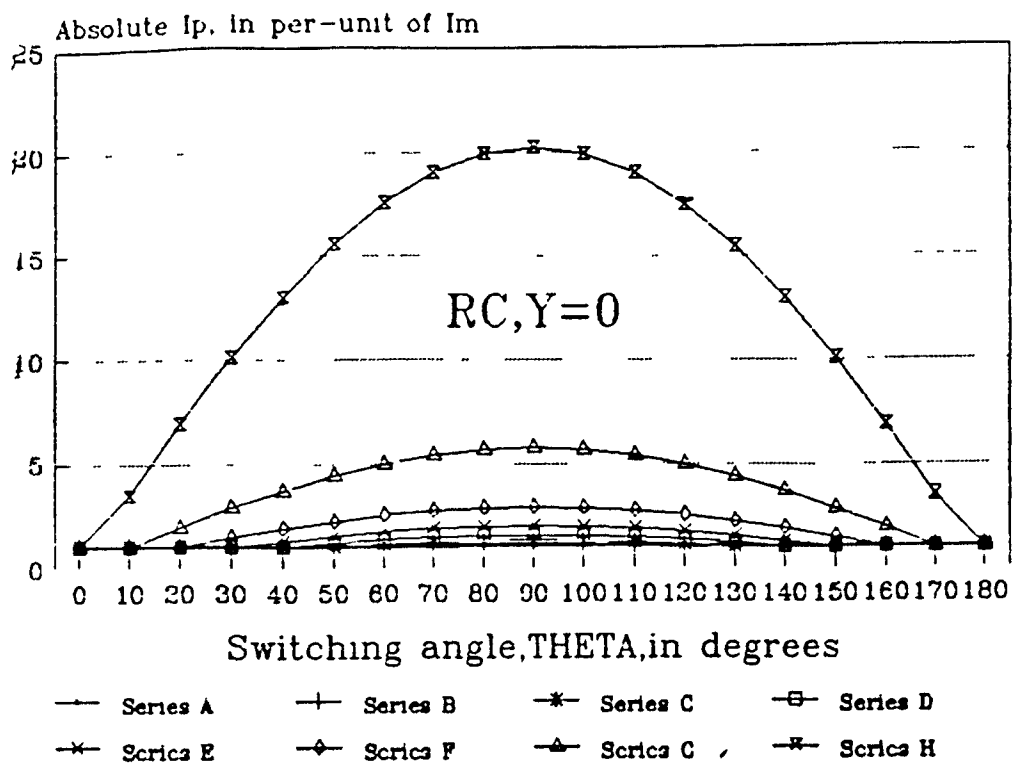

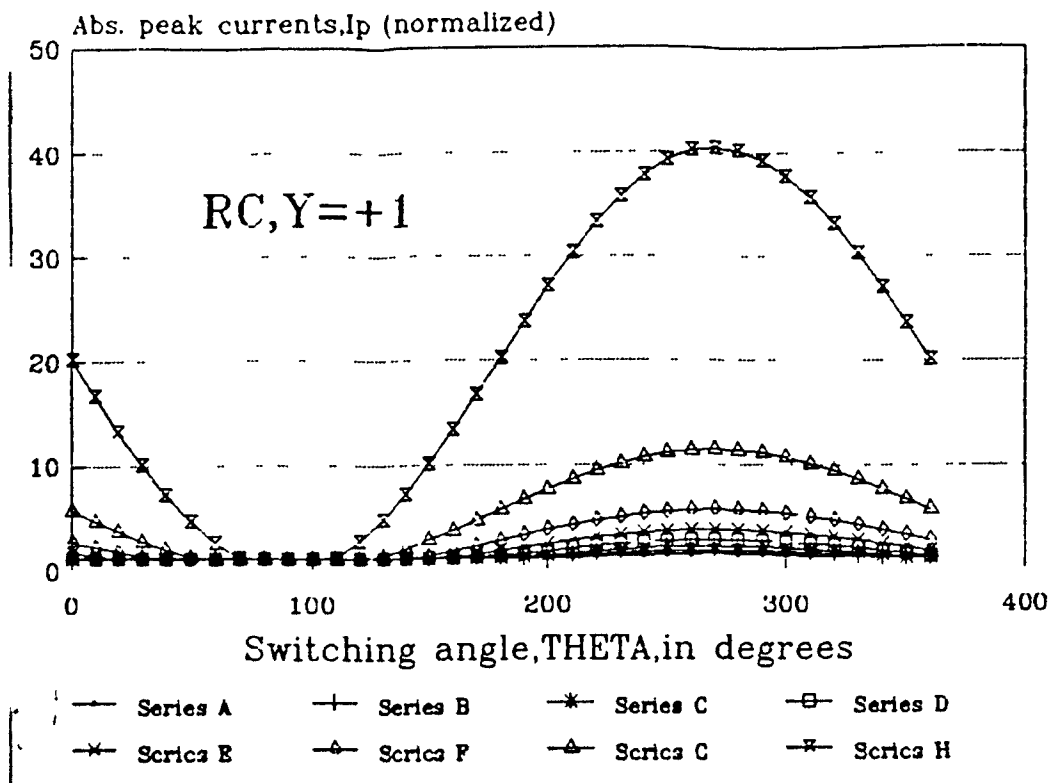

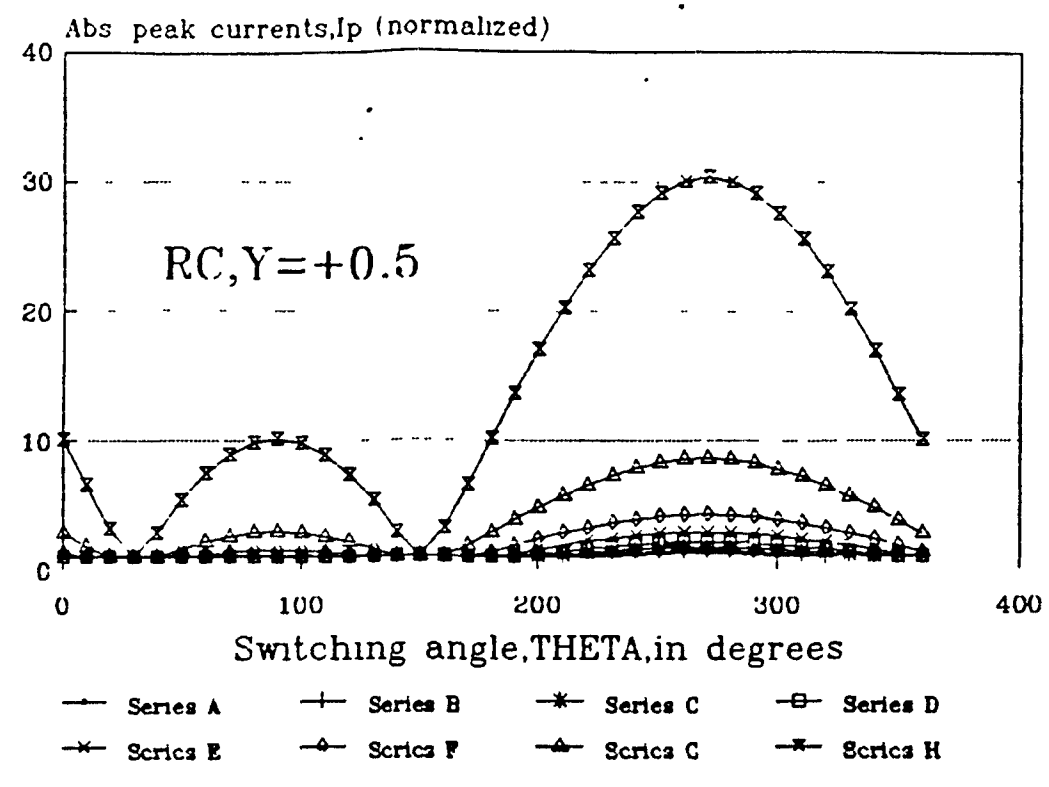

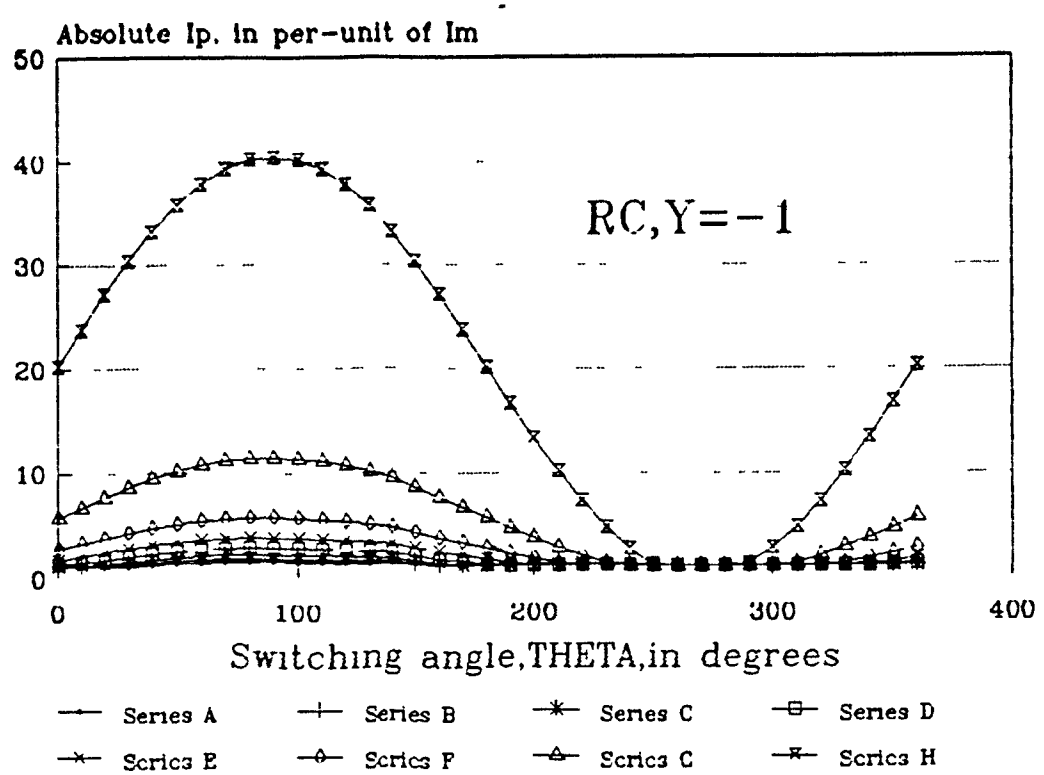

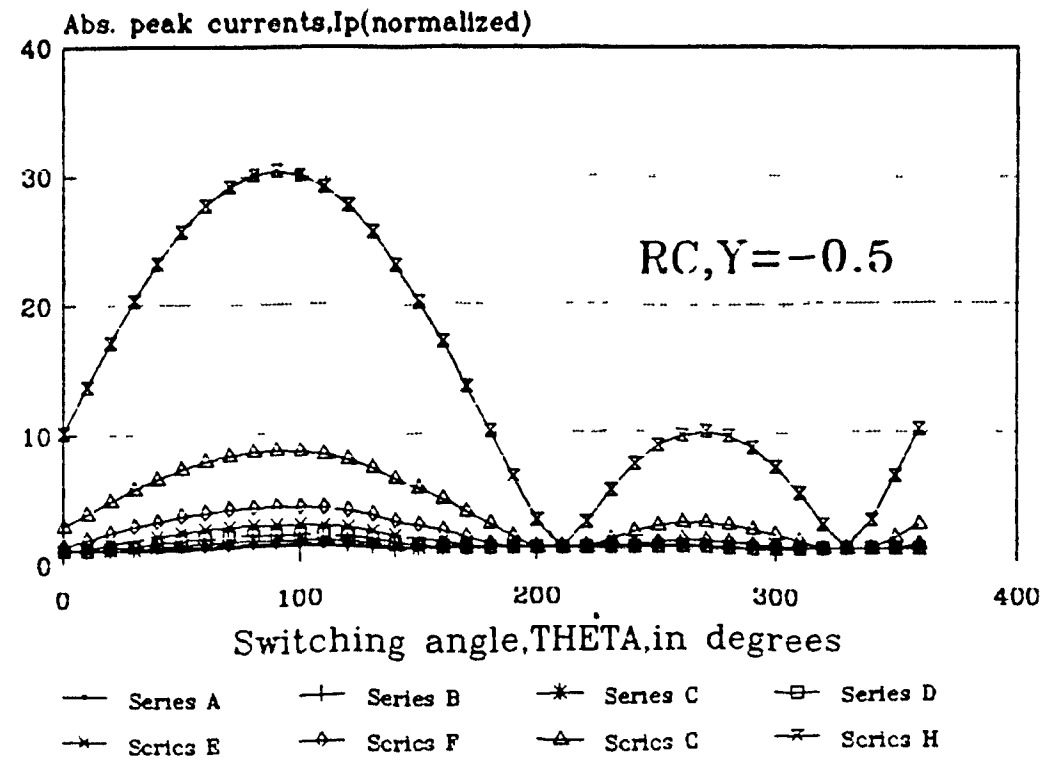

Fig. 2.11. Ip for RC circuits for different Y.

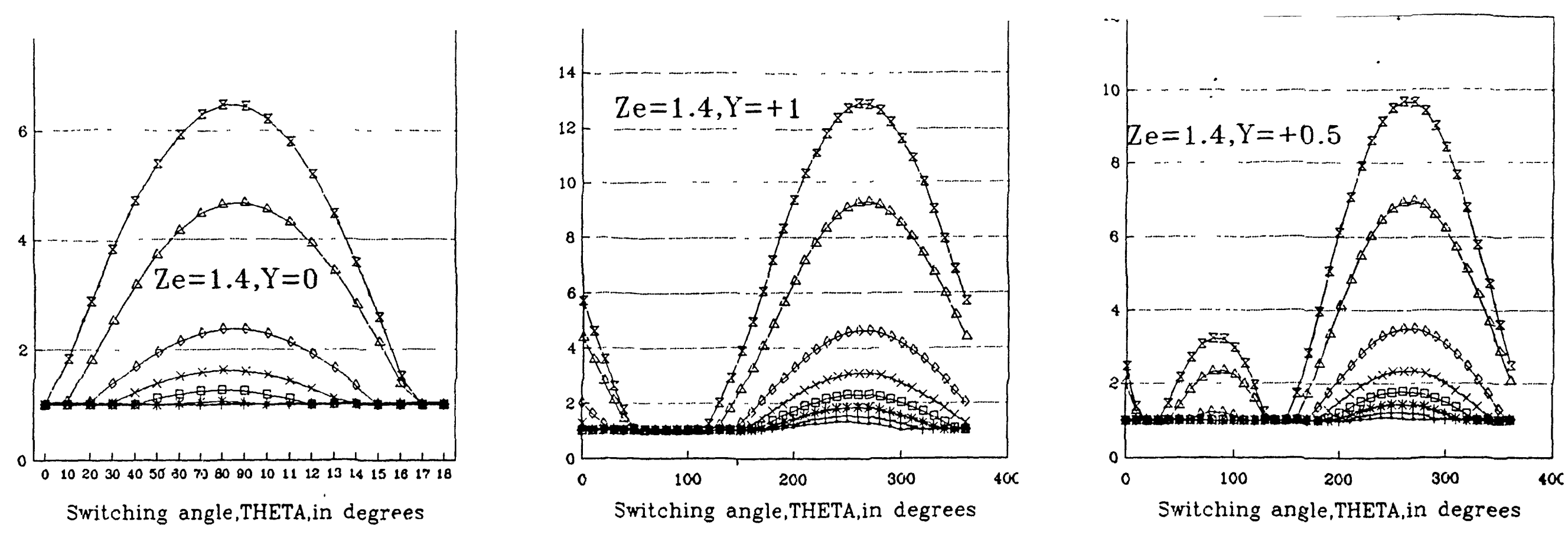

Fig. 2.12. Ip for over-damped (capacitive) circuits for different Y.

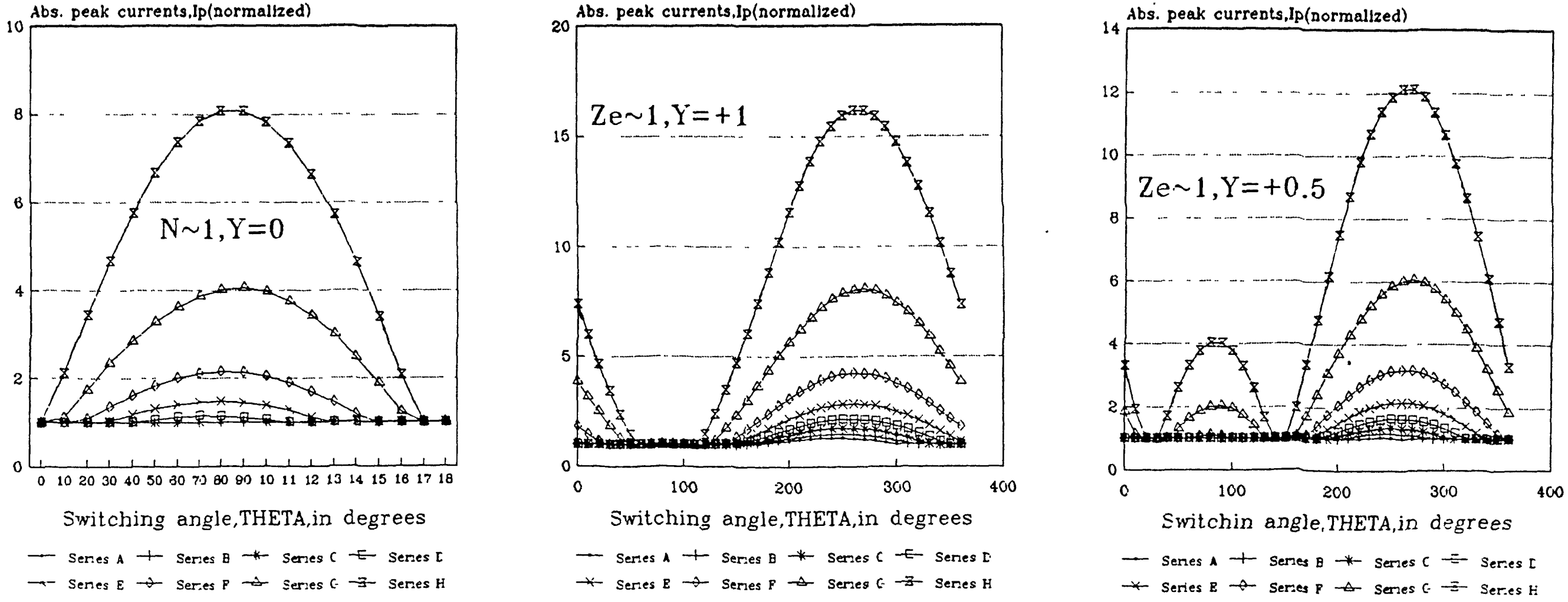

Fig. 2.13. Ip for critically-damped circuits for different Y.

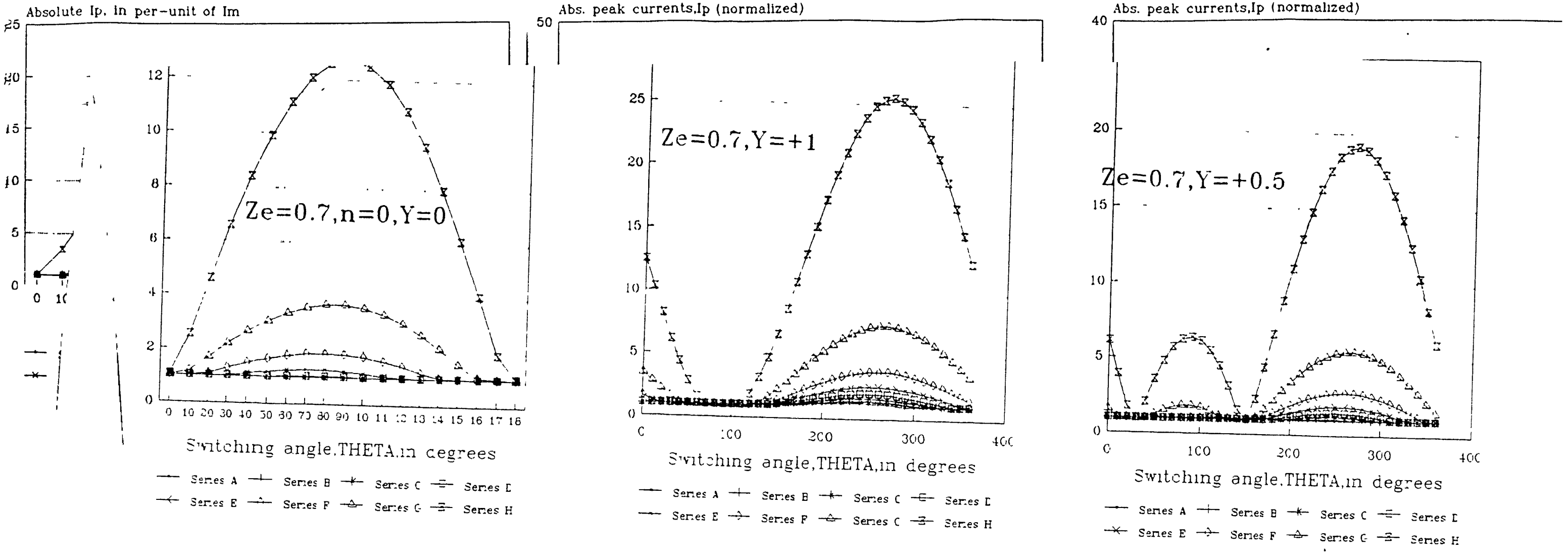

Fig. 2.14. Ip for under-damped circuits for different Y.

10°.

For the U/D circuits, Ip is calculated for Ze=0.1 to 0.9 in terms of θ, with and without stored charge on capacitor. Figure 2.14 shows the variation of Ip with θ for Ze=0.7. The condition found for the minimum and maximum transient is same as in RC circuit. In case of U/D circuits, it is found that Ip varies significantly for different values of Ze. Figures 2.15 and 2.16 show the variation of Ip for different Ze and ø.

2.3.3 Analysis of circuits with Qo and Io

For the sake of simplicity and to avoid involvement of source impedance in the calculation, a circuit configuration as shown in Fig. 2.2 is considered. Let at t=0, switch "S" be moved from A to B position. Now the current response is analyzed for various circuits. Calculation is done for various values of Ze, n, Y and ø given below:

Ze = 1.4, 1.0001(C/D), 0.7, 0.2

n = ±1.0, ±0.75, ±0.5, ±0.25, 0

Y = ±1.0, ±0.75, ±0.5, ±0.25, 0

ø = ±20°, ±30°, ±40°, ±50°, ±60°. ±70°, ±80°, ±87.13°

The effect of the initial circulating current is found significant only in case of inductive circuits. These are therefore being discussed here separately.

(a) Analysis of RL circuits:

As discussed previously θmax and θmin can be found by (i)

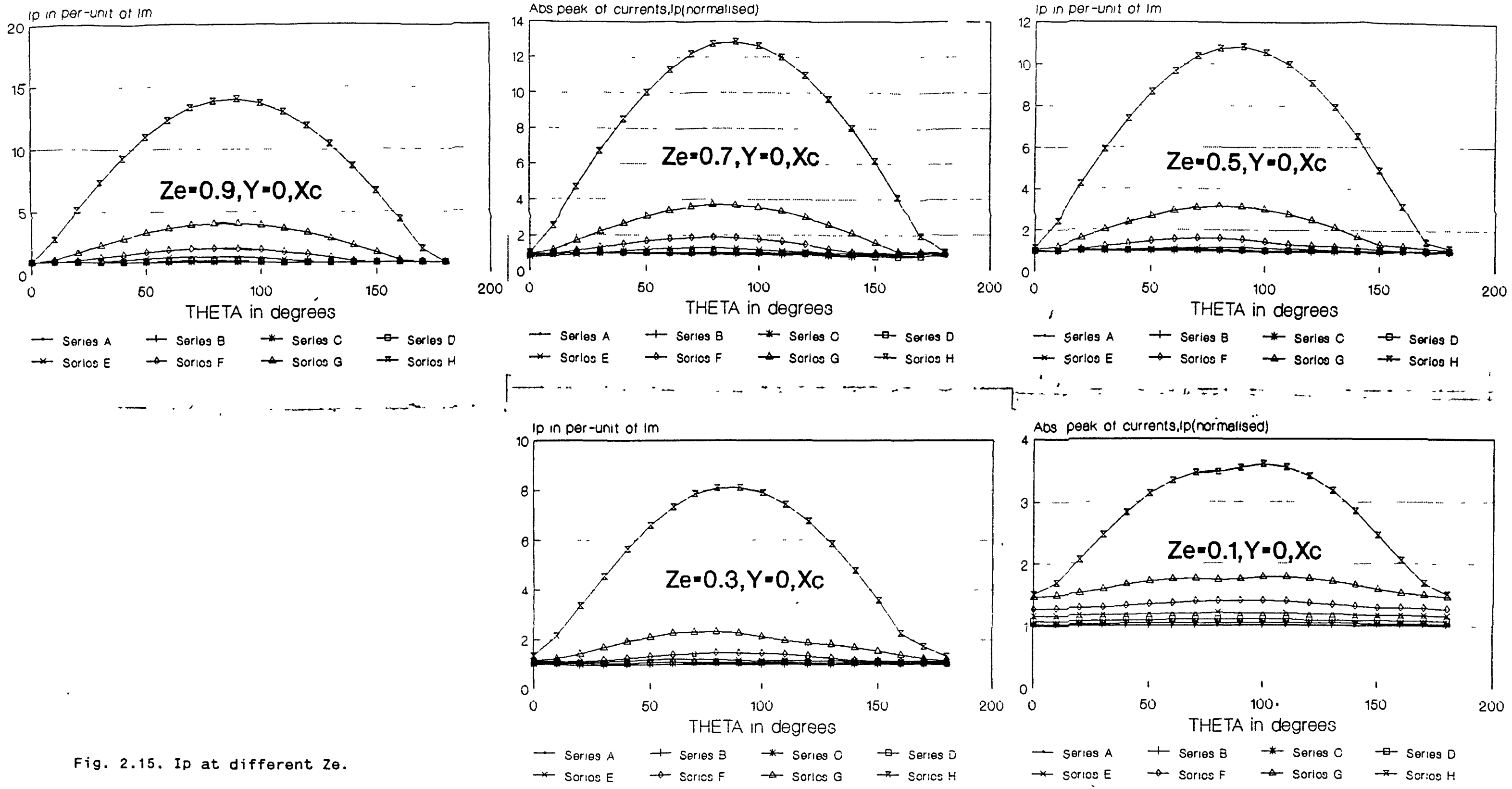

Fig. 2.15. Ip at different Ze.

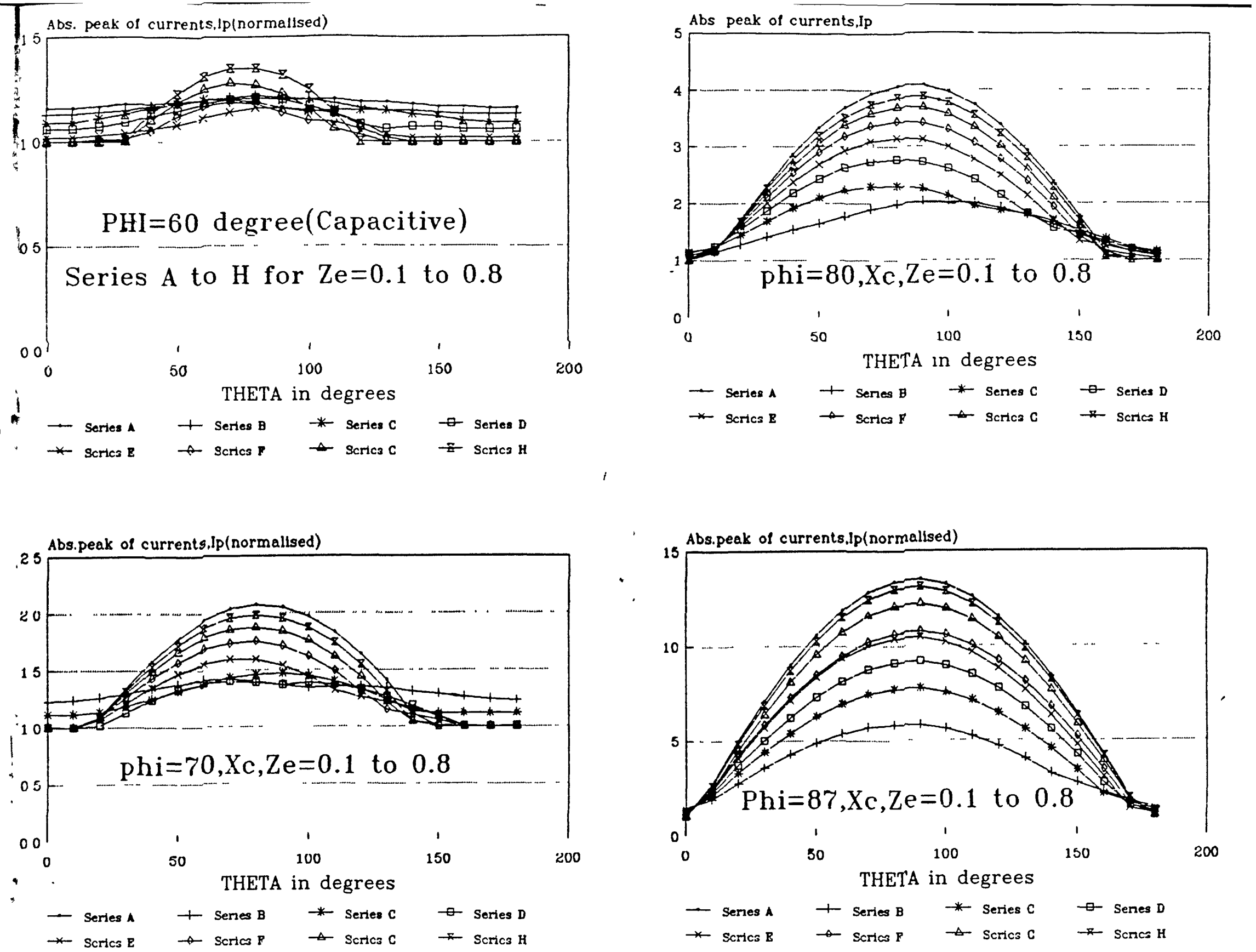

Fig. 2.16. Ip at different Ø.

optimization technique using transient term only or (ii) by direct calculation technique. Using the first technique the errors are calculated for each value of n (0.25 to 1.0) and the maximum error found is 11.5% for n= 1, if the equation 2.14 is adopted to find θmax. However, by using the second technique θmax may be taken, in most general form, without significant error, as

$$\begin{aligned} \theta max &= 0 && \text{for } n \geq 0 \\ &= \pi && \text{for } n \leq 0 \end{aligned} \qquad (2.38)$$

In this case the maximum error is found to be 5% for n= 1.

Ip depends simultaneously upon the steady-state as well as the transient term of (2.28). Fig. 2.17 shows the variation of Ip in RL circuit with different values of n. The accurate condition for the maximum Ip is determined as

$$\begin{aligned} \theta max &= \{(\pi/2)-\phi\}n && \text{for } n \geq 0 \\ &= \pi+\{(\pi/2)-\phi\}n && \text{for } n \leq 0 \end{aligned} \qquad (2.39)$$

(b) Analysis of inductive RLC circuits:

Different graphs for Ip, showing the effect of Ze, n and Y, for different ϕ are given here. Observations of the inductive circuits are given below

(i) θmin for minimum Ip is given by

$$\begin{aligned} \theta min &= \theta 1+\phi && \text{for } Y \leq 0 \\ &= \pi-\theta 1+\phi && \text{for } Y \geq 0 \end{aligned} \qquad (2.40)$$

where $\theta 1=\sin^{-1}(n)$ and is related to the value of sine function in the first or fourth quadrant depending upon the sign of n.

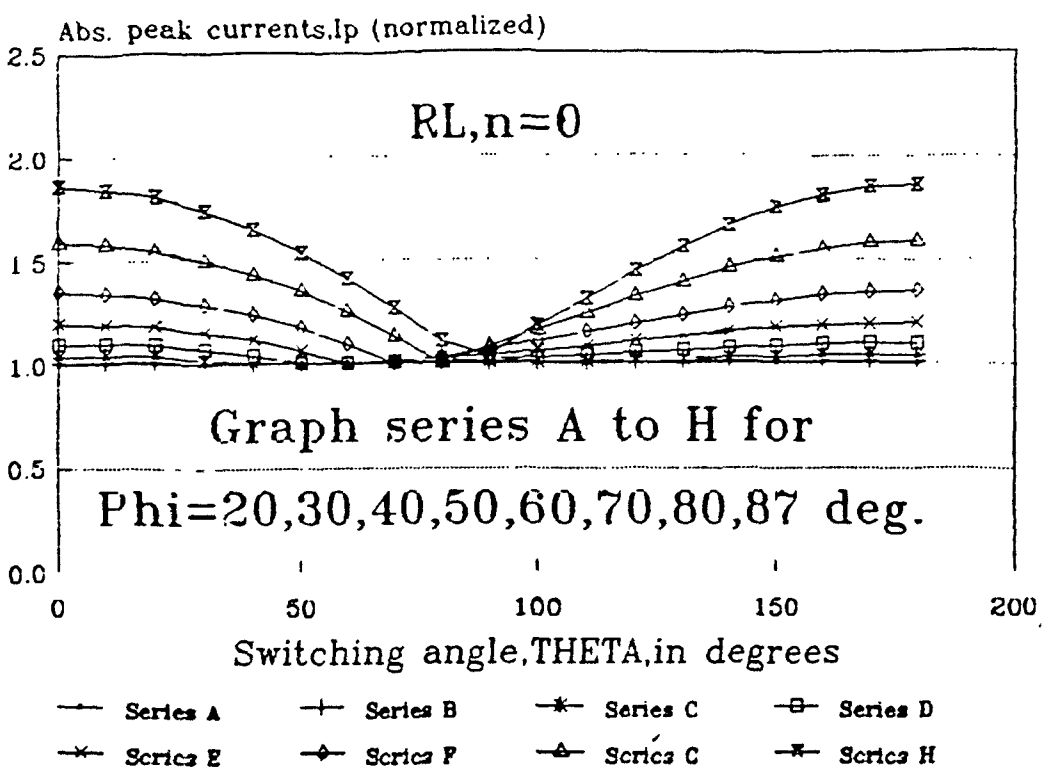

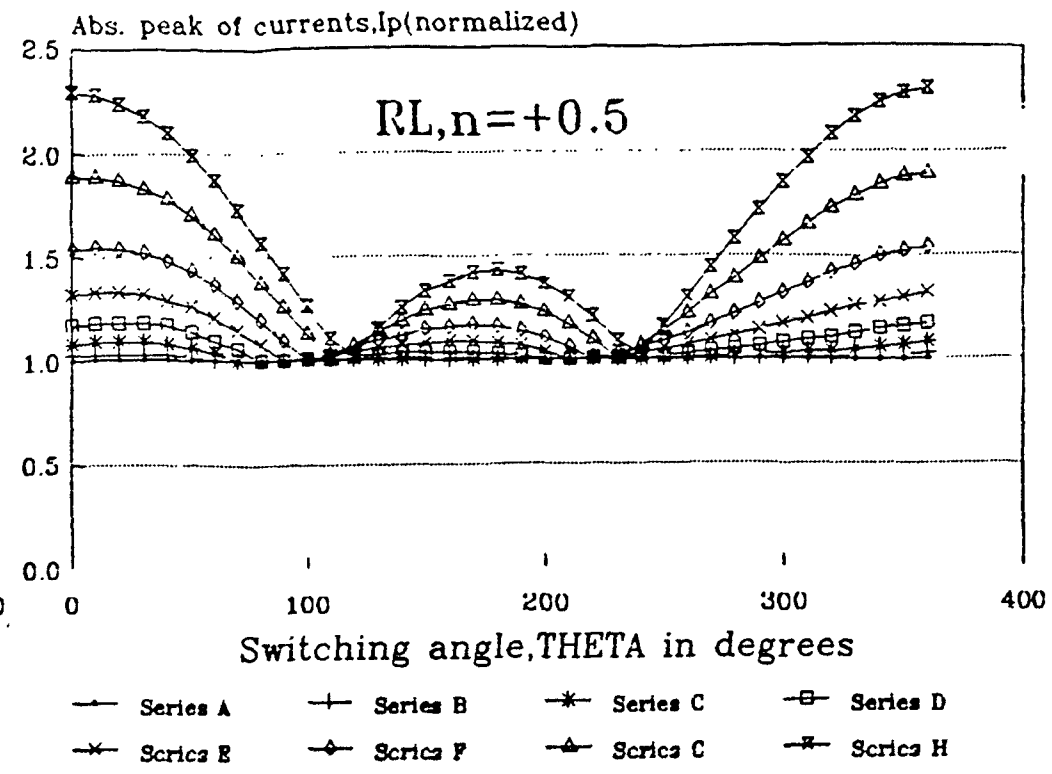

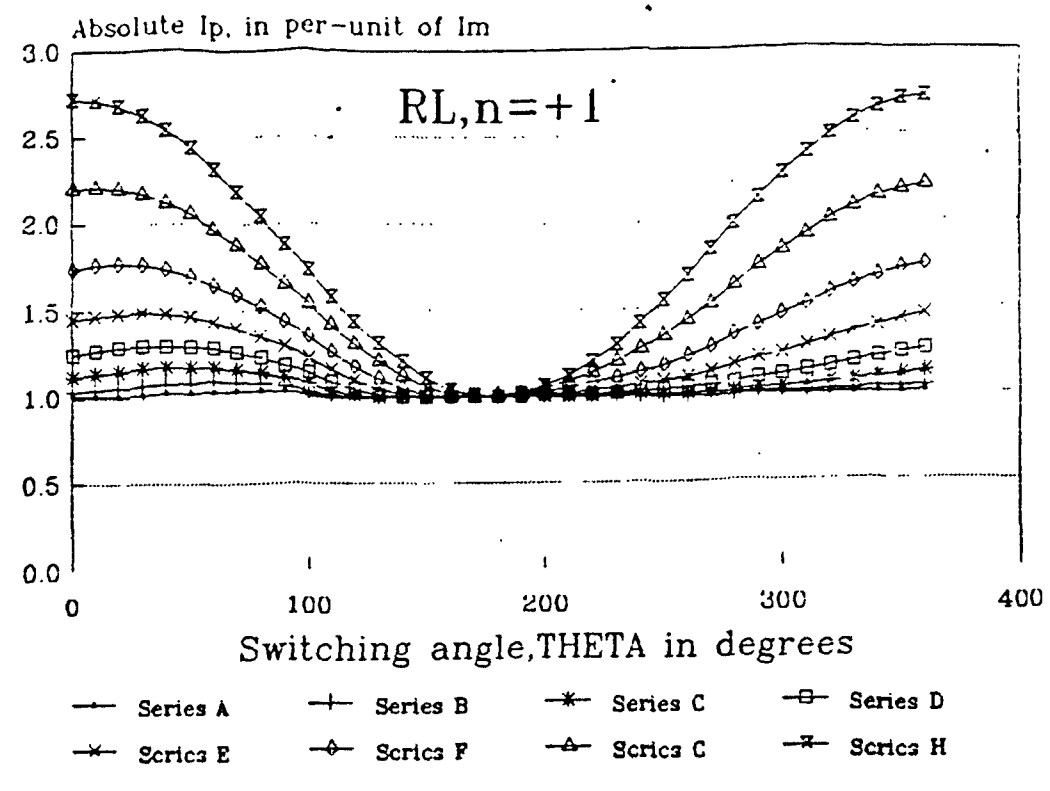

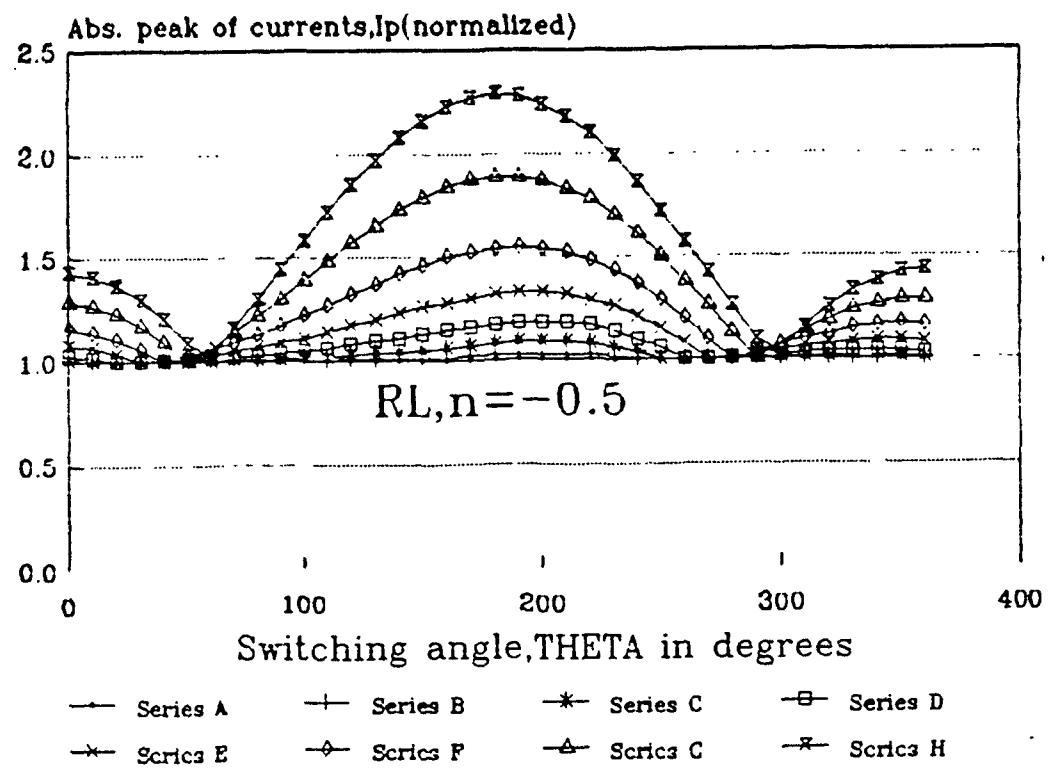

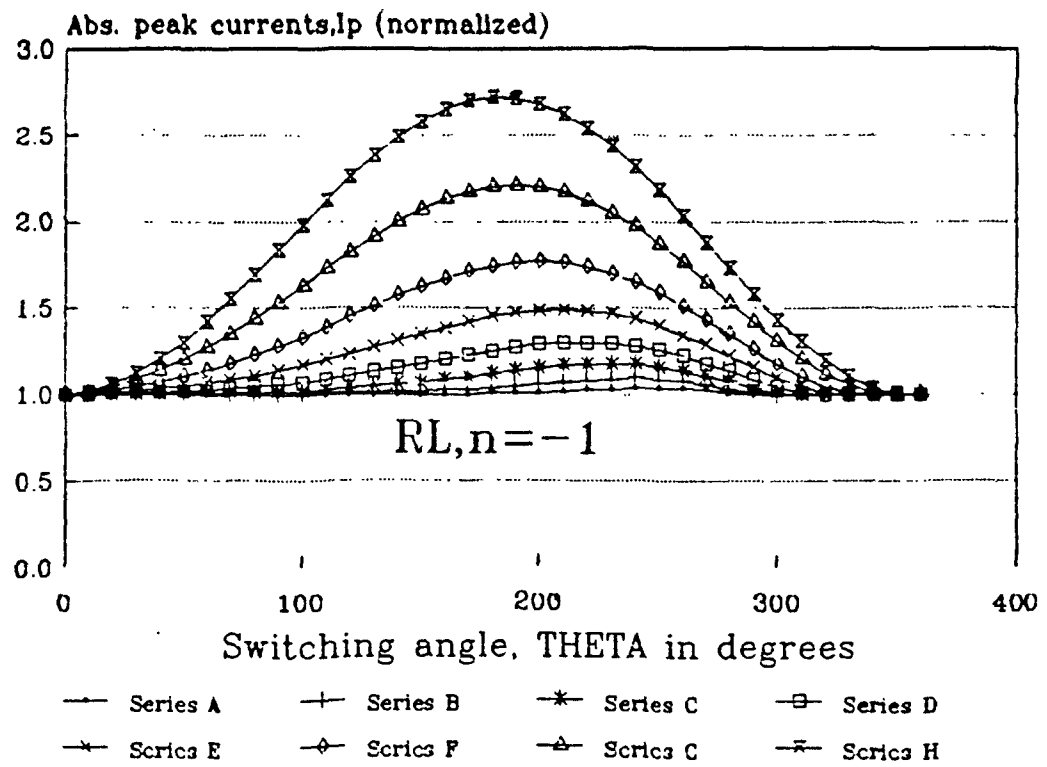

Fig. 2.17. Ip for RL circuit for different n.

(ii) For a particular value of n and Y (say $n1$ and Y1) the variation of Ip is found same as in case of $-n1$,-Y1 except that the graph is shifted by 180°. Thus θmin and θmax also shift by 180°. This is evident from Fig. 2.18 and 2.19 for O/D and U/D circuits respectively.

(iii) In general, θmax depends upon "n" and is independent of "Y".

(iv) Considerable error is found in the value of θmin for the lower values of ϕ. However, the magnitude of transient current, hence the difference of Ip and Im for such cases, are not significant.

(v) θmax occurs at 0° and 180° for all the values of $n \geq 0$ and $n \leq 0$ respectively.

(vi) the effect of Ze does not play any role in deciding the values of θmin and θmax. However for the lower values of Ze (in U/D circuits), at θmin the transient, although small, doesn't vanish completely, which is evident from Fig. 2.20 (as in case of Io=0).

(c) Analysis of capacitive RLC circuits:

General observations with such circuits are given below:

(i) The magnitude and variation of Ip with respect to θ is independent of n (Fig. 2.21).

(ii) Variation pattern of Ip with respect to θ depends upon Y (Fig. 2.22).

(iii) The maximum magnitude of Ip depends upon Ze as in case of n=0. Which is evident from Fig. 2.22.

(iv) θmin and θmax is same as in the RC circuit.

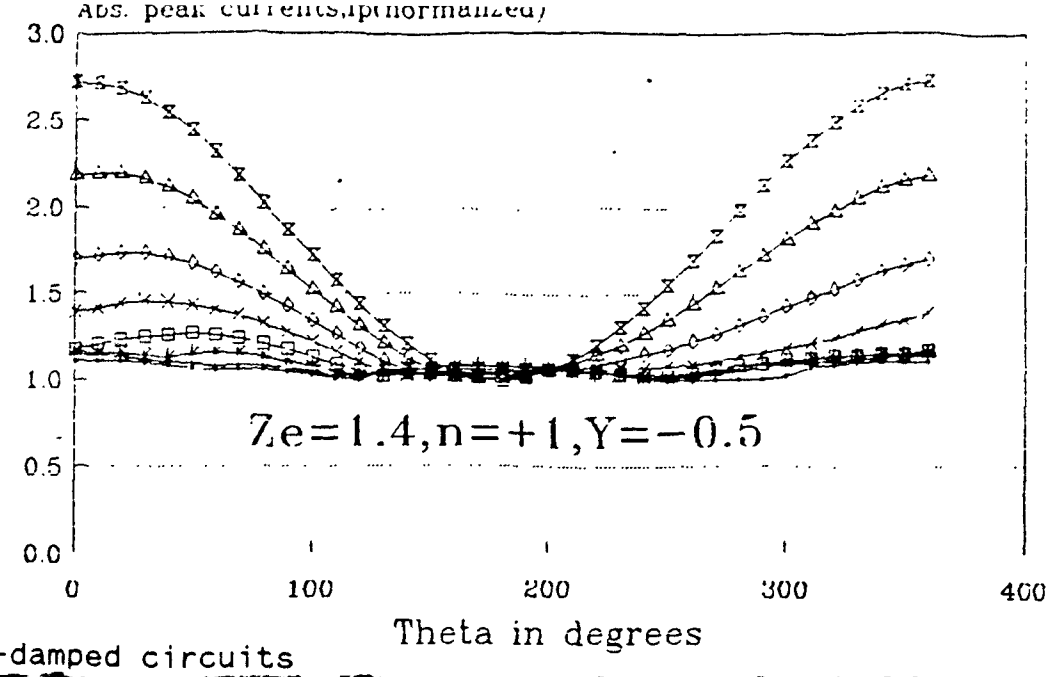

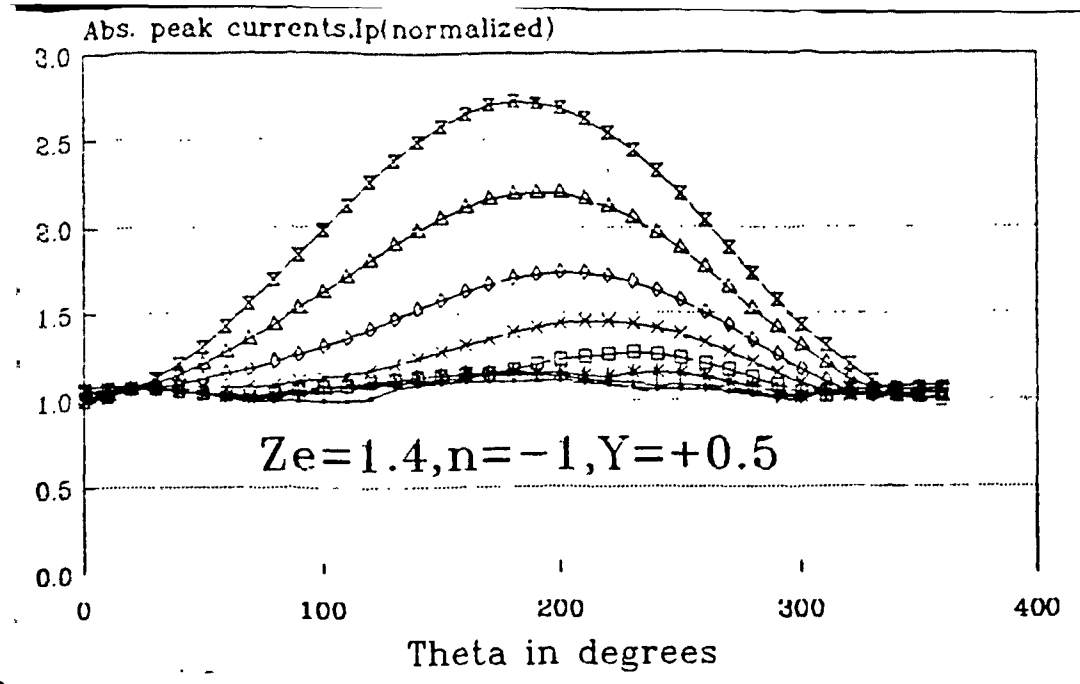

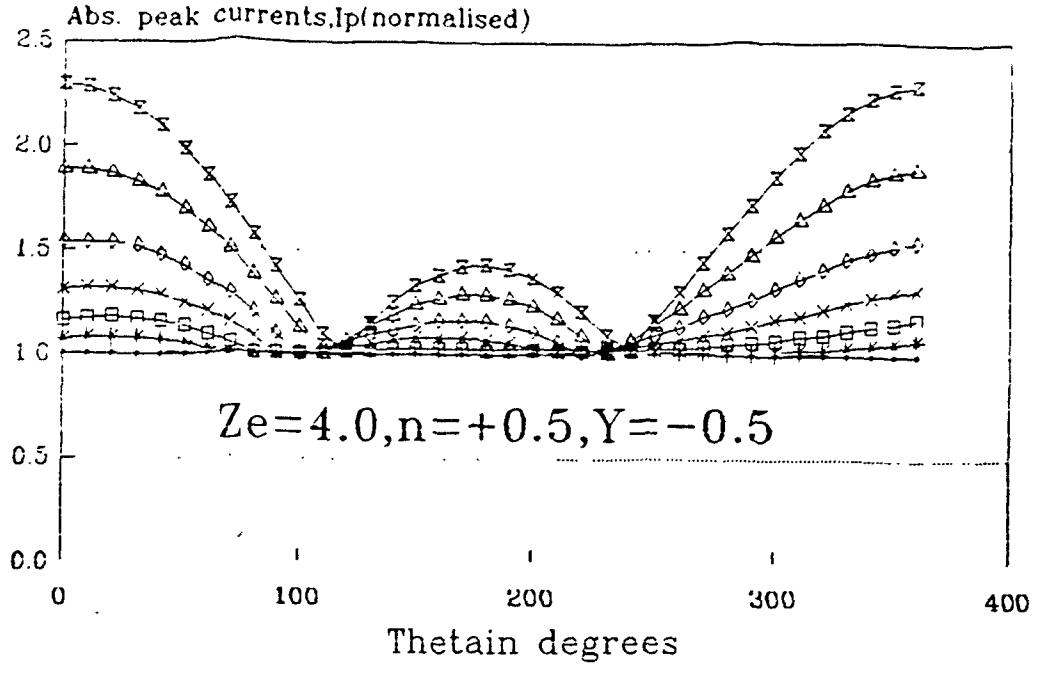

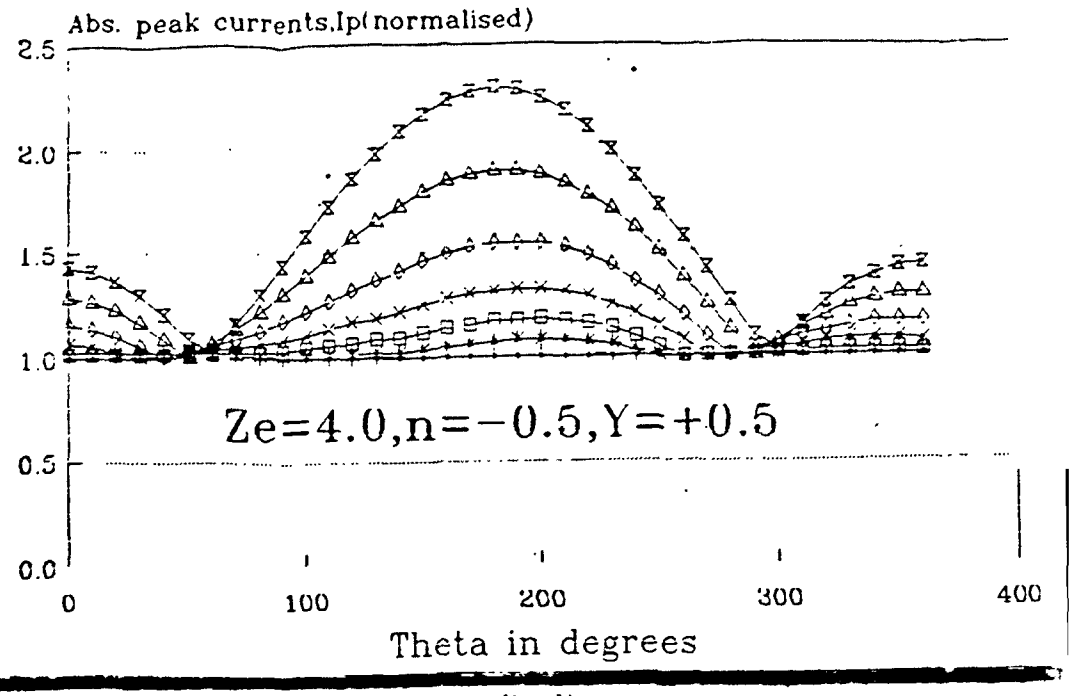

Fig. 2.18. Ip for over-damped circuits

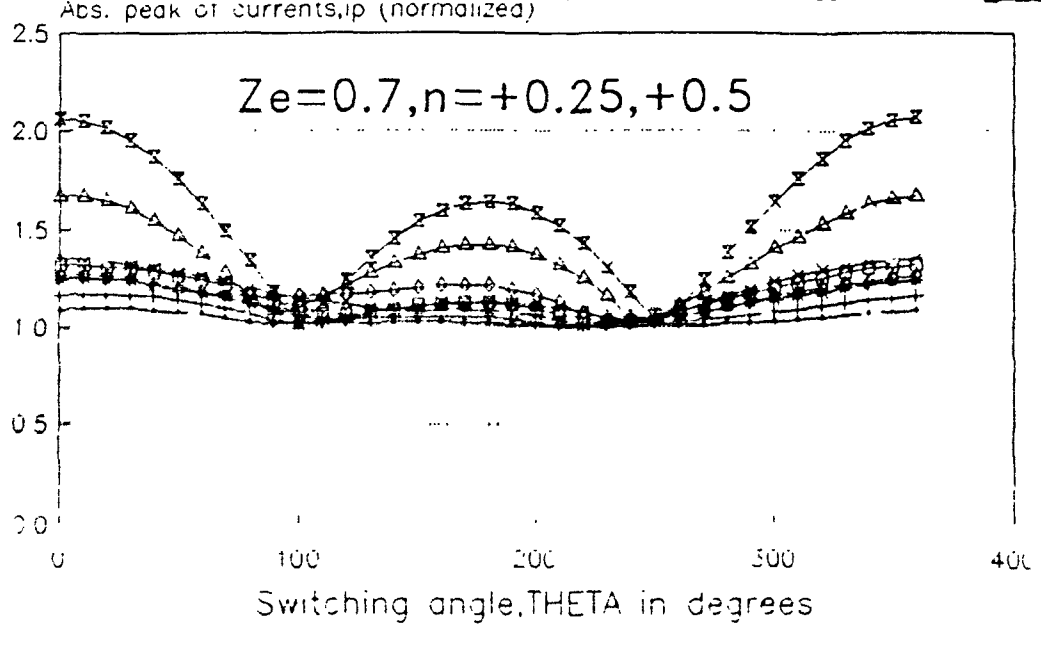

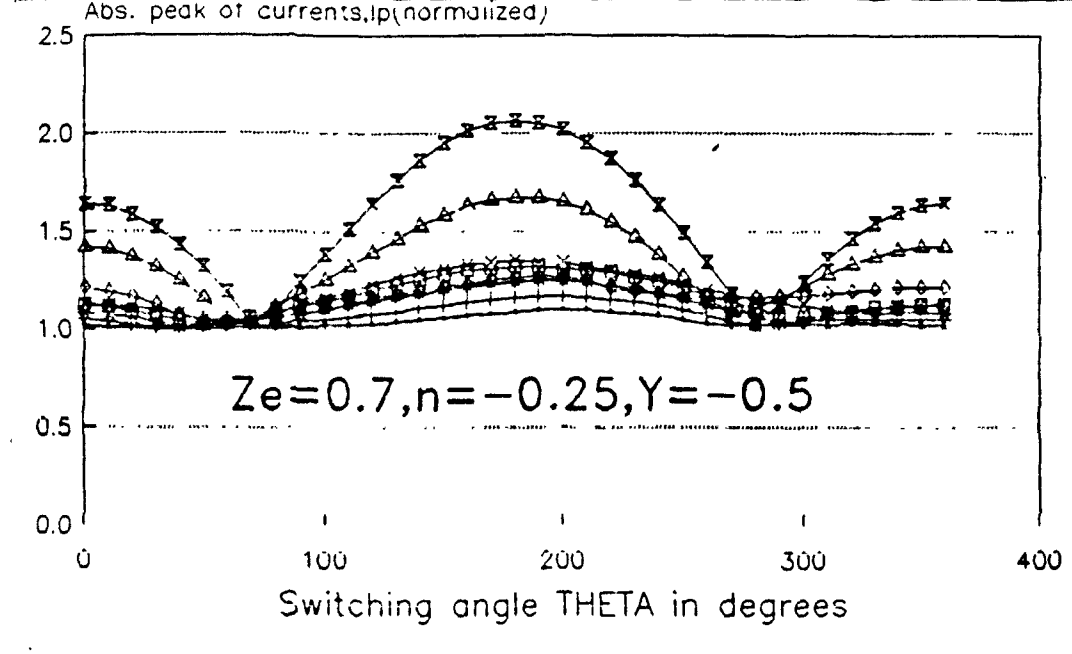

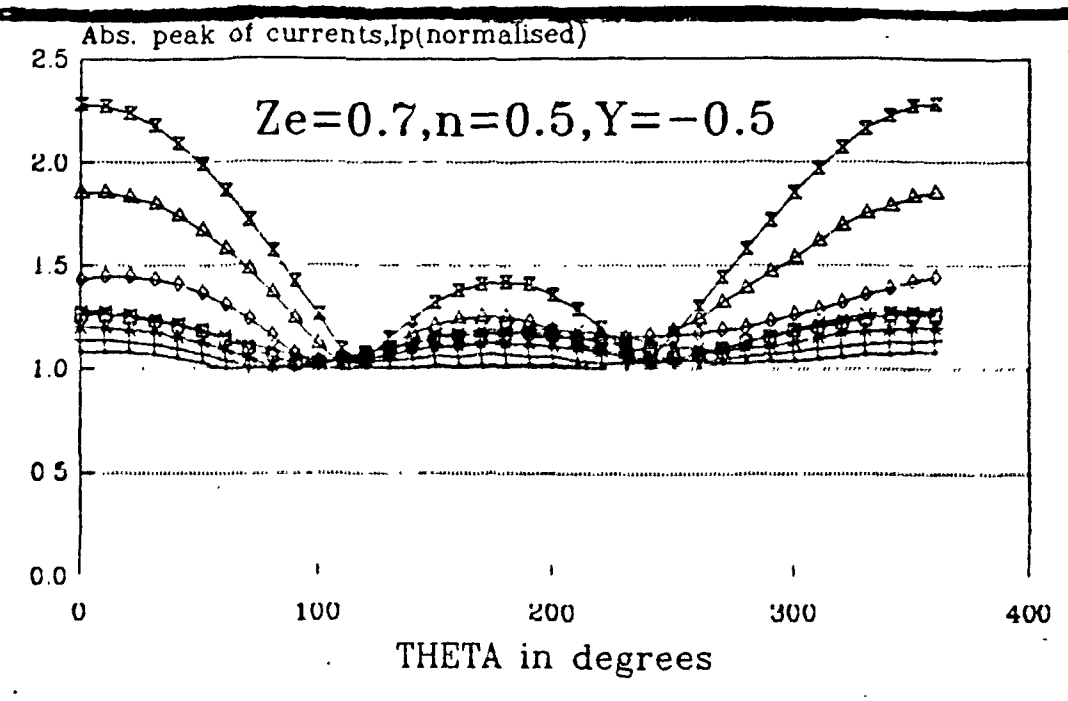

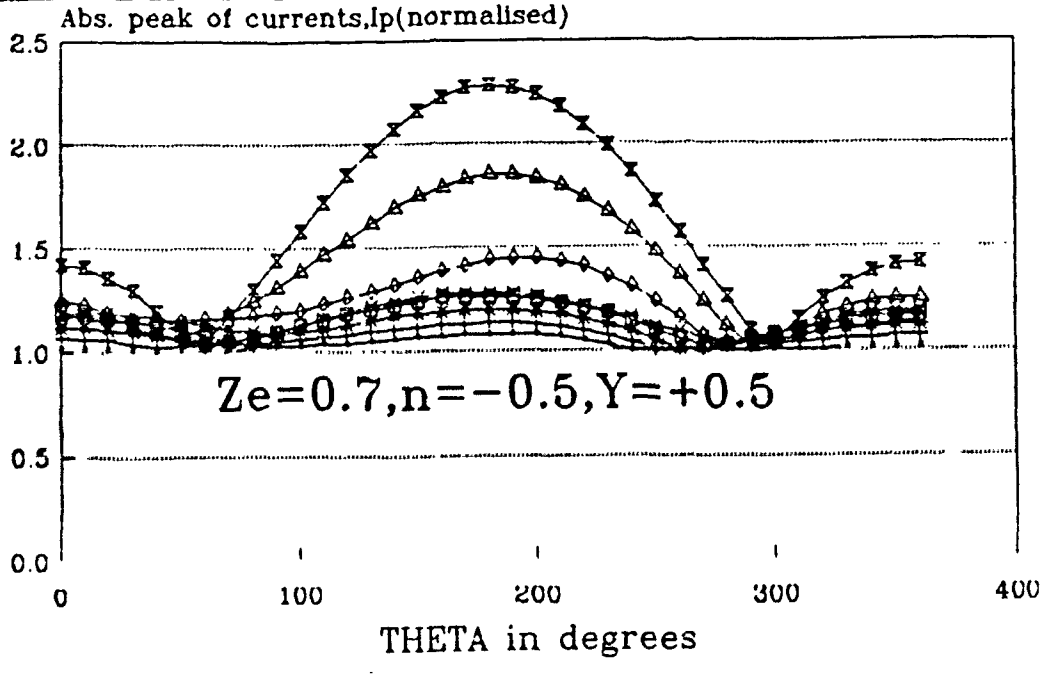

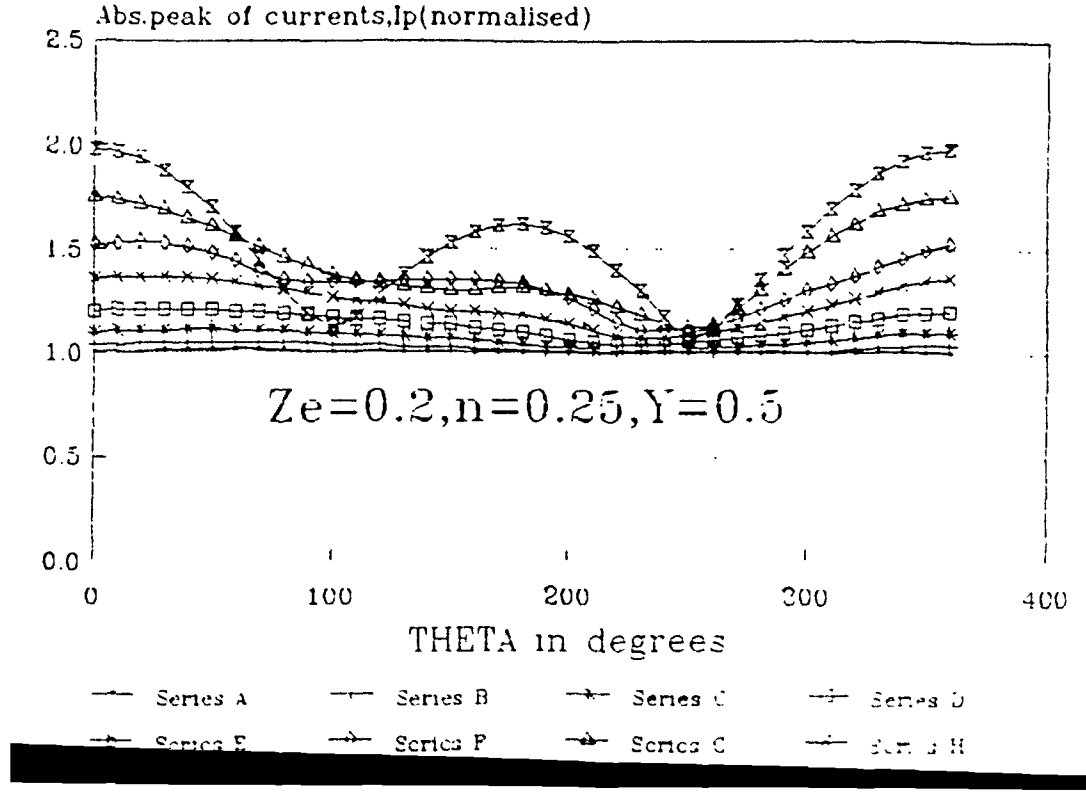

Fig. 2.19.

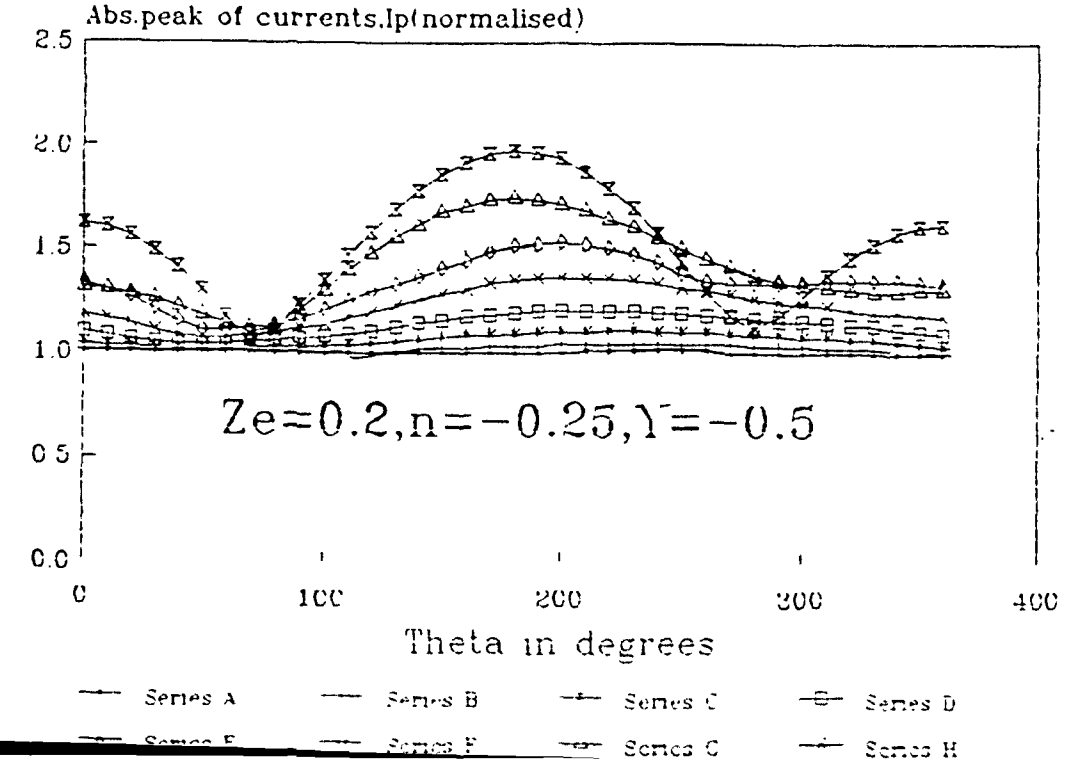

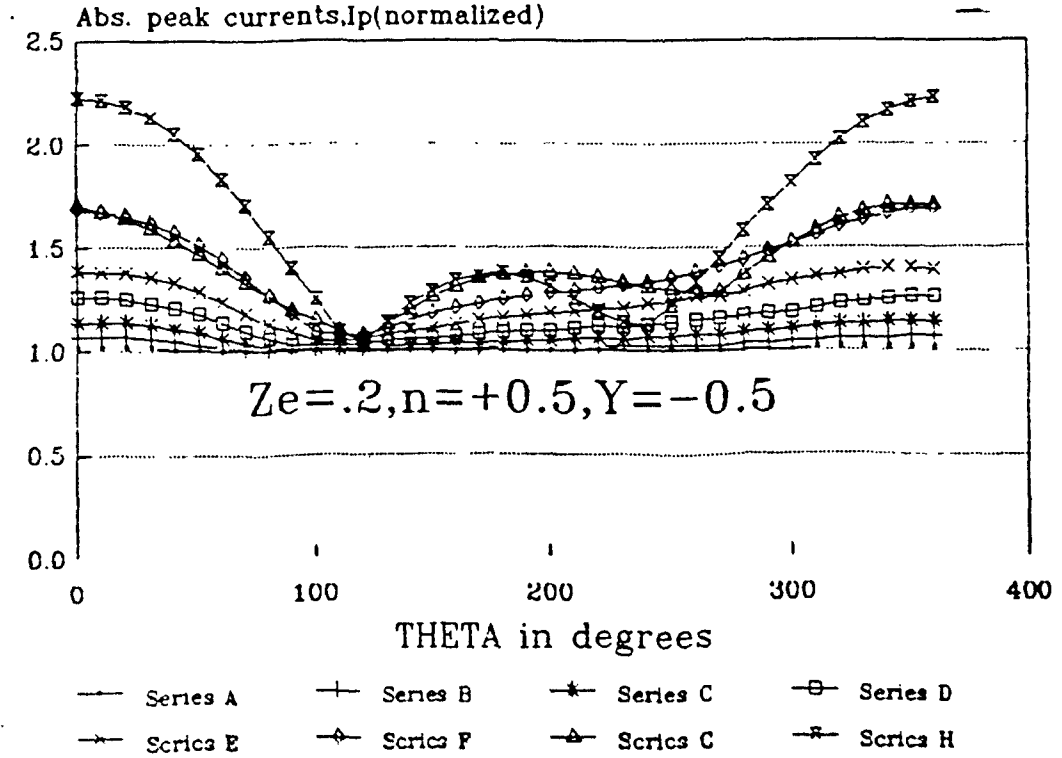

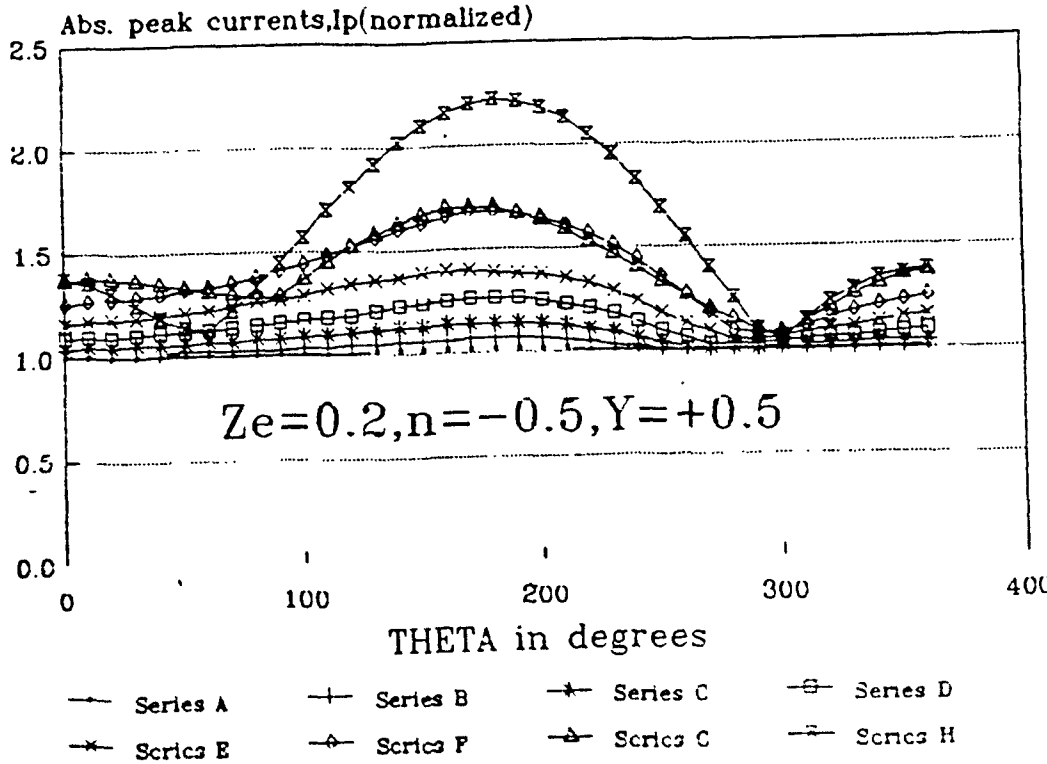

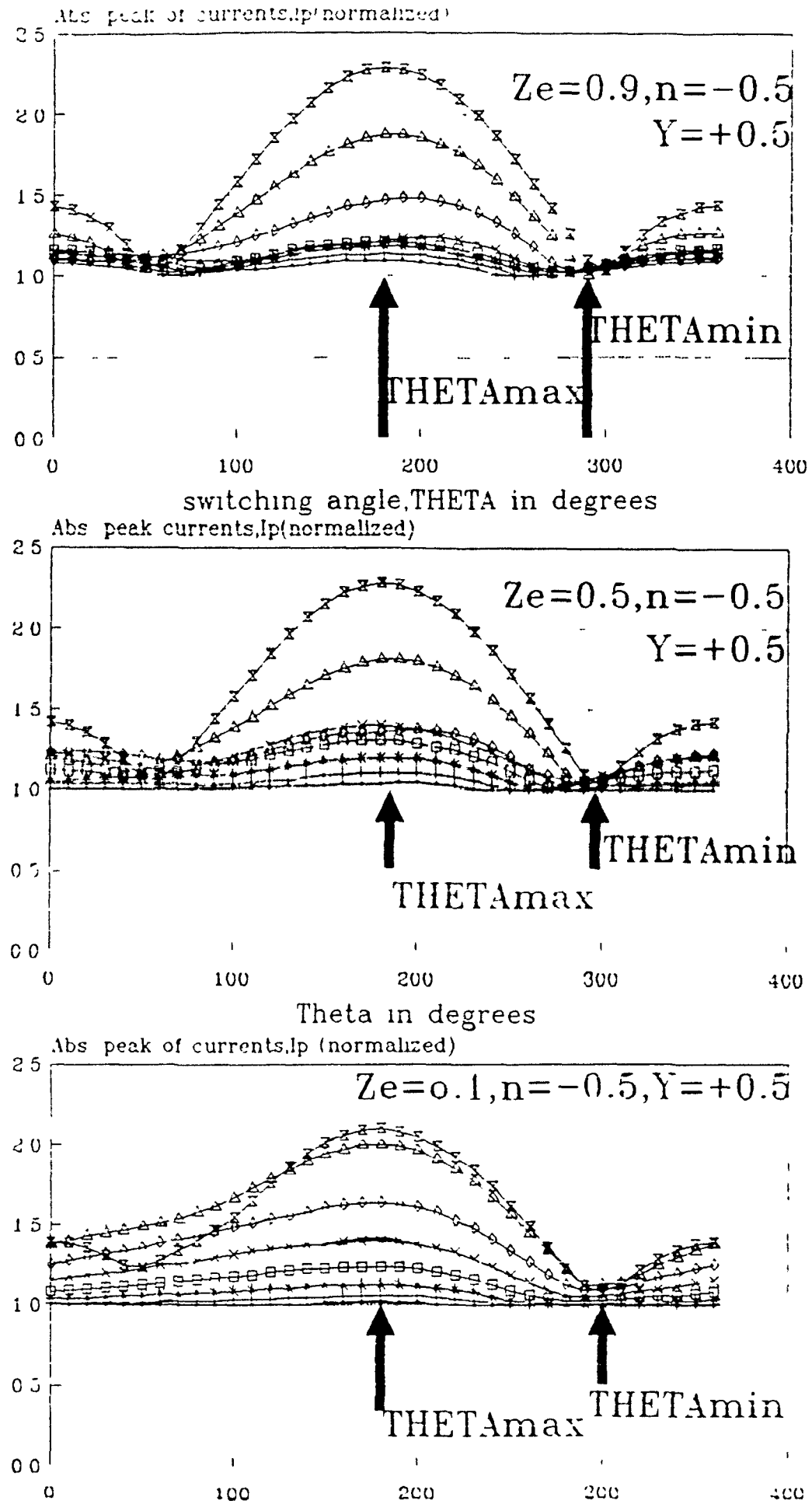

Fig. 2.20. θmax and θmin indeperdnt of Ze.

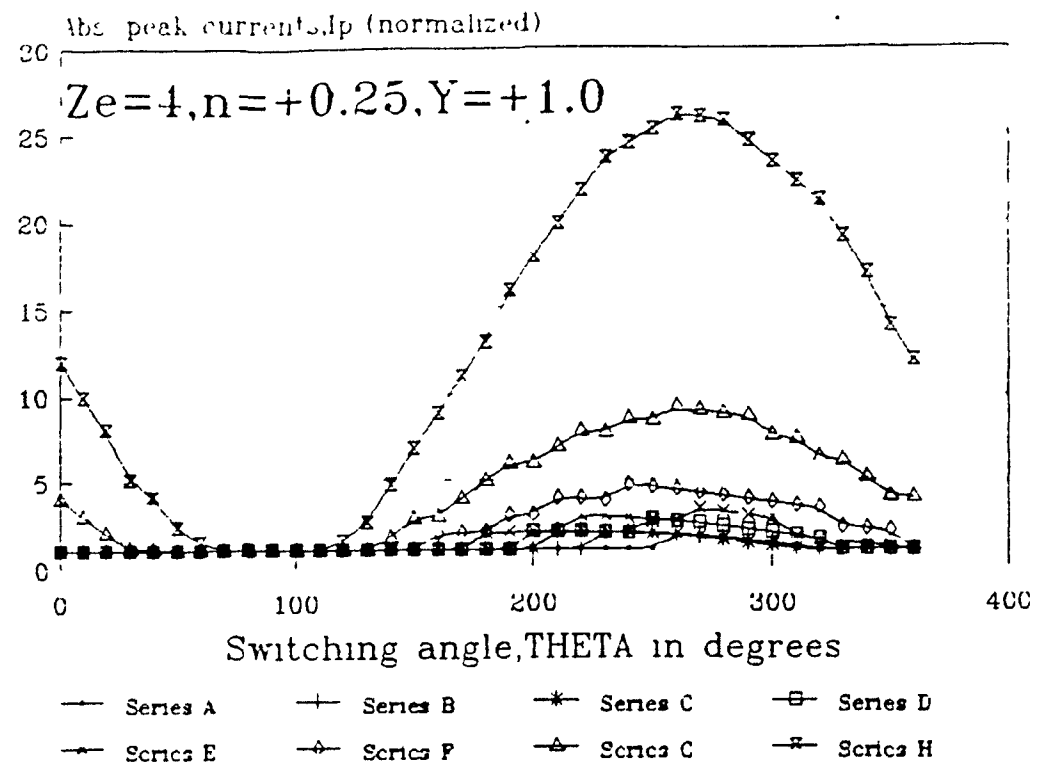

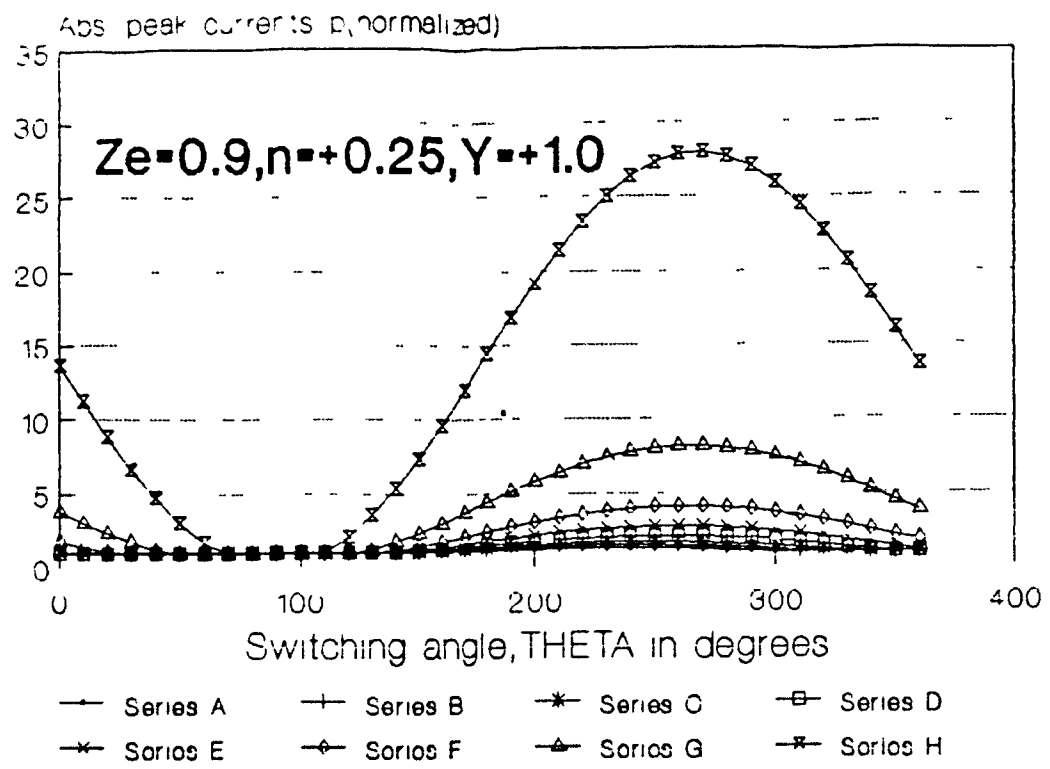

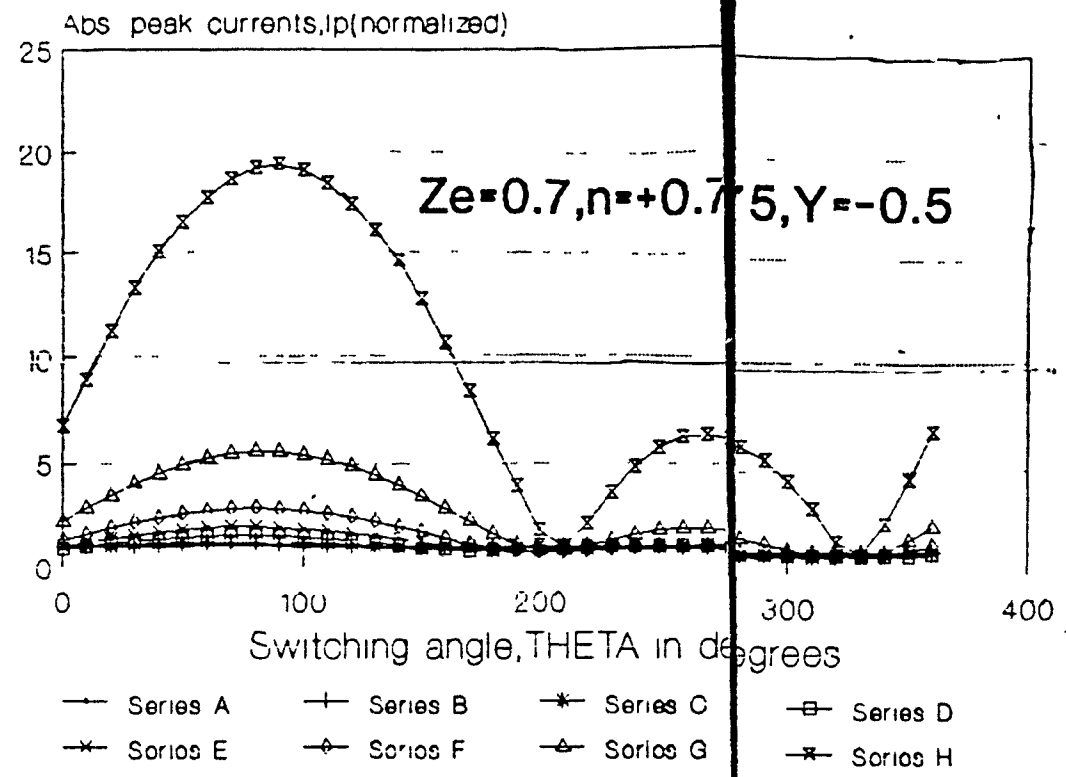

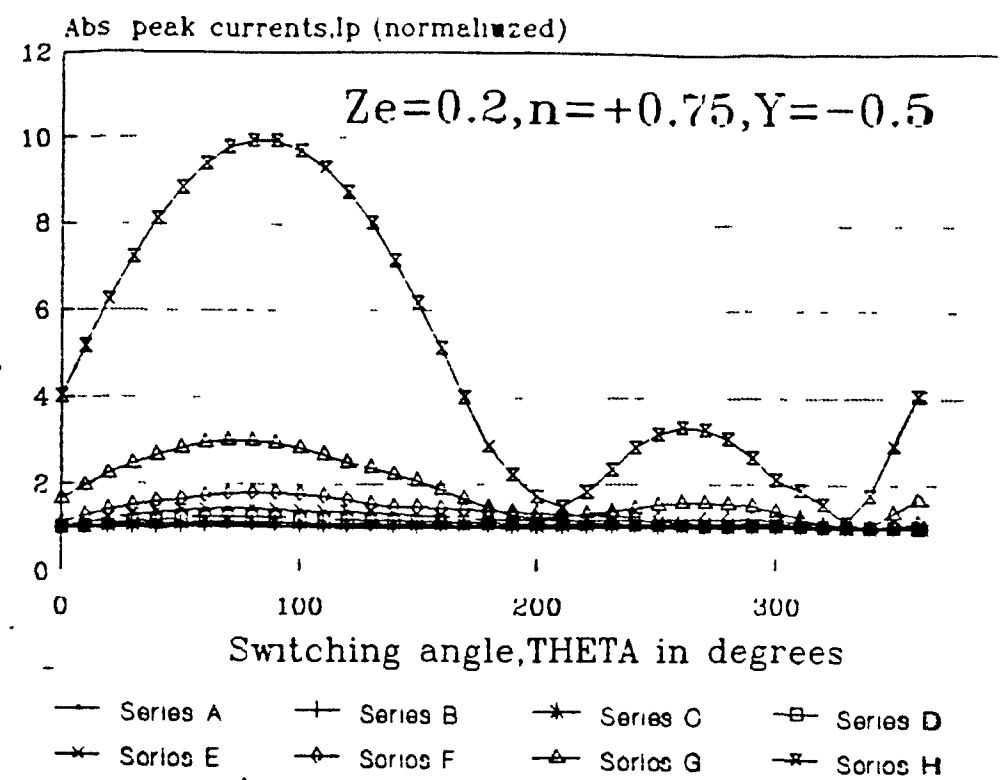

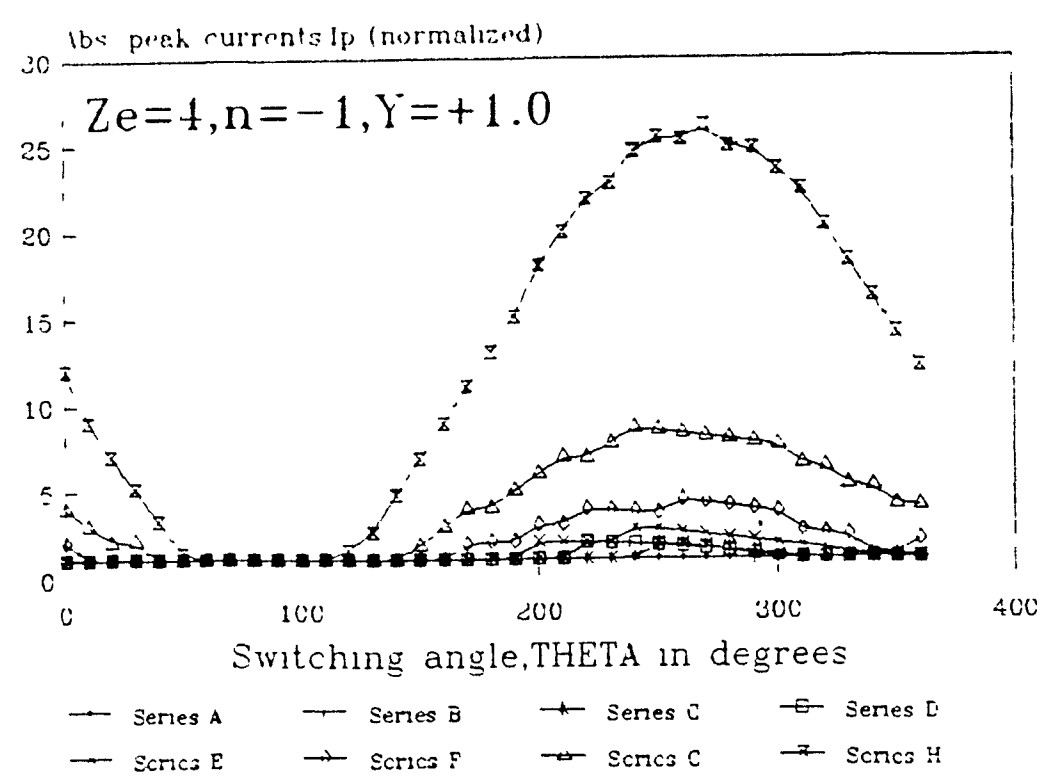

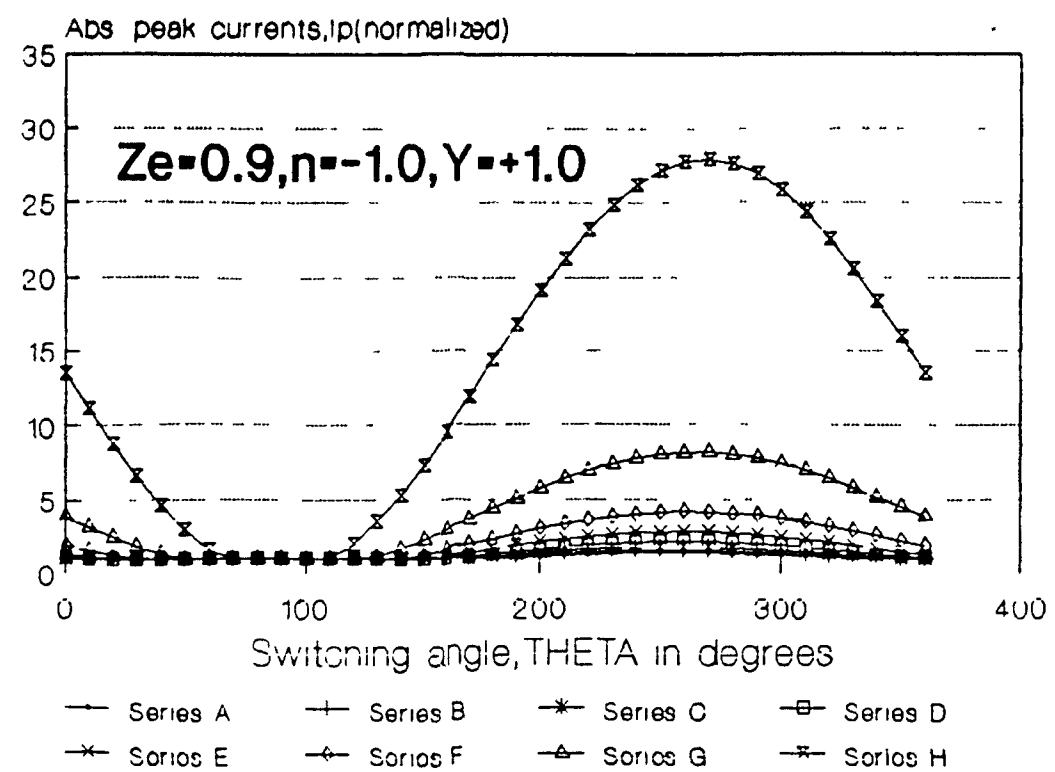

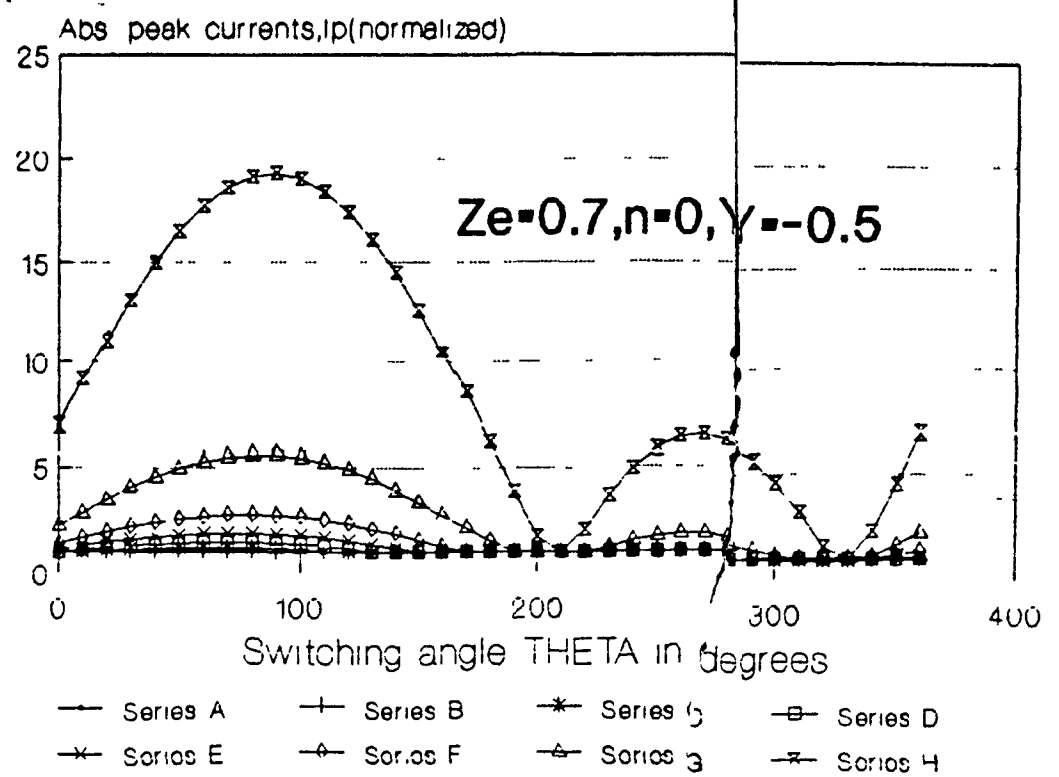

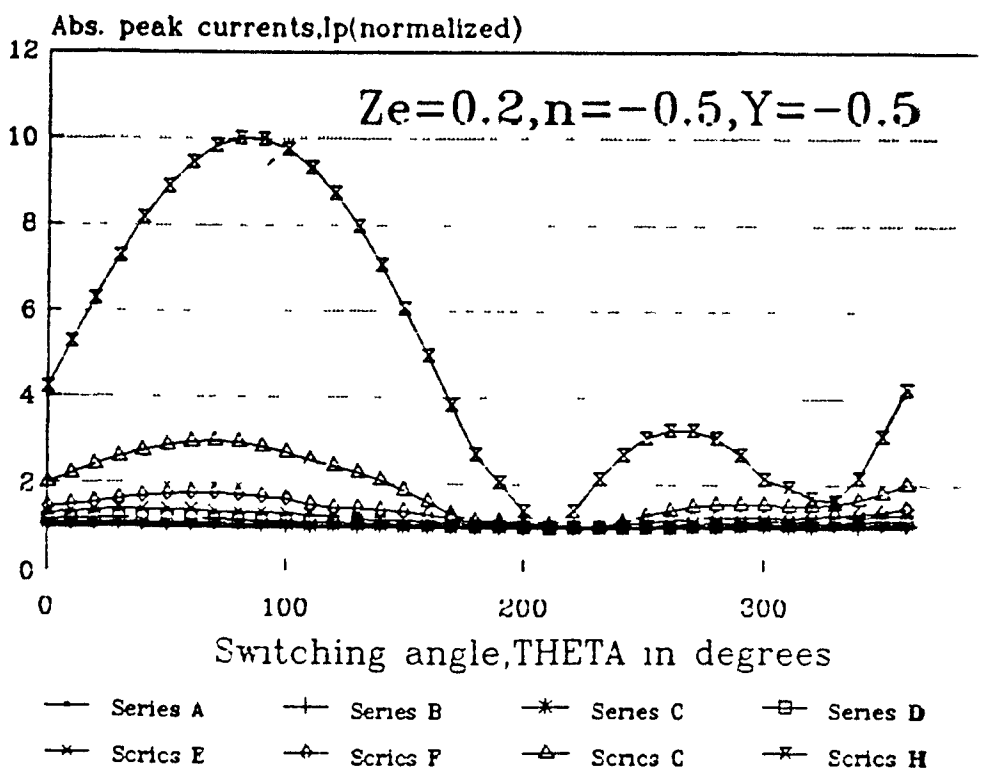

Fig. 2.21. Variation of Ip independent of n.

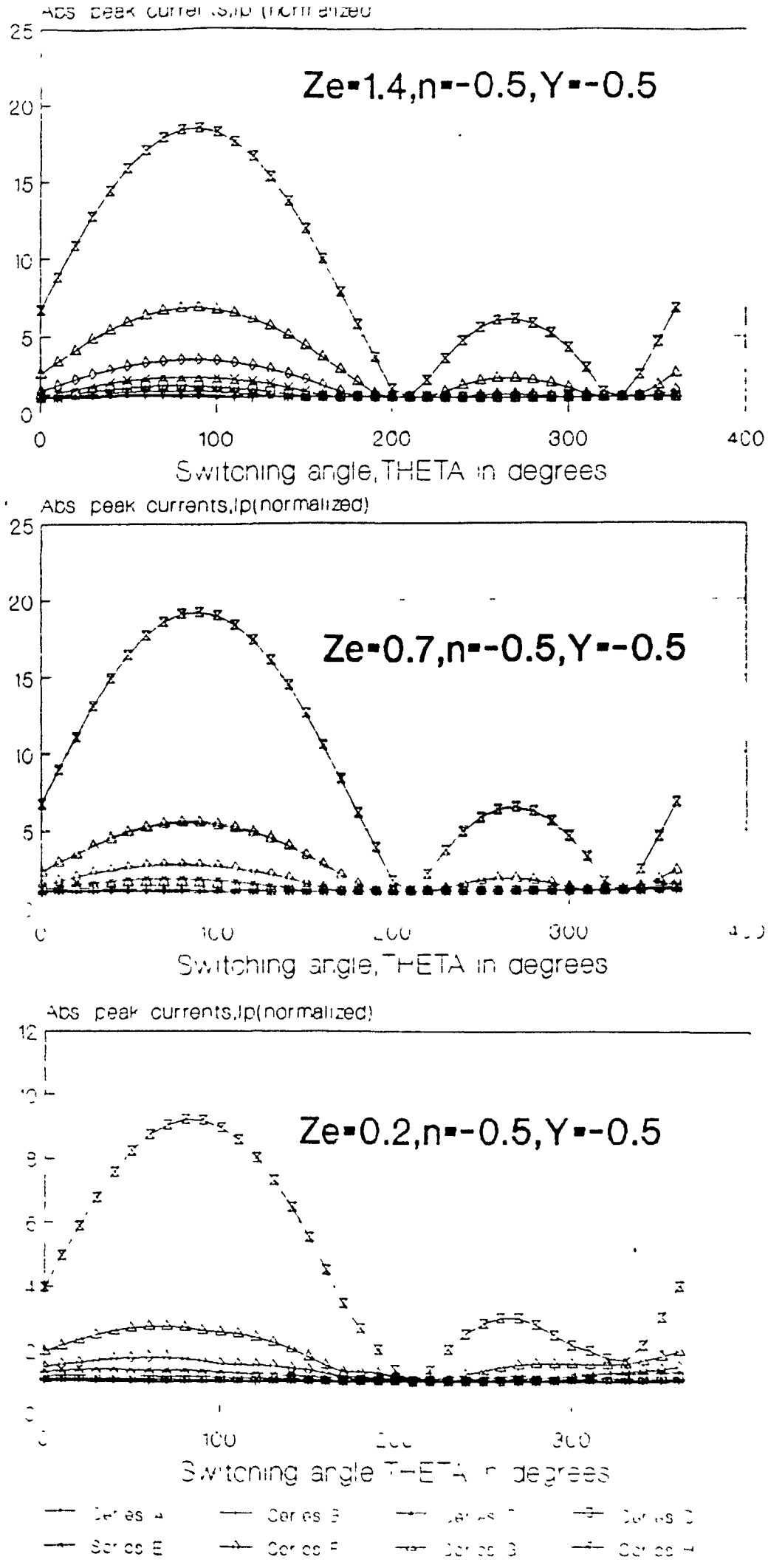

Fig. 2.22. Ip(maximum) for different Ze.

2.4 SUMMARY OF SWITCHING TRANSIENTS

The conditions for minimum and maximum switching current in the linear circuits are summarized in table 2.1 (for Qo only i.e. Io=0). The table is made only for $Y \geq 0$ and the corresponding conditions $Y \leq 0$ can be found simply by adding 180° to the respective value of θmin and θmax.

No significant effect of Io is found in capacitive circuits. The variation pattern of Ip in all inductive circuits is same and depends simply on *n* (although it is not exactly true but the error does not substantially modify the conclusion). Therefore, θmax and θmin are also same.

Summary of the switching transients in the circuits is given below.

(a) Inductive circuits:

(i) In general, the variation pattern of Ip with respect to θ is same in all inductive circuits for a particular *n* and is independent of Y.

(ii) The doubling effect (Ip $\tilde{-}$ 2) is observed for all values of Ze.

(iii) Graph of Ip for $Y \leq 0$ is mirror image (along y-axis) of the graph for $Y \geq 0$.

(iv) The maximum Ip is significant only for $\phi > 60°$ (PF<0.5).

(v) The transient persists for considerable period depending upon the damping-ratio of the circuit.

(b) Capacitive circuits:

(i) The variation trend of Ip with respect to θ basically

TABLE 2.1 Condition for minimum/maximum switching current peak, Ip.

Nature of the circuit	Circuit parameters	Condition for minimum/maximum switching current (n=0)			
		Approximate θmin	More accurate θmin	Approx. θmax	More accurate θmax
Inductive (Xl>XC)	RL	$\pi+\phi, \phi$	same	0	same
	RLC (o/d)		$-(\pi/2)-Y\{(\pi/2)-\phi\}$ for $\phi<60^\circ$ $\pi+\phi$ for $\phi\geq 60^\circ$		0 for $\phi < 60^\circ$ π for $\phi \geq 60^\circ$
	RLC (u/d)		$-(\pi/2)-Y\{(\pi/2)-\phi\}$ for $\phi<80^\circ$ $\pi+\phi$ for $\phi\geq 80^\circ$		0 for $\phi < 80^\circ$ π for $\phi \geq 80^\circ$
Capacitive (Xc>Xl)	RC	$\cos^{-1}(-Y)-\phi$	same	$-\pi/2$	same
	RLC (o/d)		$\cos^{-1}(-Y)-\phi-0.055\pi$		$-\pi/2-0.055\pi$
	RLC (u/d)		$\arccos(-Y)-\pi/2$		

depends upon Qo or Y not on n.

(ii) For a particular Y, the variation pattern of Ip is same in all the capacitive circuits. Therefore θmin and θmax are also the same.

(iii)The maximum Ip is, (1+|Y|) times the maximum Ip at Y=0.

(iv) The maximum Ip is significant only for ϕ>60° (PF<0.5).

(v) Transient current is very large but exists for very short period as the damping-ratio is large.

(vi) The effect of Io or n is not significant.

2.5 EXPERIMENTAL RESULTS

The switching current during the transient condition is recorded by a storage oscilloscope. The SI or θ is controlled by using an instant-controlled switching circuit (discussed in the next chapter in detail). A 230 volts and 50 cycle, AC voltage is applied to different circuits of impedance, Z=100 ohms (source impedance is neglected). The value of ϕ is kept 70° in all cases. Photographs are given here in pairs showing maximum and minimum Ip of the same circuit when switched at θmax and θmin. Fig. 2.23 shows the switching arrangements employed for generation of different initial conditions in circuits.

Fig.2.24(a) shows the switching currents in a RL circuit (R=34.2 ohms and L=300 mH) when it is switched on at θ=0° (upper photograph) and at θ=70° (lower photograph).

Fig. 2.24(b) shows the switching currents in a RLC (U/D) circuit (R=34.2 ohms, L=438 mH, C=73 μF, Ze=0.22 and Xl>Xc) with

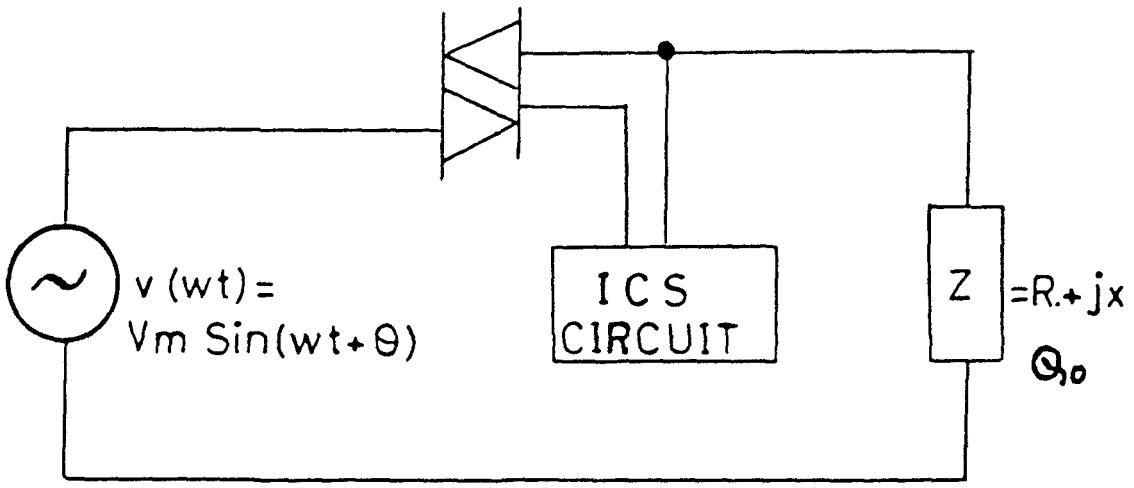

(a)

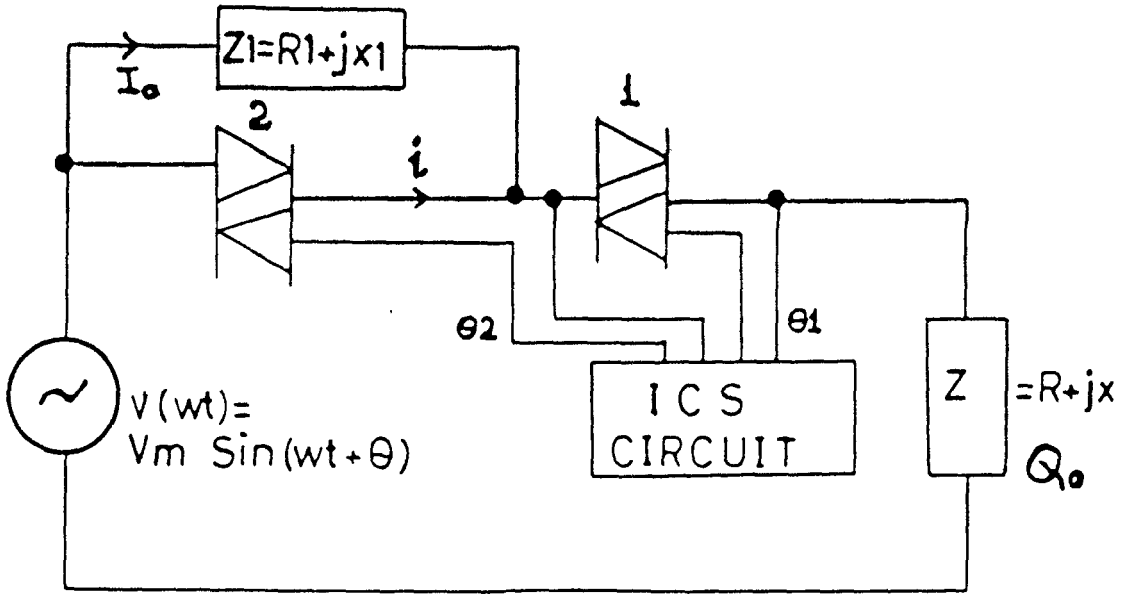

(b)

FIG. 2.23. SWITCHING WITH (a) Qo ONLY AND WITH (b) Qo & Io.

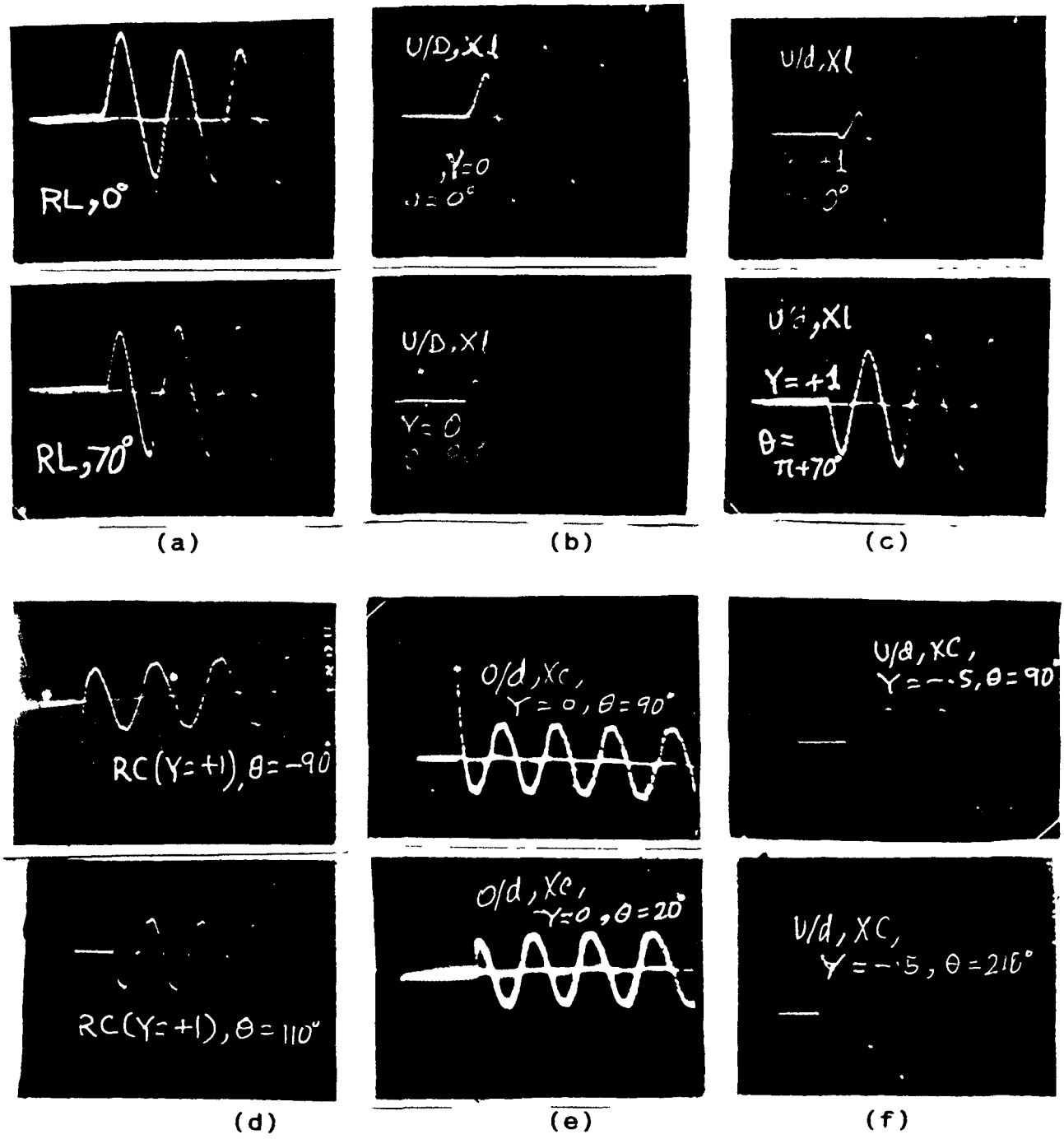

Fig.2.24.Oscillographic records of the switching currents (Qo only).

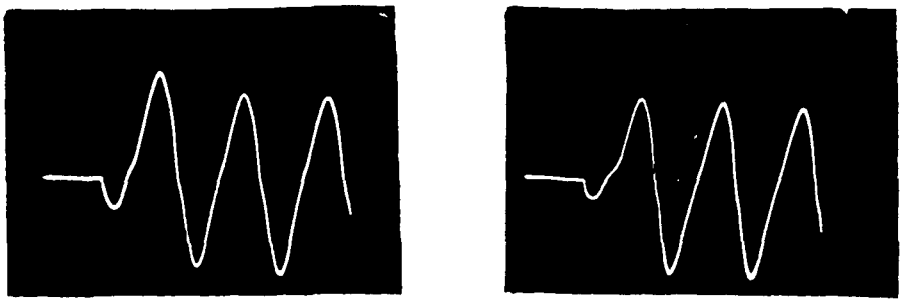

Fig.2.25.Oscillographic records of the switching currents (with Io).

zero initial condition (Y=0) and switched on at $\theta=0^\circ$ (upper photograph) and $\theta=90^\circ$ (lower photograph).

Fig. 2.24(c) shows the switching currents in the above circuit with initial condition (Y=+1) and switched on at $\theta=0^\circ$ (upper photograph) and $\theta=180^\circ+70^\circ$ (lower photograph).

Fig. 2.24(d) shows the switching currents in a RC circuit (R=34.2 ohms and C=34 μF) with the initial condition, Y=0 and switched on at $\theta=90^\circ$.

Fig. 2.24(e) shows the switching currents in a RLC (O/D) circuit (R=34.2 ohms, L=5 mH, C=33 μF, Ze=1.4 and Xc>Xl) when it is switched on at $\theta=90^\circ$ (upper photograph) and $\theta=20^\circ$ (lower photograph).

Fig. 2.24(f) shows the switching currents in a RLC (U/D) circuit (R = 34.2 ohms, L =19 mH, C = 32 μF, Ze =0.7 and Xc>Xl) with Y = -0.5 and switched on at $\theta = 90^\circ$ (upper photograph) and $\theta=\pi+[\cos^{-1}(-0.5)-90^\circ] = 210^\circ$ (lower photograph).

Fig.2.25 shows the effect of Io on the switching current in a RL circuit ($Z1=7.0+j19.2$, $\phi=70^\circ$). The circuit arrangement as shown in Fig. 2.23(b) is used here. Initially triac-1 is switched at $\theta1=-45^\circ$ ($=135^\circ$) to provide Io ($n=0.2$) in Z1 impedance circuit. Then triac-2 is switched in the next cycle to by pass Z2 (inductive circuit). Ip is maximum and minimum at $\theta2=0^\circ$ (left photograph) and $\theta2=70^\circ$ (right photograph) respectively.

The maximum and minimum values of Ip are found in agreement with the computed values (those are shown in graphs).

3. DESIGN OF INSTANT CONTROLLED SWITCHING CIRCUITS

3.1 INTRODUCTION

As discussed in the previous chapter an instant-controlled switching (ICS) circuit is required for switching a circuit or a phase (of load) at a predetermined and precisely set switching instant (SI) on the voltage wave. Different types of ICS circuits developed here for 1-phase as well as 3-phase applications. Initially a digital circuit was designed and realized based on counting of high frequency pulses. An improvement was then made by realizing an analogue circuit for the same purpose which was frequency invariant and much simpler. Finally, a hybrid circuit was evolved which was much more versatile and useful for many other purposes. For the later two types of devices a measurement of phase-angle was needed. To accomplish this a frequency-invariant phase-angle meter was also developed.

3.2 DIGITAL ICS CIRCUIT

A control pulse generated at the required SI or angle, in each cycle of the supply voltage, may be used to trigger a switching device which in turn closes the main power switch. The two possible methods for obtaining such a control pulse are as

follows:

(i) Generating a pulse at the positive zero-crossover instant (PZI) and then delaying it for a known period using a monostable or a delay network.

(ii) Counting, starting from the PZI, a precalculated number of high-frequency (HF) pulses and then generating the control pulse.

In the first method the presence of a monostable may lead to undesirable operation due to noise and stray pulses. Moreover it is difficult to set the delay period precisely. In the proposed scheme, therefore, the latter technique is adopted. The block diagram of the scheme is shown in Fig. 3.1. The counter starts counting the HF (6 KHz) pulses from the PZI. Each pulse at this frequency corresponds to 3° of a 50 Hz cycle and gives a sufficient resolution. Only 6 bits of the binary counters (7493) output are needed for counting the 60 HF pulses corresponding to half of the 50 Hz cycle. The parallel outputs of the counter are connected to a combinational logic block which produces the control pulse at the terminals A,B,C,.....N after counting the appropriate number of the HF pulses. In order to produce the control pulses at 0°, 30°, 60°, 90°, 120°, 150° and 180°, i.e. after 0, 10, 20, 30, 40, 50 and 60 counts, a combinational logic circuit, comprising of three AND gates (IC chip 7408) is connected at the output of the counter. Only combinational logic has to be changed for triggering at any instant other than the above. Moreover, with the help of different combinational logic, a 3-phase circuit or different circuits can be switched on sequentially.

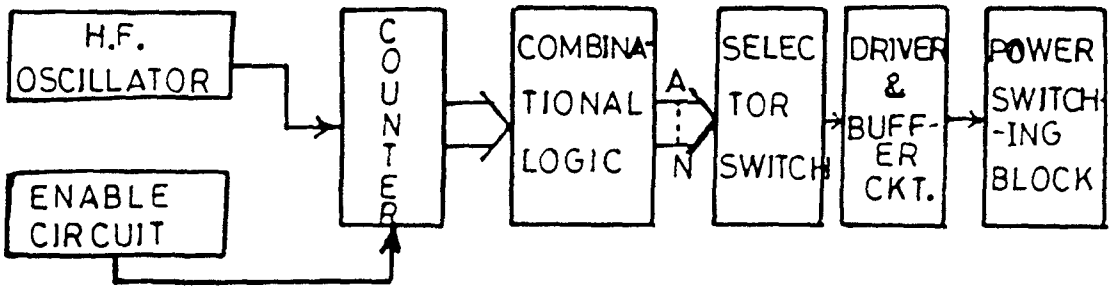

FIG.3.1. BLOCK DIAGRAM

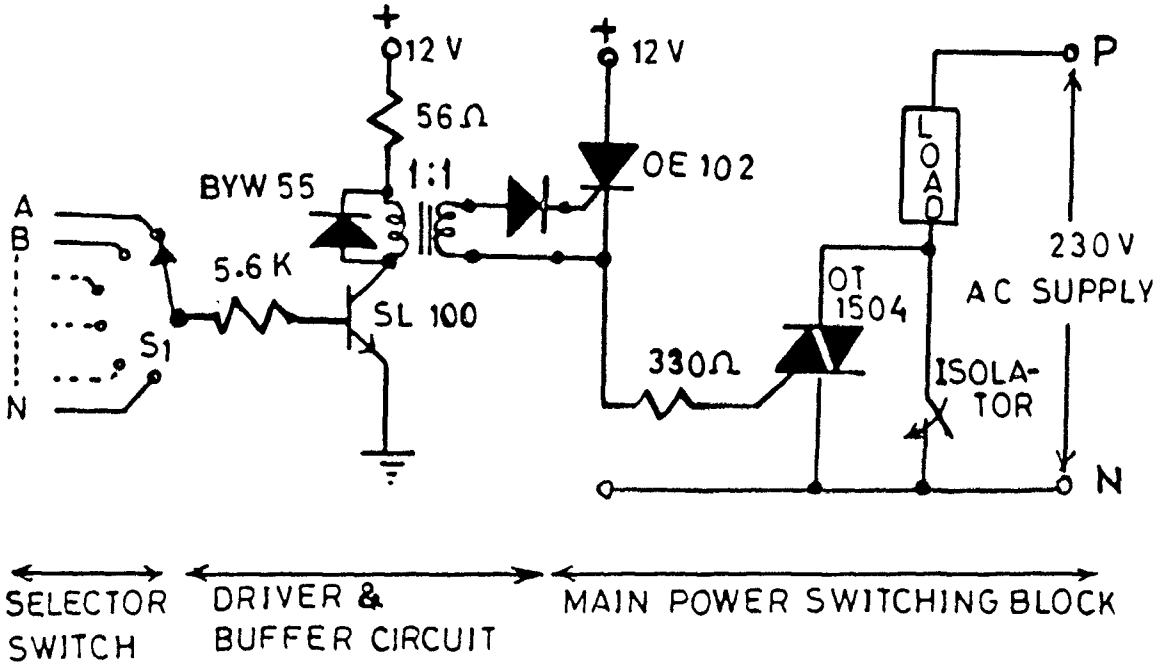

FIG.3.2. POWER SWITCHING BLOCK

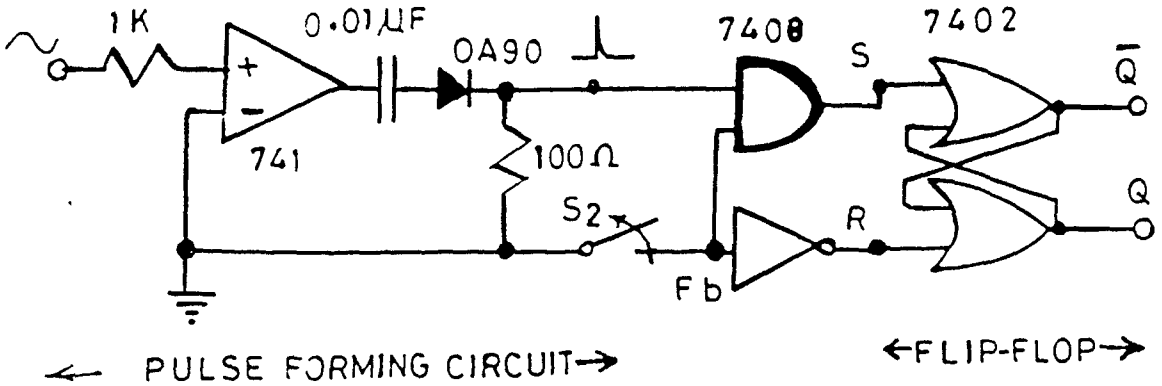

FIG. 3.3. ENABLE CIRCUIT.

The selector switch S1 can be set to tap any one of the combinational logic outputs according to the desired SI (Fig. 3.2). This output triggers an auxiliary SCR through a driver and buffer circuit (DBC), which provides the permanent gate supply needed to switch on the triac and keep it on during subsequent cycles. An isolator switch in parallel with the whole switching circuit may be used to replace the switching circuit after the switching-on operation. To ensure that the counter starts counting only from the PZI, an "Enable circuit" is used. It has a pulse-forming circuit (PFC) and a SR flip-flop (FF) as shown in Fig. 3.3. The PFC generates a sharp positive pulse at the PZI of the applied voltage which when allowed (by opening the switch S2) sets the FF through the AND gate and enables the counter to start counting the HF pulses from the PZI.

Experiments were carried out to switch a 50 Hz power supply to a resistive load at different instants in a cycle. Photograhic records were obtained (Fig. 3.4) and carefully examined. The SIs were found to be in close agreement with the pre-set values.

3.3 ANALOGUE ICS CIRCUIT

The circuit described in the previous section was basically a delay type of circuit and they are susceptible to variation in power frequency. The same function was realized by an analogue circuit which is not only simpler and cheaper but also independent of frequency variations. The block diagram of the proposed circuit is shown in Fig. 3.5. In order to obtain switching at any required instant or angle, a, first a voltage

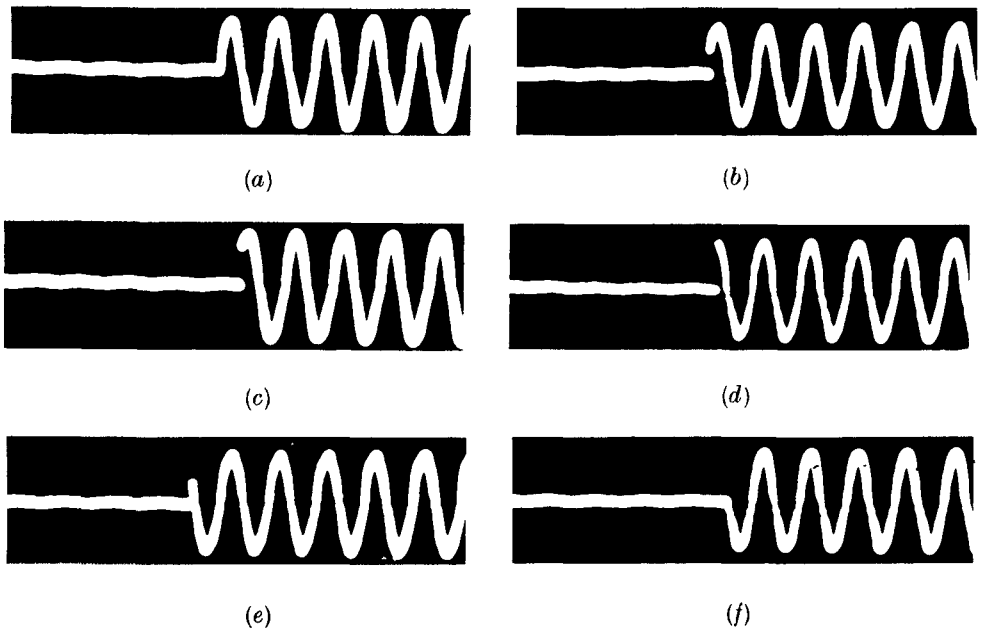

Fig. 3.4.Photographs at different switching instants: (a)0°,(b)30°,(c)60°,(d)90°,(e)150°,(f)180°.

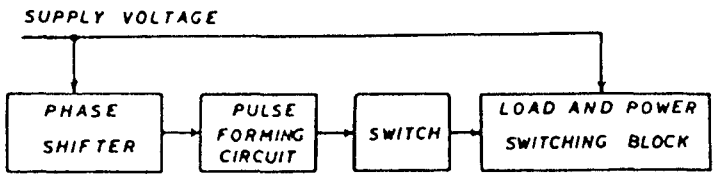

Fig. 3.5.Block diagram of the switching circuit.

signal, Va, shifted in phase from the supply voltage by the same angle is produced. The phase shift is accomplished by an AC thyratron-type circuit [12], as shown in Fig. 3.6. The advantage of this circuit is that it can easily give a phase-shifted voltage signal of constant magnitude and any phase-angle between 0 and π (leading or lagging) and can be achieved simply by varying the resistance R. The value of a is given by

$$a = 2 \tan^{-1}(wCR) \qquad (3.1)$$

The range of a can be extended from π to 2π by interchanging, the input terminals of the transformer or of the operational amplifier, or by the positions of C and R. The complete switching circuit is shown in Fig. 3.7. On opening the switch S1, the pulse from the PFC at an angle a with respect to the supply voltage Va, is passed over to to the gate of the auxiliary SCR and it is continuously triggered. This in turn triggers the triac as shown in Fig. 3.8. Thus supply to the load is switched in at the angle 'a'.

To set the switching angle accurately, a simple solid-state phase-angle meter is designed as shown in Fig. 3.9. The phase-difference between two AC signals A and B can be measured in terms of the time elapsed between their PZIs. Sharp positive pulses, corresponding to the PZIs are obtained using a PFC. The pulse A sets and B resets the FF. The phase-difference between A and B is equal to the duration for which the output Q of the FF remains 'high'. This duration can be measured by converting it to a DC level using period-to-voltage converter and measuring it by

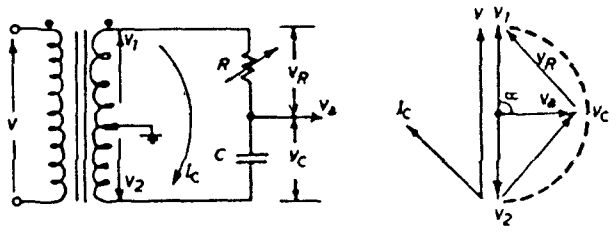

Fig. 3.6 AC thyratron-type phase-shifting network and its phasor diagram

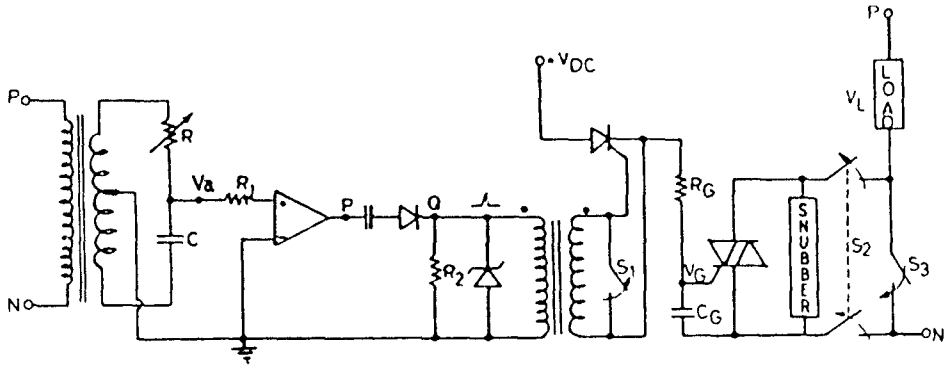

Fig. 3.7 Complete switching circuit

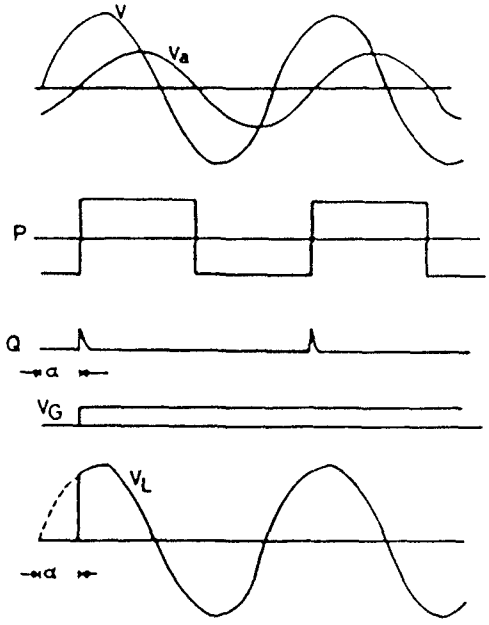

Fig. 3.8 Wave shapes at various points of the circuit

a voltmeter. The voltage during this period is amplified, clipped and the average DC voltage measured by a moving-coil instrument (micro-ammeter in series with a high resistance of 30 K-ohms). The timing diagram of the circuit is shown in Fig. 3.10. If "t" is the duration corresponding to the phase difference and "T" the time-period of the input signals then the average DC voltage to be measured depends on the ratio t/T and is independent of the frequency. The output characteristic is shown in Fig. 3.11. The phase-angle meter was tested to confirm that a variation in frequency from 4 Hz to 5 Khz neither affected the accuracy nor the calibration. For the measurement of the power-factor, the normal range of interest lies between 90° leading and 90° lagging. Therefore an inverted B signal can be used instead of B to give the deflection of the voltmeter in the range -180° (leading) to 180° (leading) as shown in Fig. 3.12.

3.4 HYBRID ICS (MASTER-CONTROLLER) CIRCUIT

Different types of firing angle controllers for converters and inverters are available in literature since last three decades. However these firing circuits are either meant for a particular application or are quite complex involving large hardware. A number of techniques for polyphase converter/inverter control had been discussed in detail [13,14]. Le and Berg had reported a 3-phase triggering circuit where three sets of active phase-shifter circuits (PSC) are employed [15]. However each PSC requires four operational amplifiers in addition to some combinational logic gates. Similarly other firing angle

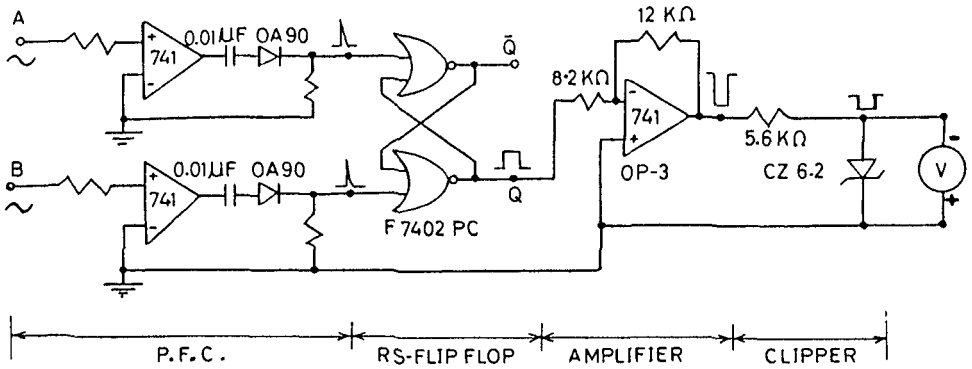

Fig. 3.9 Proposed circuit diagram for the phase-angle measurement.

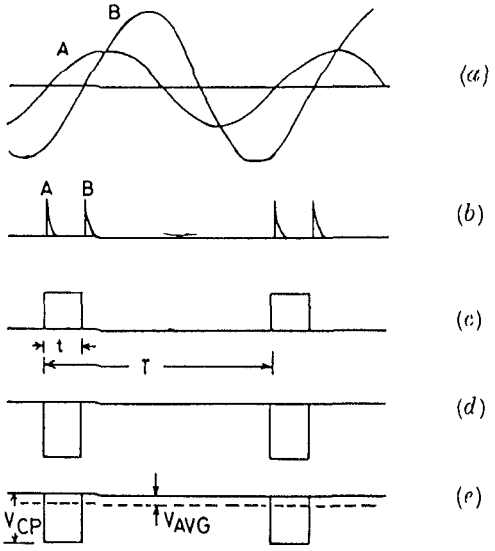

Fig. 3.10 Waveshapes at different stages. (*a*) AC signals, (*b*) output pulses of PFC, (*c*) output Q of the flip-flop, (*d*) output of amplifier, (*e*) clipped and averaged DC voltage.

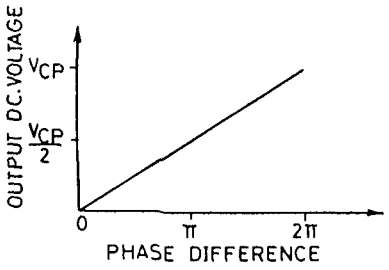

Fig. 3.11 Characteristic of phase-angle meter.

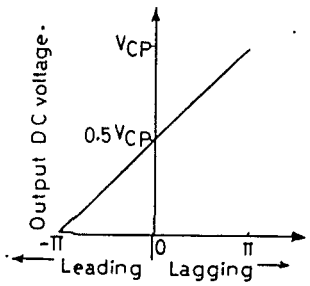

Fig. 3.12 Characteristic of power-factor meter.

controllers (including the integral-cycle power control/zero-voltage switching) are also reported for three phase systems by phase-locked loop and microprocessor based methods [16,17,18]. In these cases also lengthy circuitry is involved.

The principles of the ICS by the digital and analogue circuits are extended to develop a versatile master-controller circuit (MCC) for different applications. It is equally useful for converters, inverters, choppers, ICS, zero-voltage switching and integral-cycle control using thyristors, BJTs, FETs and MOSFETs etc. in the power circuits. Moreover it is successfully tested as a phase-comparator by phase-sequence detection techniques for realizing various distance characteristics for the protection of the transmission line. It easily controls as well as generates polyphase reference sinewave over wide frequency range (5Hz-40 KHz) which is otherwise difficult to be realized by simple circuits for cycloconverters and PWM inverters in speed control application over a frequency range within 100 Hz [14].

The block diagram of the MCC is shown in Fig. 3.13. Which has phase-shifting or phase-split circuits (PSC) as it is used in analogue ICS circuit (Fig. 3.8). Several phase-shifted signals (leading or lagging) are generated by adding more RC series branches at the secondary of the center-tapped auxiliary transformer (audio-interstage coupling transformer, Delta 13A74A) as shown in Fig. 3.14. Different voltage signals V1, V2 and V3 of required phase-shifts $\theta 1$, $\theta 2$ and $\theta 3$ respectively, are generated with respect to the reference sinusoidal voltage, V. The PFCs give sharp positive pulse at PZIs to set or reset the different

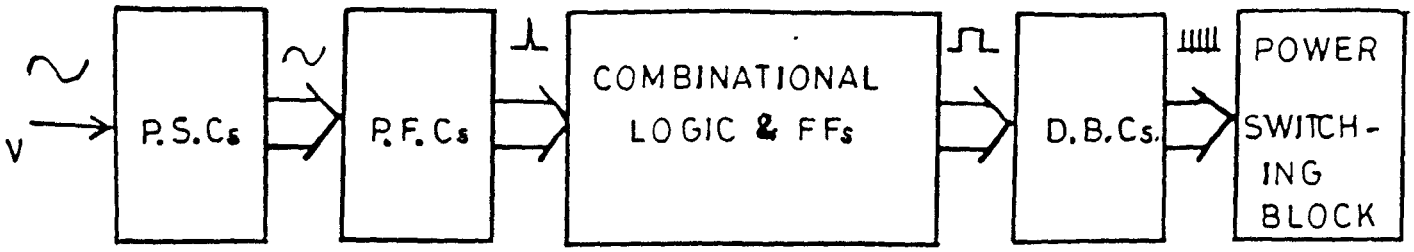

FIG. 3.13. BLOCK DIAGRAM OF MCC.

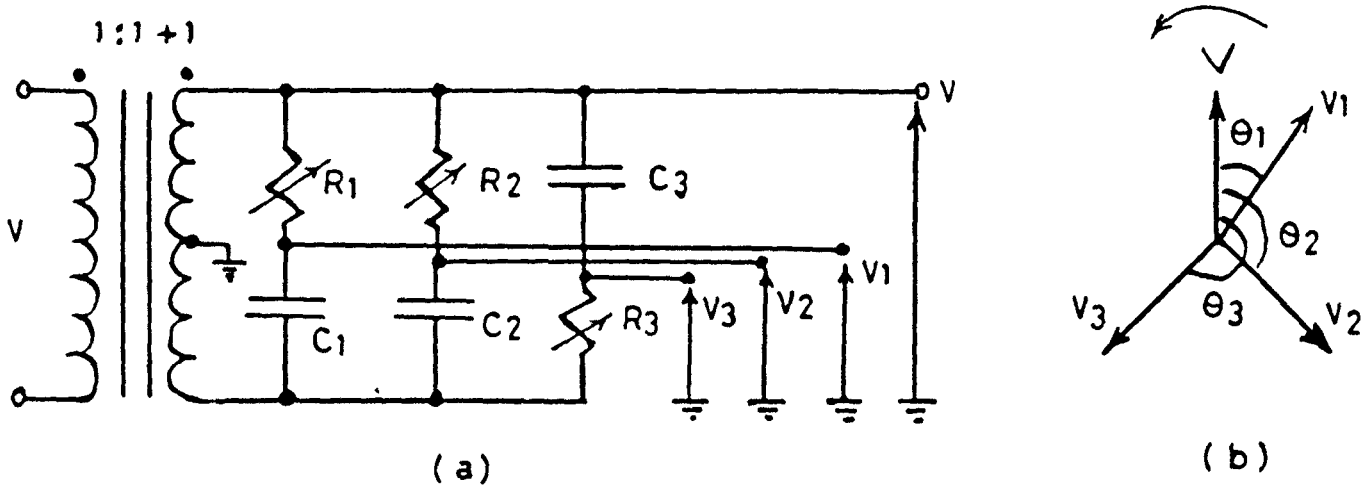

FIG. 3.14. PSC WITH PHASOR DIAGRAM

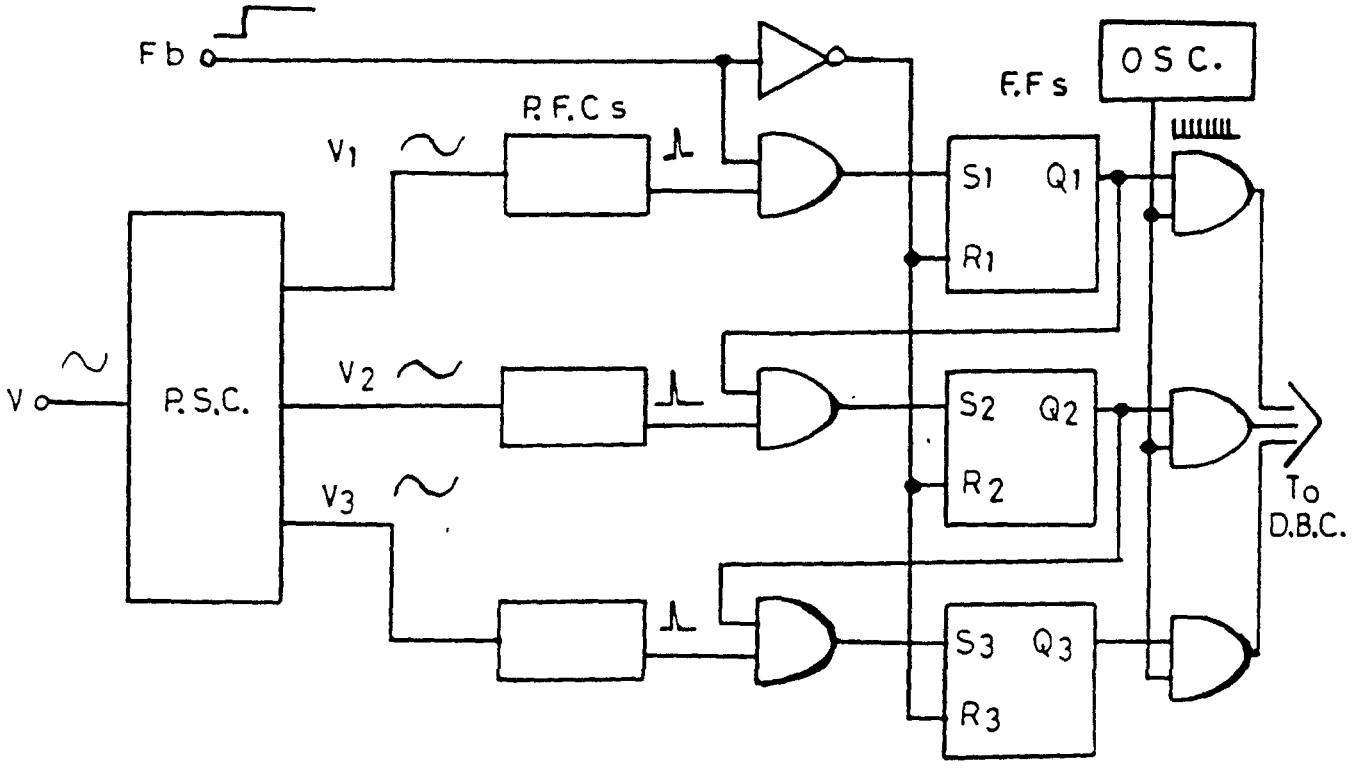

FIG. 3.15. M.C.C. IN I.C.S. MODE.

FFs according to the logic combinations. High output of the FF (Q=1), enables the carrier signal (10 KHz) from the oscillator to reach the DBC. Which inturn controls the switching and conduction period of different power semiconductors in the power switching block. The DBC circuit used here is same as shown in Fig. 3.2.

3.5 APPLICATIONS OF THE DESIGNED MCC

The applications of this circuit for various purposes are discussed below for individual cases separately.

3.5.1. ICS mode

Different load circuits or phases of a supply can be switched at the same or at sequentially different SIs (e.g. θ1, θ2, θ3 etc.) with respect to V. The MCC connections for 3-phase or three load-circuits are shown in Fig 3.15. As discussed earlier the generated voltages V1, V2 and V3 are applied to three PFCs. The control pulse of the first PFC at θ1, when allowed (Fb terminal is set to logic '1' level for burst control), sets the first FF as shown in Fig. 3.16. This part of the circuit is same as that of the "enable circuit" used in digital ICS circuit (Fig. 3.3). Now it enables the second FF to set at θ2 and so on. Thus switching takes place sequentially at required SIs only and continuous conduction of thyristors are maintained through the DBC.

3.5.2. Zero-voltage switching mode

In this case power control in both the modes, burst as well

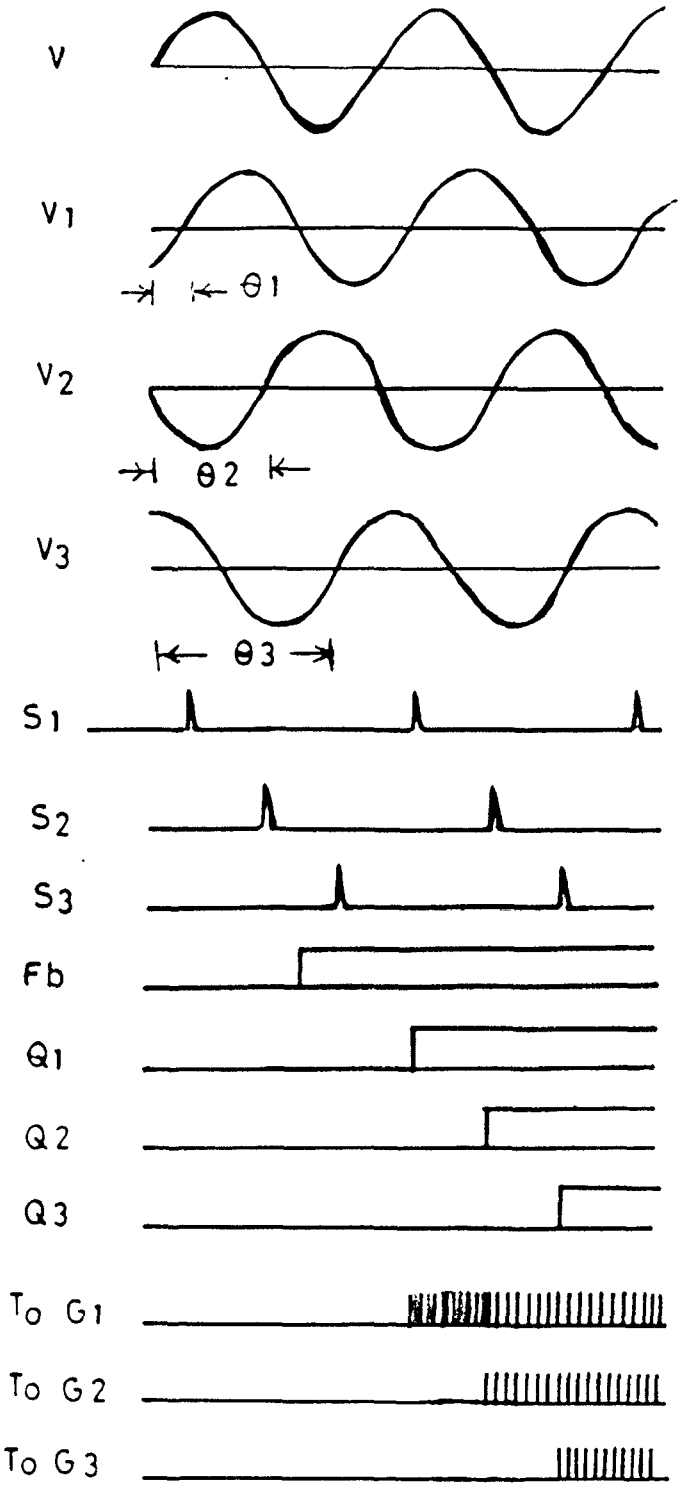

(a) WAVE FORMS FOR I.C.S.

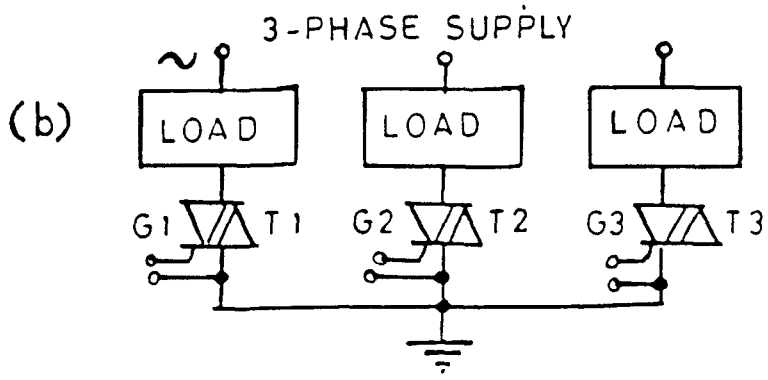

FIG.3.16. POWER SWITCHING BLOCK

as integral-cycle control, are possible. The connections in MCC are same as in Fig. 3.15 except that the burst or ON/OFF control signal at Fb controls the overall conduction period. When Fb goes to low level it resets all the FFs. Hence all thyristors switch off when their respective currents drop to zero (below holding current level).

3.5.3. Chopper control mode

As in previous cases, two AC signals V2 and V3 are generated by the PSC in MCC at the required frequency as shown in Fig. 3.17. The control pulse at $\theta 2$ and $\theta 3$ from the PFCs sets and resets FF corresponding to the PZIs of these signals (Fig. 3.18). The outputs of the FF, go to the main and auxiliary SCRs through the DBC . The variation of phase-difference $|\theta 3-\theta 2|$ between them is made in accordance with the desired duty-cycle of the chopper. The phase-difference of 90°, 180°and 270° correspond to 25%, 50%, and 75% of duty-cycle respectively. Therefore,

$$\text{duty-cycle} = 100.|\theta 3-\theta 2|/2\pi \quad \% \qquad (3.2)$$

The frequency control is achieved by varying the frequency of the reference voltage, V from the sinewave oscillator and time-ratio control is achieved by the phase-difference. The phasor position of V2 and V3 vary in between 0 and π, and π and 2π, by varying R2 and R3 respectively in PSC (Fig. 3.14). Thus the duty-cycle can be continuously controlled from 0 to 100%.

3.5.4. Converter/Inverter control mode

For 1-phase and 3-phase converter/inverter bridges four and

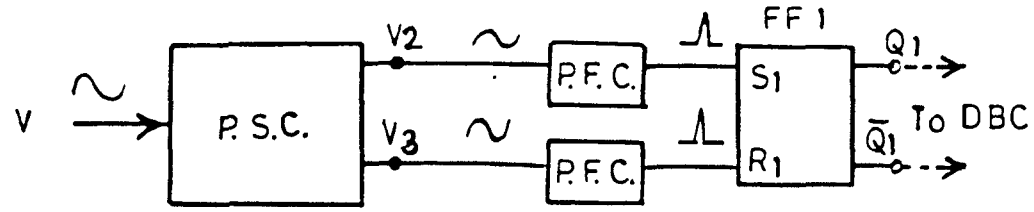

FIG.3.17. M.C.C. IN CHOPPER MODE

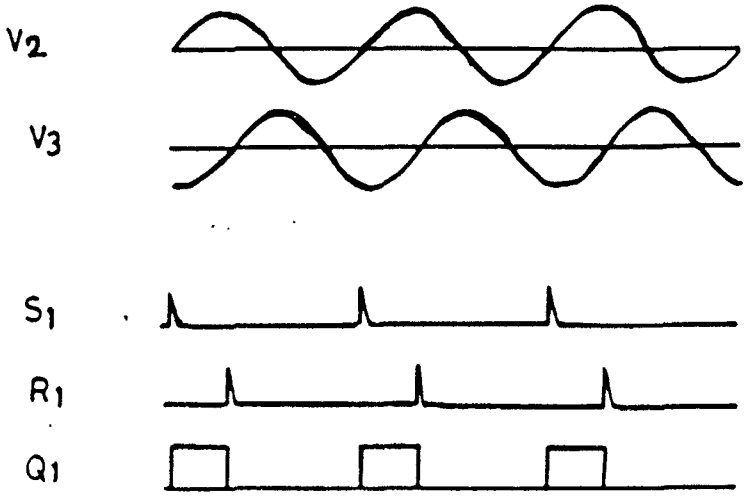

FIG.3.18. WAVEFORMS FOR CHOPPER.

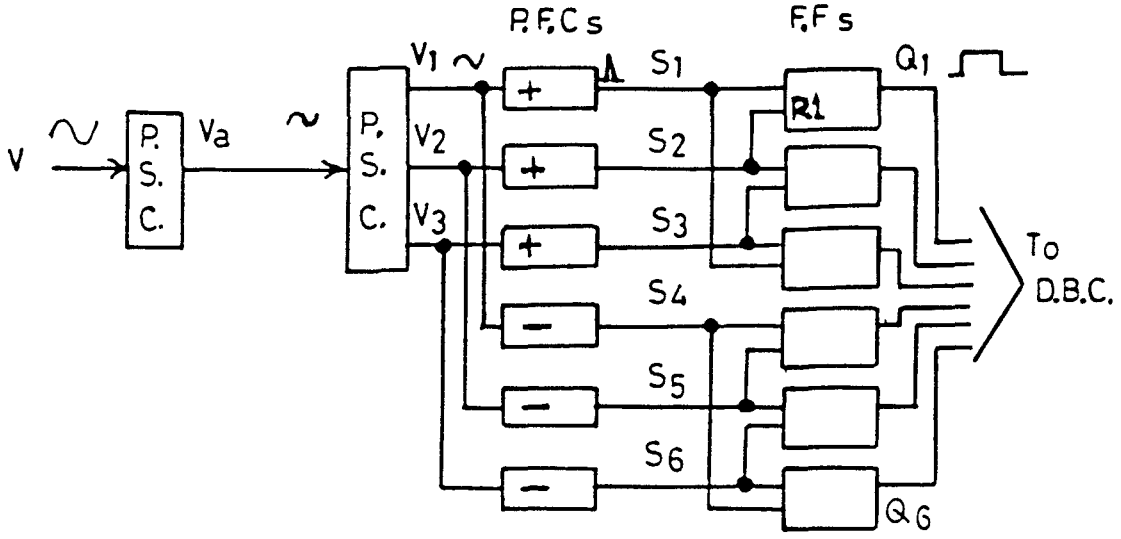

FIG.3.19. M.C.C. IN CONVERTER/INVERTER MODE.

six switching pulses respectively are required. Fig. 3.19 shows connections in MCC for 3-phase applications in 120° conduction mode. Here θ1, θ2 and θ3 are set at 0°, 120° and 240° and V1, V2 and V3 are applied to the six PFCs. Three PFCs give positive pulses at PZIs while the remaining PFCs give pulses at negative zero-crossover instants. Now these pulses (at 0°, 120°, 240°, 180°, 300° and 60°) set and reset the FFs for the desired duration as shown in Fig. 3.20. Thus they control the triggering pulses reaching the power semiconductor through DBC. The triggering/switching-angle control is accomplished by the variation of phase-angle 'a' of the reference voltage, V by a pre-PSC.

3.5.5. Realization of distance relay characteristics

In case of a long transmission line, the difference in impedance under heavily loaded condition and fault condition is small. But a considerable difference in phase angle exists [19]. Therefore static phase comparator are most suitable for distance protection. Different authors have reported the realization of directional [20] and quadrilateral characteristics [21,22] by the phase-sequence detector (PSD). However the circuits reported by them contain very large number of discrete components and devices such as mixing transformers, replica impedances in the form of reactor coils and large transistorized network. These circuits, therefore, have the inherent drawbacks of more power drainage, lack of compactness and difficulty in realization of large number of non-linear devices and components. The reliability of the

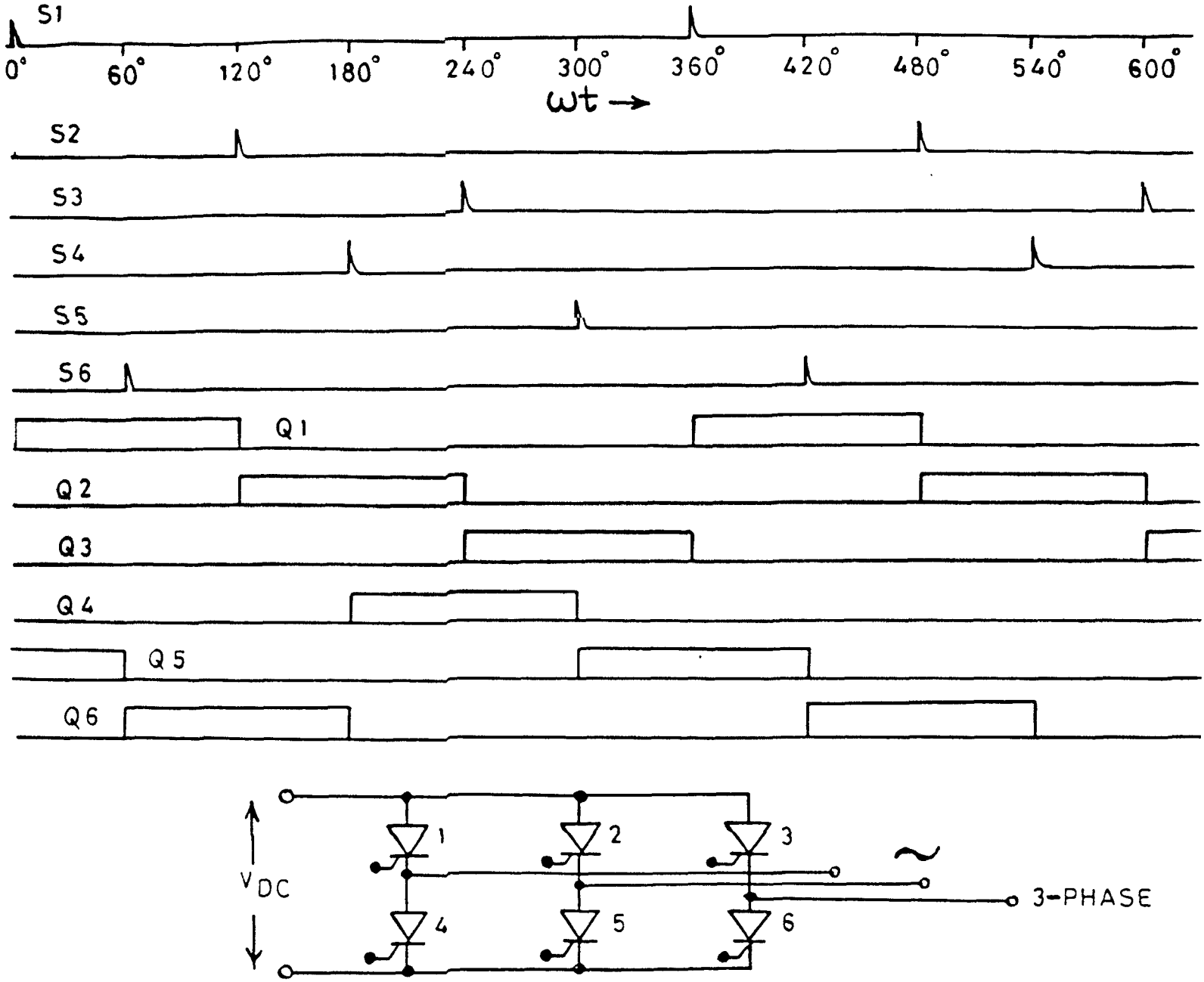

FIG 3.20 WAVEFORMS AND BRIDGE CONFIGURATION .

circuit, which is very important for protective devices, depends upon the proper functioning of all these components and is obviously adversely affected by their large number.

Here the MCC is used in such a way that it works as a versatile static phase-comparator which can realize all the characteristics of the distance relay viz. directional, general-directional, reactance, angle-impedance and general-angle impedance. It dispenses with the use of actual replica-impedances, mixing transformers and a large transistorized network. The design flexibility and ease of practical realization is obtained by simulating continuously adjustable replica impedances instead of actual ones.

A line impedance, Z, seen by the relay is shown on the impedance plane in Fig. 3.21. If the current signal, I, is taken as reference, then the line voltage signal V (=IZ), will represent Z. A directional characteristic is given in Fig. 3.22(a). The sequence of replica-impedance signals IZ1 and IZ2, V at the fault or trip condition will be IZ1, V, IZ2. A 3-input PSD can distinguish between the fault and normal condition as it is given in circuit I of Fig. 3.23. Similarly the sequence at the fault condition for reactance relay (Fig. 3.23c) is IZ'1, IZ3-V, IZ'2 and is realized by circuit-II of Fig. 3.23. Several other characteristics i.e. general-directional, angle-impedance and general-angle impedance are also realized by detecting the phase-sequence among these signals.

The connections of MCC to realize different relay characteristics are shown in Fig. 3.23. A combination of characteristics (b) and (e) gives a general quadrilateral characteristic as shown

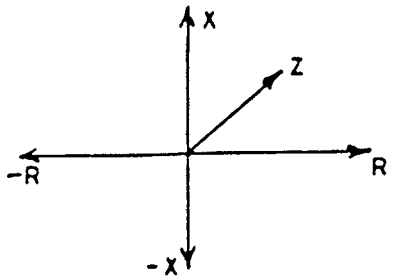

Figure 3.21 Line impedance, Z seen by relay on impedance plane.

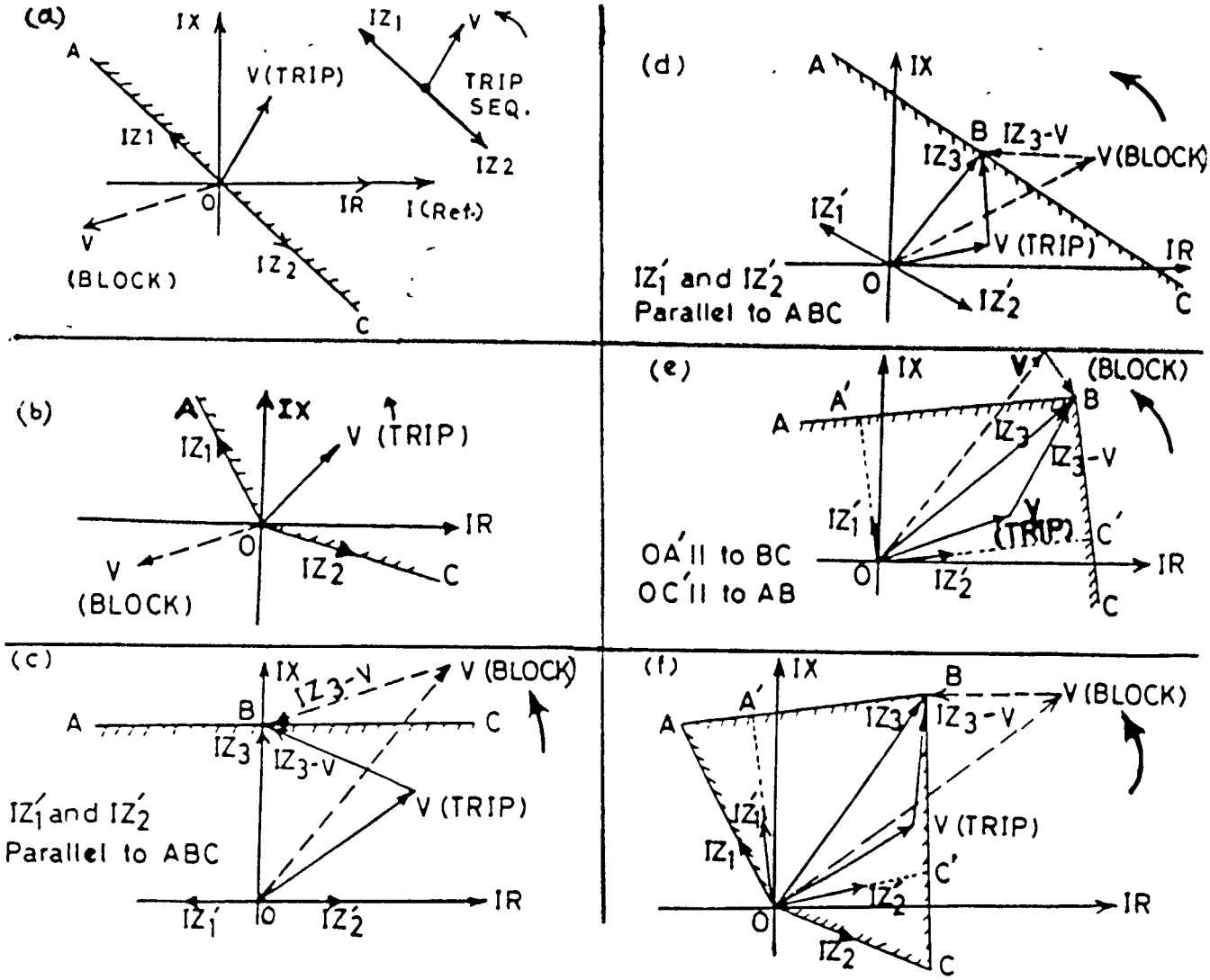

Figure 3.22 Directinal characteristics and inputs to PSD; (a) directinal, (b) general directinal, (c) reactance, (d) angle-impedance, (e) general angle-impedance and (f) general quadarilateral characteristic.

in Fig. 3.22(f). This can be realized by connecting the outputs of circuit-I and II with an AND gate.

With the help of a replica-impedance a current signal is converted into a voltage signal of required magnitude and phase-shift. Here the function of replica impedance is realized separately for versatile control by PFC. The phase-angle of the generated signal is controlled independently by the PSC and magnitude is controlled by the gain of an amplifier (operational-amplifier, 741 in closed-loop mode). A voltage signal in phase with the current is obtained by taking the voltage across the shunt resistance of the secondary of a current transformer (CT). It is applied to the PSC to generate V1, V2 and V3 or IZ1, IZ2 and IZ3 signals respectively as before. A difference amplifier is used instead of the mixing transformers for generating the IZ3-V signal. The PFCs give positive pulses at the PZIs whose sequence has to determined by PSD. Since the operational amplifier in PFC is connected in open loop mode, the magnitude of signals are not much important for PSD. However, except in case of IZ3, the magnitude of the IZ3 decides the phasor position of IZ3-V signal in circuit-II as shown in Fig. 3.23.

Two AND gates and two FFs are connected to make PSD as shown in Fig. 3.24. The pulse from the PFC of V1 sets the first FF while the pulse corresponding to V3 sets the second one for the sequence V1, V3, V2. The output of the PSD, Q2, remains high as long as the above sequence is maintained otherwise low. The relay is tested successfully with an artificial transmission line consisting of eighteen π-sections, for the normal, fault and

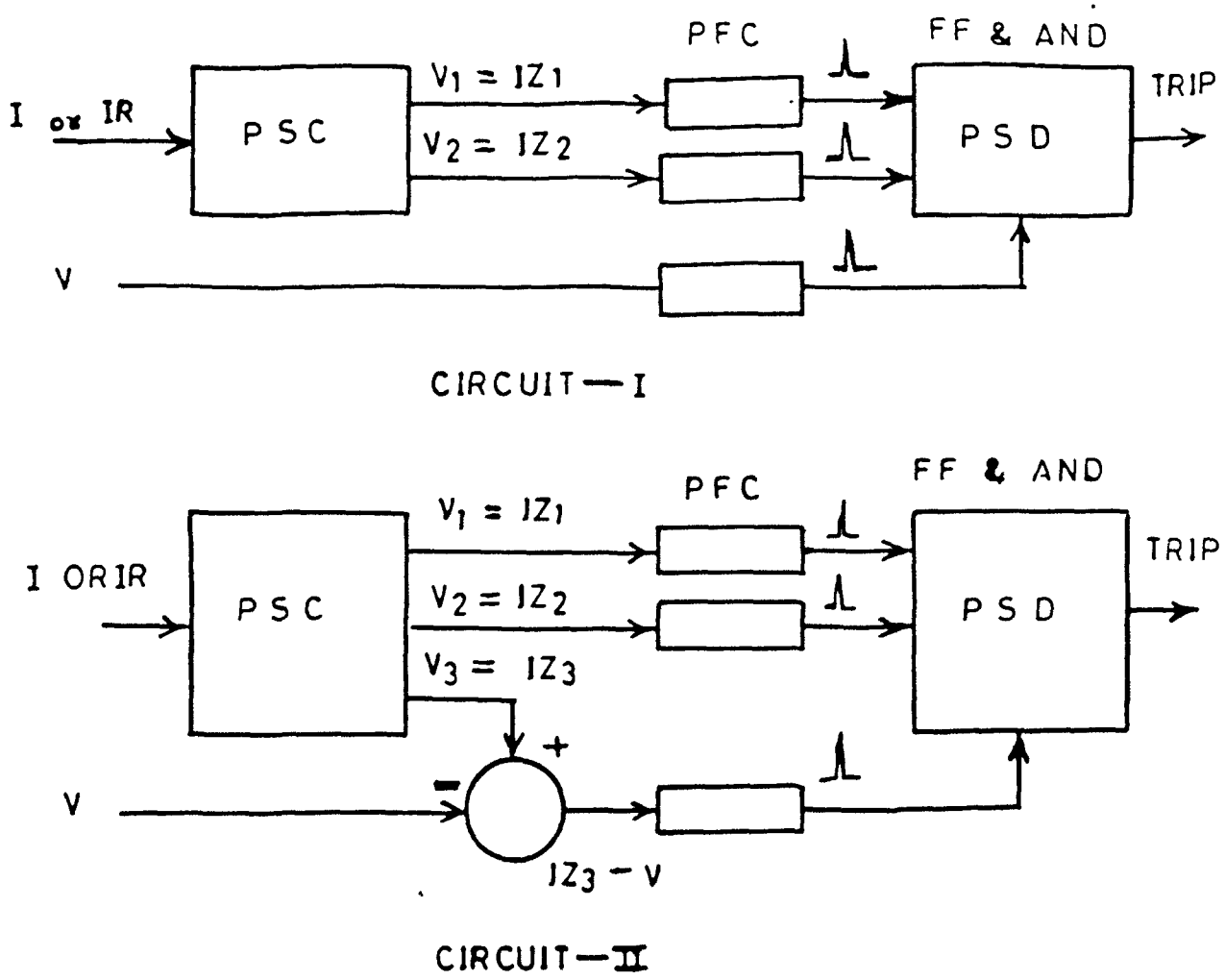

FIG.3.23. M.C.C. IN RELAY MODE.

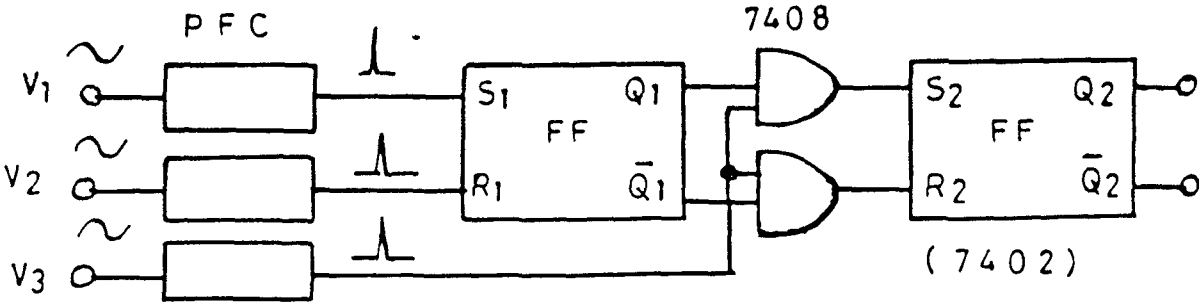

Q_2 HIGH FOR SEQUENCE V_1, V_3, V_2.

FIG.3.24. PSD CIRCUIT

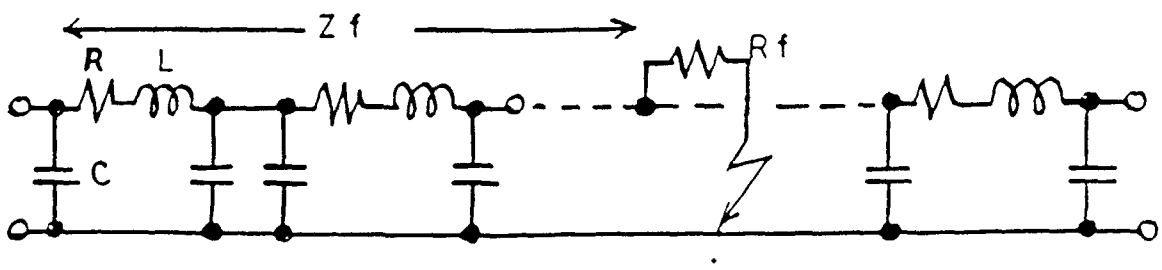

FIG.3.25. ARTIFICIAL TRANSMISSION LINE.

thorough-fault conditions. Each section of the transmission line has a series resistance and inductance of of 2.1 ohms and 21 mH and a shunt capacitance of 0.04 μF as shown in Fig. 3.25. The zone of protection was extended up to sixteenth section of the line, leaving the last two sections for simulation of thorough faults. The fault was created by using a variable (fault) resistance, Rf to determine the performance of the relay for different locations on R-X plane (Zf+Rf). All the characteristics of the phase comparator are tested successfully. The maximum operating time of the relay is one cycle during which the phase-sequence measurement completes. However it can be reduced to half cycle if another pair of PFCs, PSD and an OR gate are also used. Here PFCs generate the pulse at negative zero-crossover instants instead of PZIs, as it is used in 3-phase converter/inverter circuit (Fig. 3.19 and 3.20). Thus the phase sequence for the fault condition will be detected within one cycle (maximum) by either PSD. Performance of the relay under dynamic/actual conditions can be improved further, replacing RC branch in PSC by a RL branch, to avoid the effects of power system oscillations.

4. INSTANT CONTROLLED SWITCHING APPLICATIONS

4.1 INTRODUCTION

The ICS technique can be applied to study, estimate and control the transients in different circuits and systems. Here its application for controlling the performance and switching current of different types of load circuits, estimation and elimination of inrush current of transformers, and switching current as well as speed control of 1-phase and 3-phase induction motors are discussed. The results are experimentally recorded and verified.

4.2 ICS FOR INTEGRAL-CYCLE POWER CONTROL

As discussed in section 3.5, with the help of the "Fb" signal the MCC can be made to operate in integral-cycle control (ICC) mode. Fb controls the ON period which is realized by the PFC and two monostables.

4.2.1 ICC of 3-phase resistive loads

The ZVS technique is extensively used in heat controllers where otherwise phase-controlled converter circuit generates radio-frequency interference (RFI) and heavy inrush current while

switching-on the furnace element at cold (due to high thermal coefficient of resistivity). By ZVS at large power level, the use of bulky and expensive line filters to reduce the RFI can be avoided. Custom-made IC for ZVS are available [23]. But they are designed for low voltage (240 volts) and single phase applications and thus three sets with separate three phase sensing is required for 3-phase applications. Moreover at start or at initial switching, in case of critical applications like furnace to be heated from cold, another set of ZVS is required [16]. Bhat had reported two circuits based on phase-locked-loop method and direct digital proportional control method for 3-phase ZVS using single phase sensing [16,17]. However the circuitry involved in both the cases consists of large number of discrete components as well as IC chips.

The IQS method as discussed in chapter-3, section 3.5.2 can be used for three phase ZVS using single phase sensing. Switching pulses to the FFs are generated at PZI of all the phases. Which in turn switch the thyristors in the power switching block of MCC on the arrival of "Fb" or ON signal by enabling the AND gate to set FF1. Fb controls in burst as well as integral cycle control (ICC) mode. However in ICC mode, the number of ON cycles may not be equal for each phase at different "ON periods" causing an unbalanced load current. To remove this drawback another circuit configuration of MCC is used to control equal number of ON cycles in all phases as shown in Fig. 4.1. Fb is generated by two non-retriggerable monostables (74221) in between PFC for phase A to FF1. The first monostable sets the total number of cycles (ON+OFF) to be controlled while the second one sets the ON period

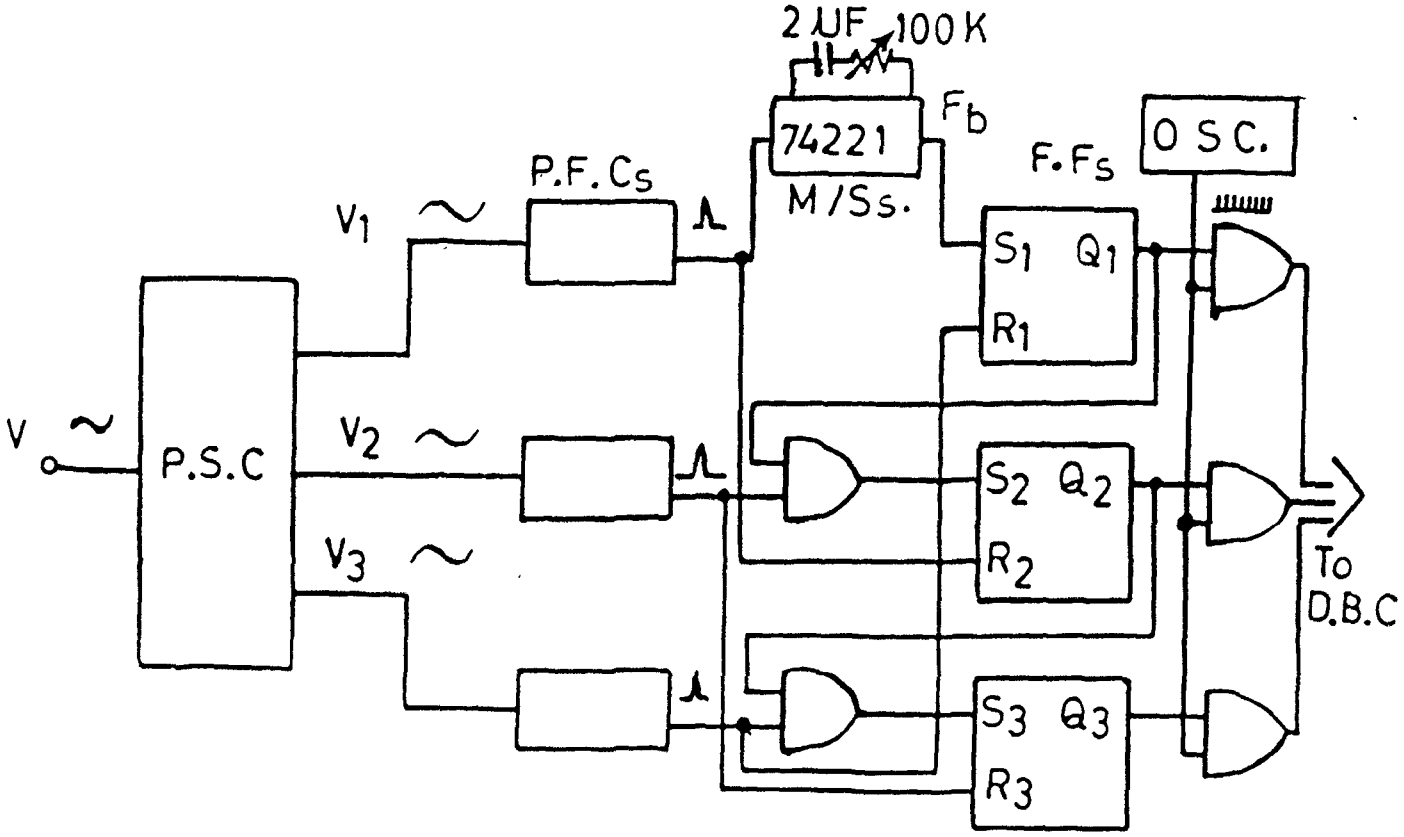

FIG.4.1. M.C.C. IN ZVS MODE

only. Triggering pulses are available between 0° to 240° only for each phase during the ON period, enable the thyristors to be switched in both the half-cycles. The timing diagrams of MCC in this mode for 3-phase application and the oscillographic records are shown in Figures 4.2 and 4.3 respectively.

4.2.2 ICC of 3-phase inductive loads

For all RL loads, the transient is found significant only when $\phi \geq 60°$ and it can be eliminated while switching at PF angle ($\theta=\phi$) as discussed in chapter 2 (sections 2.2 and 2.3). Moreover it can be shown that for such cases if the SI or θ is fixed to 90° then the transient is almost eliminated for any ϕ and the magnitude of Ip confines to Im as it was shown in Fig. 2.6. Which is also evident from the current response of RL circuit of different ϕ as shown in Fig. 4.4.

Thus this technique can be applied to control the transients in 3-phase RL loads. Pulses generated at 90° of each phase of 3-phase, 4-wire system can be used to switch A, B and C phases sequentially. The conduction will be maintained till ON (or Fb) signal persists as discussed for resistive loads in the previous section However number of switched half-cycles in each phase will not be same due to the non-simultaneous switching of all phases which causes different ON periods for each phase. Thus saturation in the core of inductor and unbalance in the load current may take place. This drawback was removed by changing the sequence of switching as A, C, B i.e. the C phase is switched in advance at its -90°. Thus if Va is the reference voltage to PSC,

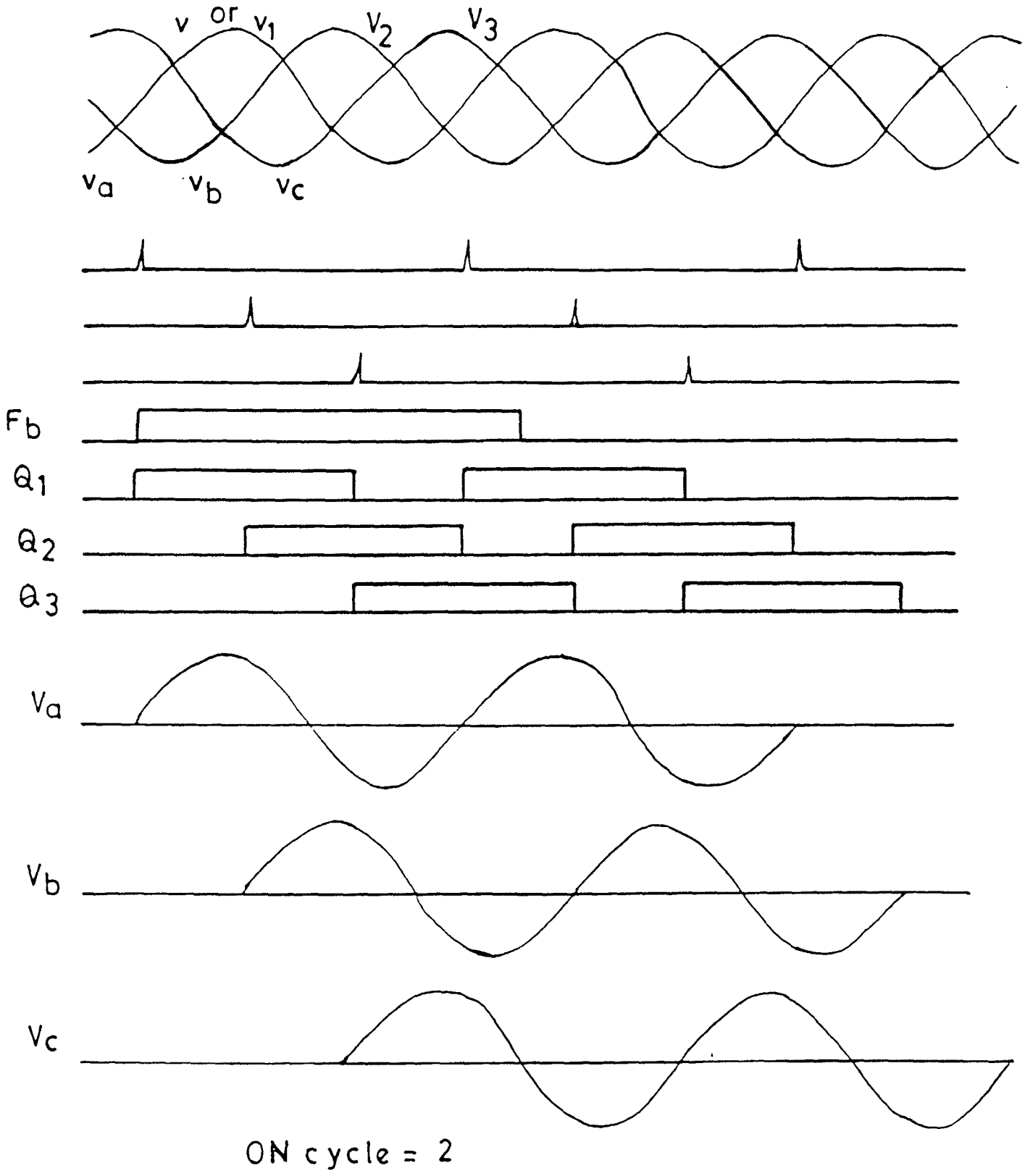

FIG.4.2. TIMING DIAGRAM FOR ZVS.

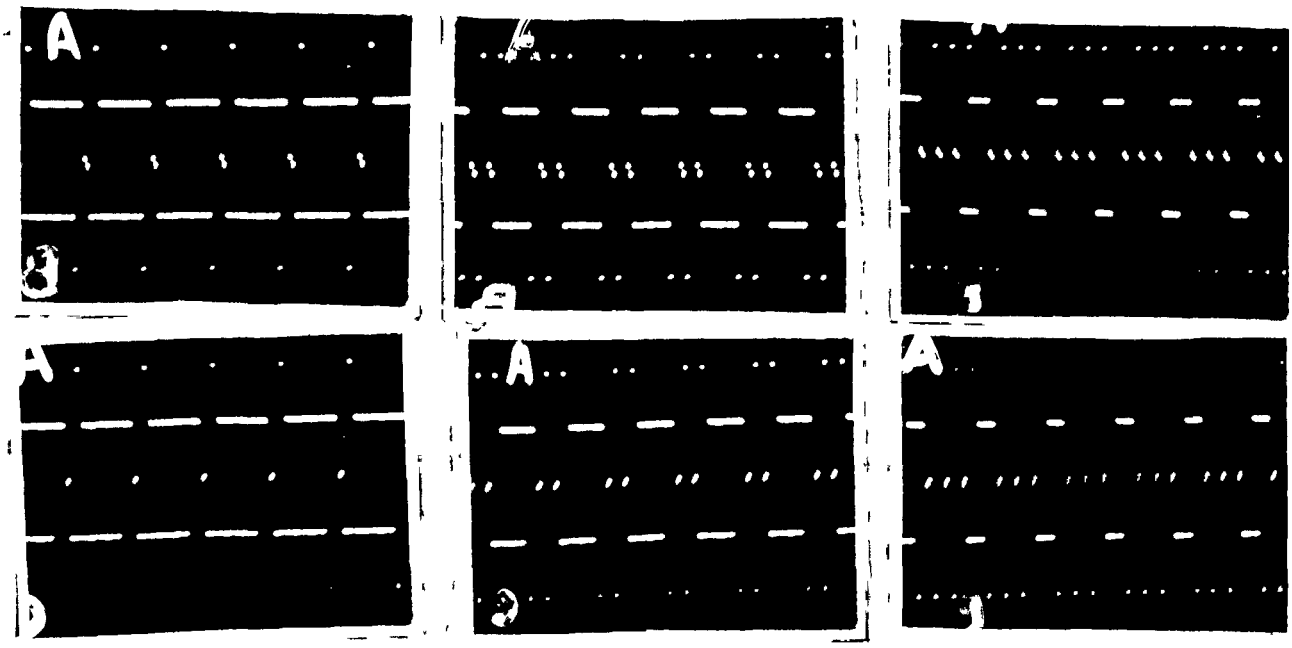

Fig. 4.3. Oscillographic records of ICC of 3-phase reactive loads (ZVS).

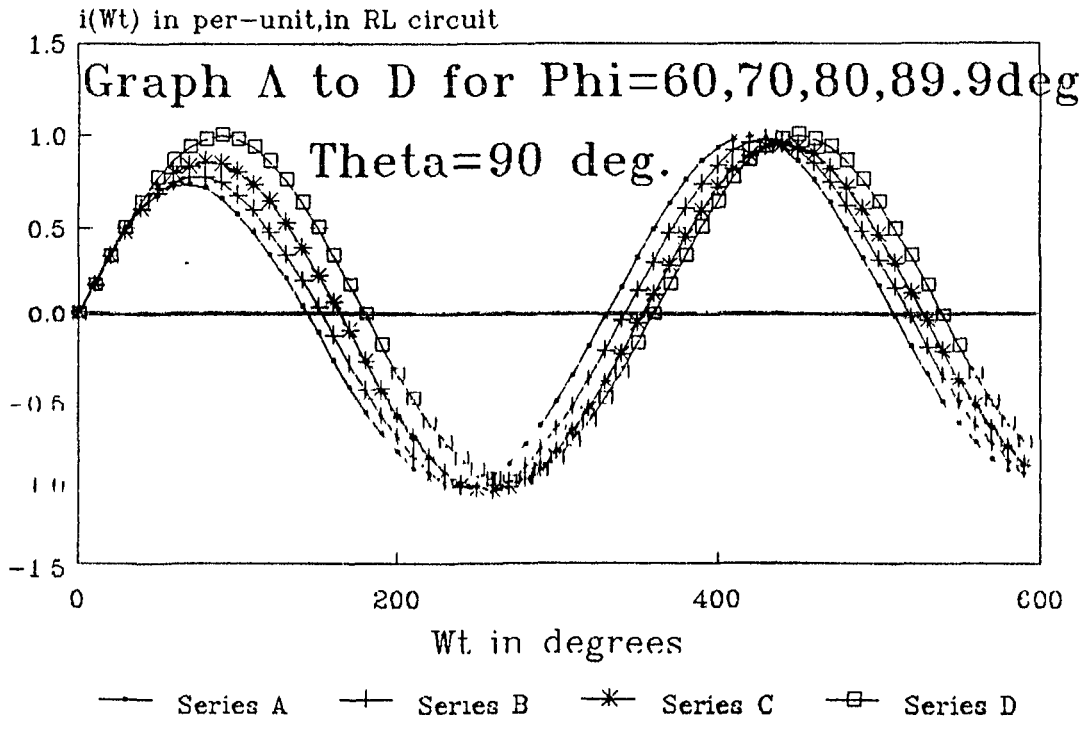

Fig. 4.4. Current response of RL circuit for different Ø, at Θ=90°.

then

$\theta 1 = 90^{\circ}$ For phase A

$\theta 2 = -120^{\circ} - 90^{\circ} = 150^{\circ}$ For phase C

$\theta 3 = 120^{\circ} + 90^{\circ} = 210^{\circ}$ For phase B

The timing diagram is shown in Fig. 4.5 for MCC in ICS mode and the photographic records for a 3-phase, 4-wire load are shown in Fig. 4.6.

4.3 ICS FOR DETERMINATION OF INRUSH CURRENT

For a transformer with an air-core or unsaturated core the maximum transient current (inrush), due to switching at or near ZCI, would be only twice the normal magnetizing current. However transformers are normally designed with some saturation. Hence the magnetizing inductance, which is proportional to the slope on B-H curve, is no more constant but decreases drastically with increase of the flux density, B as shown in Fig. 4.7. This collapse of the magnetizing reactance, Xm, raises the magnetizing current, im, to several times the full-load current. The residual flux density, Br, if present in the core may further aggravate the situation when it supports the initial magnetizing flux.

For proper selection/design of switchgear, it is necessary to determine magnitude as well as nature of decay of inrush current of power transformers, which depends upon the magnetization (B-H) curve of the core material and the SIs, besides other usual factors. Normally B-H curve with several assumptions has been used for estimation of the the inrush current [24,25,26,27, 28]. But the details of the magnetic properties of the core

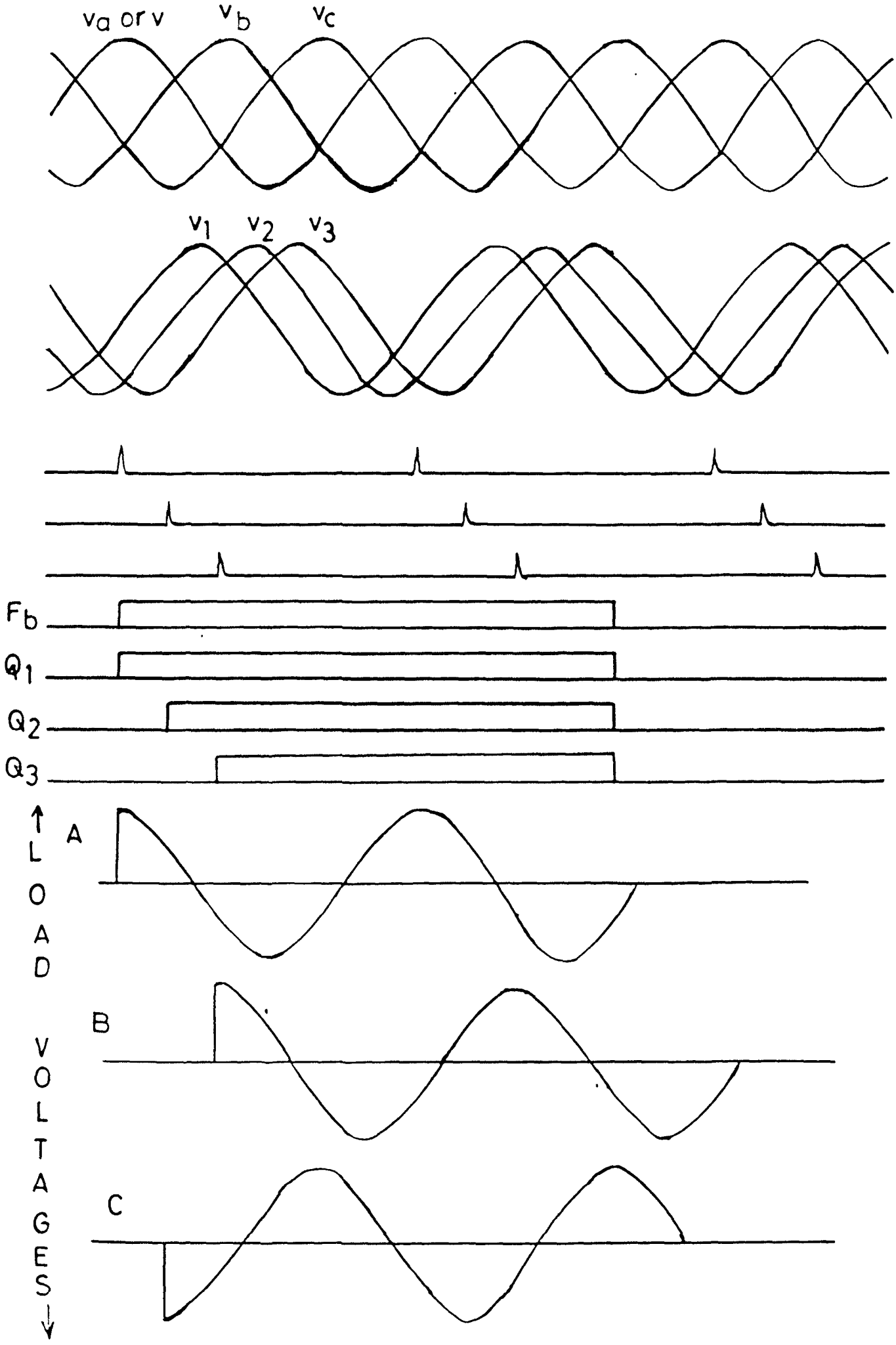

FIG. 4.5. ICC FOR INDUCTIVE LOADS

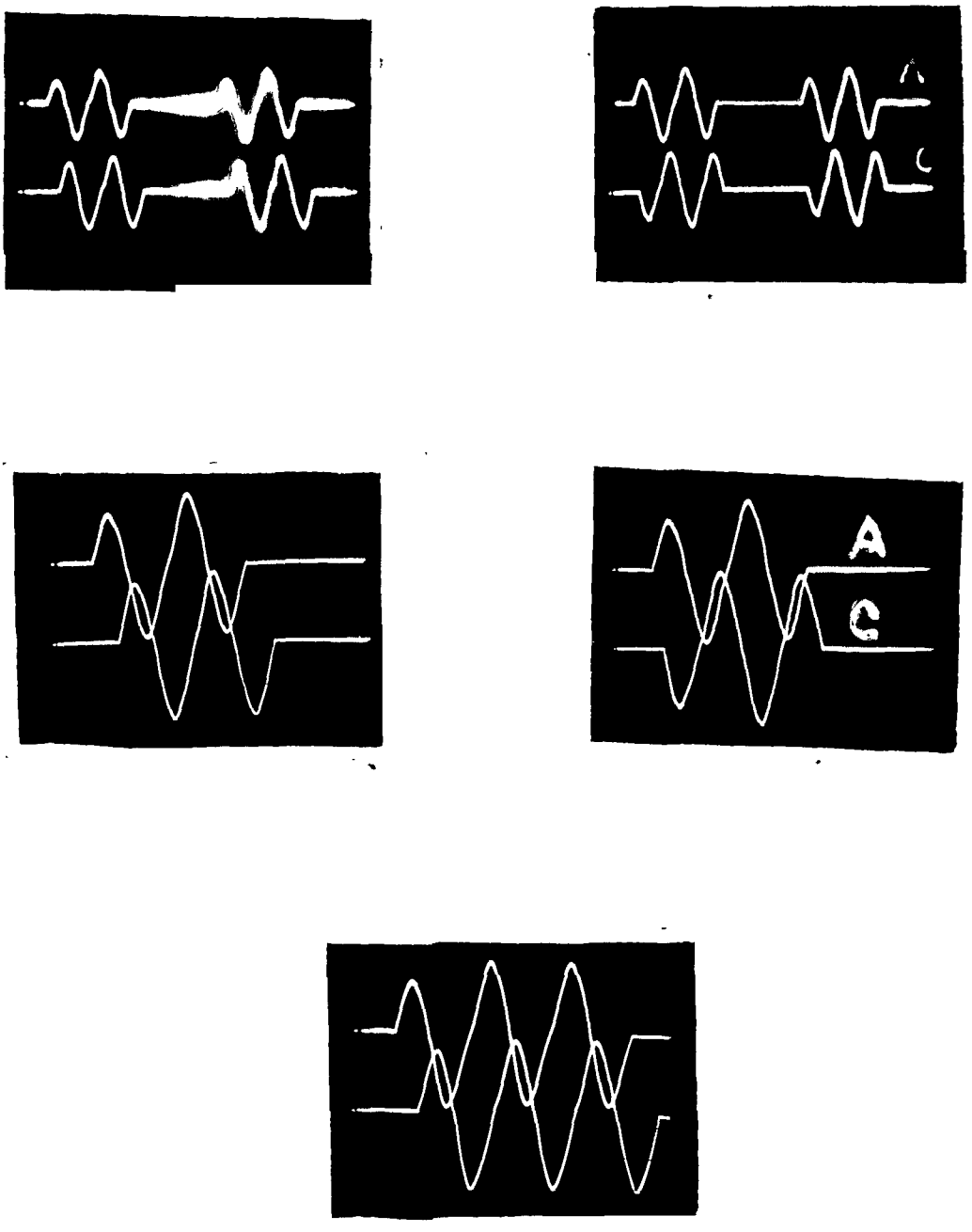

Fig. 4.6. Photograpic records of ICC of 3-phase inductive loads.

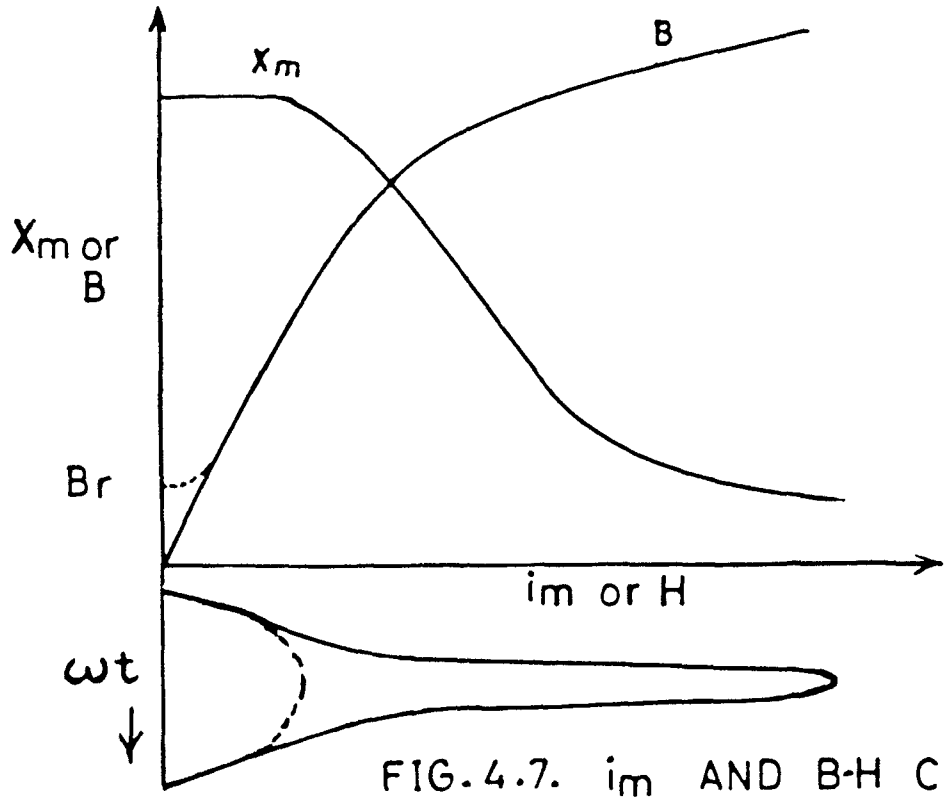

FIG. 4.7. i_m AND B-H CURVE

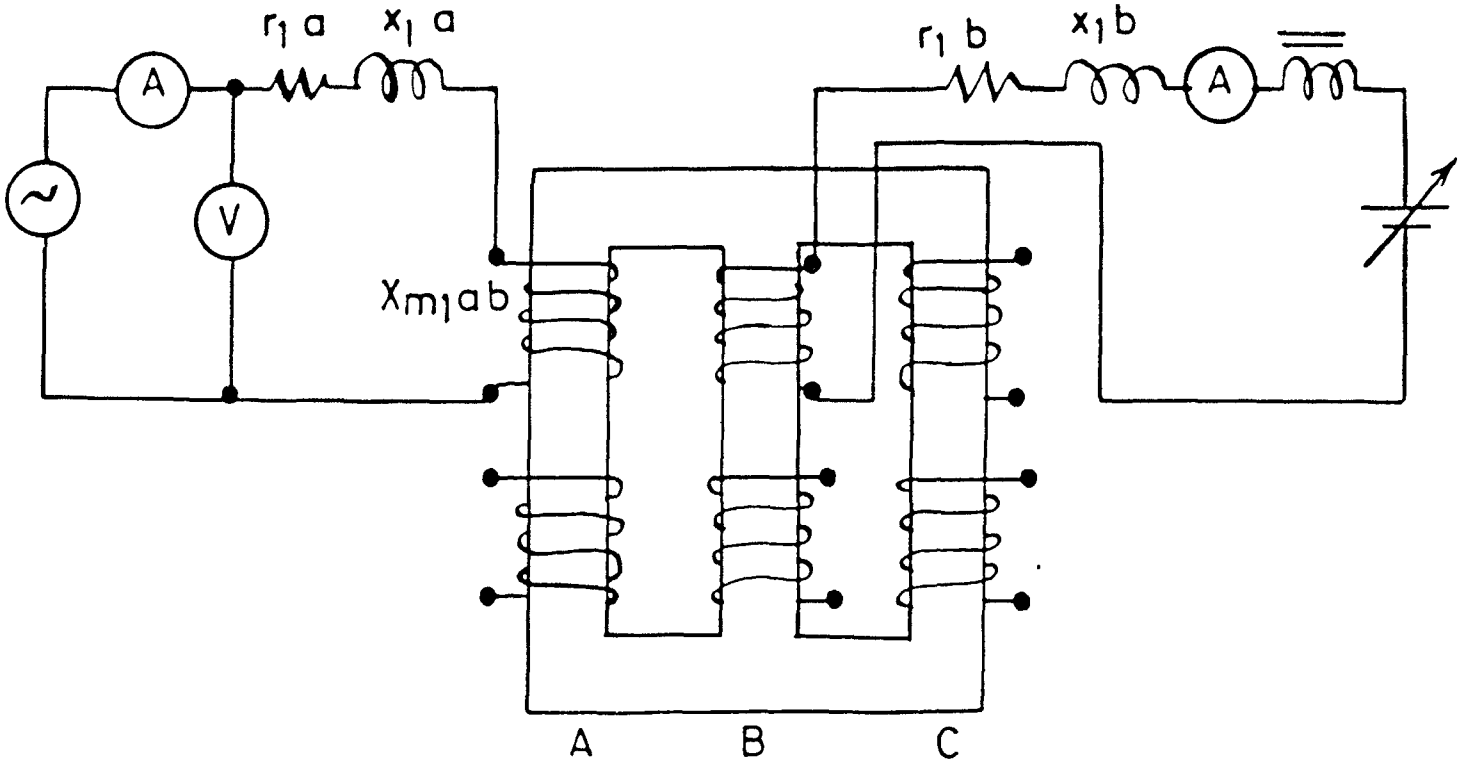

FIG. 4.8. MEASUREMENT OF MUTUAL AND MAGNETIZING REACTANCES.

material, and its physical dimensions are normally not available to the user. Moreover the methods so far available for the determination of B-H curve for the core material of a built-up transformer are not very simple and straight forward. The conventional methods available are step-by-step method and method of reversals [3]. But these methods require a search coil to be placed around the core and also the knowledge of the dimensions of the core (without the insulation around the stampings) of a built-up transformer and therefore the core cross-sectional area is assumed to be same as that of a coil [25,27]. This assumption could lead to errors ranging from 50% in a small transformer to 150-250% in case of a large transformer where windings are quite away from the core [28]. Spect had used piecewise linear magnetization curve and a particular conduction period in each cycle for calculation of the inrush current [24]. Rehman and Gangopadhyay combined the techniques reported in [24] and [25] for simulation of the inrush current in 3-phase transformers based on zero-sequence impedance and mutual coupling methods [29]. The sequence impedance method was used with the assumption that all the phases are electrically connected and magnetically isolated. But this assumption is valid only for a bank of three 1-phase transformers or a 3-phase shell type transformer. The second method (mutual coupling) was used with the assumption of constant mutual inductances between various phases. Practically it is not correct as the saturation or the presence of flux in each core (limb) causes variation in the flux linkages or flux distribution. This will be evident by finding the magnetizing and mutual inductances at different degrees of saturation of the core.

4.3.1 Measurement of magnetizing reactances

For this purpose, primary winding of 2 KVA, 230/115V, 3-phase, core-type transformer in series with a high inductor is energized by a variable DC source. The phase A winding is supplied from a small AC source as shown in Fig. 4.8. A very small alternating current is made to flow and corres-ponding impedance is calculated. The alternating flux, being very weak, will produce negligible iron loss in the core. The large value of the series inductance will not allow any significant amount of AC to flow in phase B winding (DC circuit). The circuit arrangement is similar to a saturable reactor. The resistance of the no-load branch of the equivalent circuit of a transformer, is large enough to be neglected as compared to the Xm under saturated condition of the core. The no-load current can therefore be safely taken same as the magnetizing current and the primary winding impedance and Xm constitute a simple RL series circuit. Hence the measured value of the impedance

$$Z_{1a} = \sqrt{[(r_{1a})2 + (Xm_{1ab} + x_{1a})2]} \qquad (4.1)$$

where r_{1a} and x_{1a} are resistance and leakage reactance of the primary winding of phase A, and Xm_{1ab} is mutual reactance between primary windings of phase A and B.

This impedance is calculated at various saturation levels of the limb of phase B. This gives the mutual impedance between the primaries of phase A and B i.e. Xm_{1ab}. Same technique is employed for the measurement of magnetizing reactance, Xm_{12}, of each phase (limb) by applying DC to the respective secondary winding also

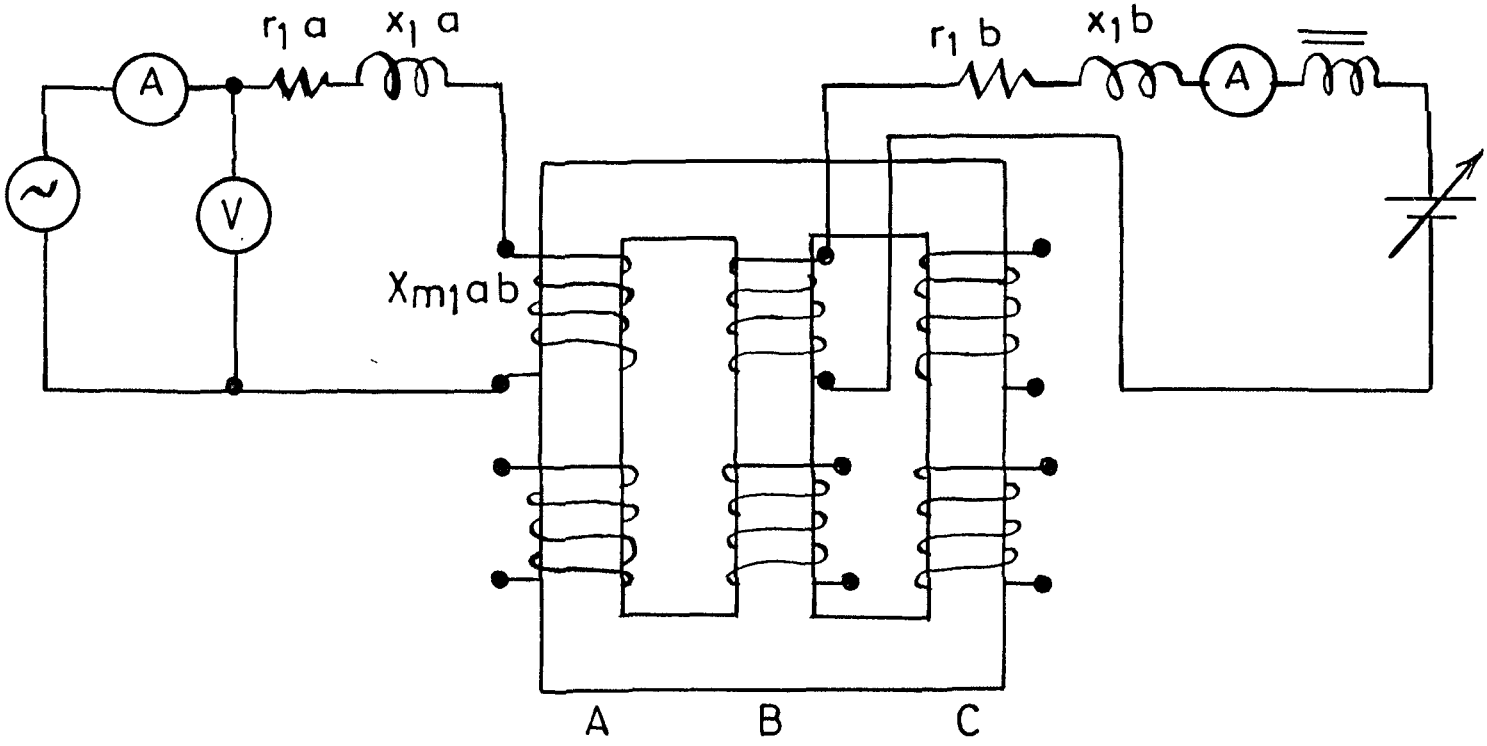

FIG.4.8. MEASUREMENT OF MUTUAL AND MAGNETIZING REACTANCES.

(which is required for estimation of inrush current when secondary is in delta mode). Graphs in Fig.4.9 clearly show that the magnetizing and mutual reactance do not remain constant at different levels of saturation.

4.3.2. Experimental records of inrush currents

ICS technique can thus be employed for determination of actual inrush current in the 3-phase as well as in 1-phase transformers. The actual inrush current in different configurations or with different initial conditions (SI as well as residual magnetization) can be found easily in a single attempt instead of repeated attempts by random switching which obviously does not guarantee the accuracy and will unnecessarily require more time and power wastage and create repeated disturbances by introducing harmonics in the line current, dip in the terminal voltage and RFI to neighboring lines. Similarly different switching current patterns can be obtained, at different conditions/configurations of machine and systems, by ICS for various purposes (e.g. pattern required for digital protection of power system).

The records of inrush current by ICS technique show the magnitude as well as nature of variation of the inrush current. Fig 4.10 shows the photographic records of the switching currents in phase A and B, at differentent SIs in a 3-phase transformer in star-star and star-delta configurations. To avoid large current peaks applied voltage are fixed at 40% of the rated voltage (near the knee point). The scale of currents in all the configurations of 3-phase transformer, are kept same for easy comparison.

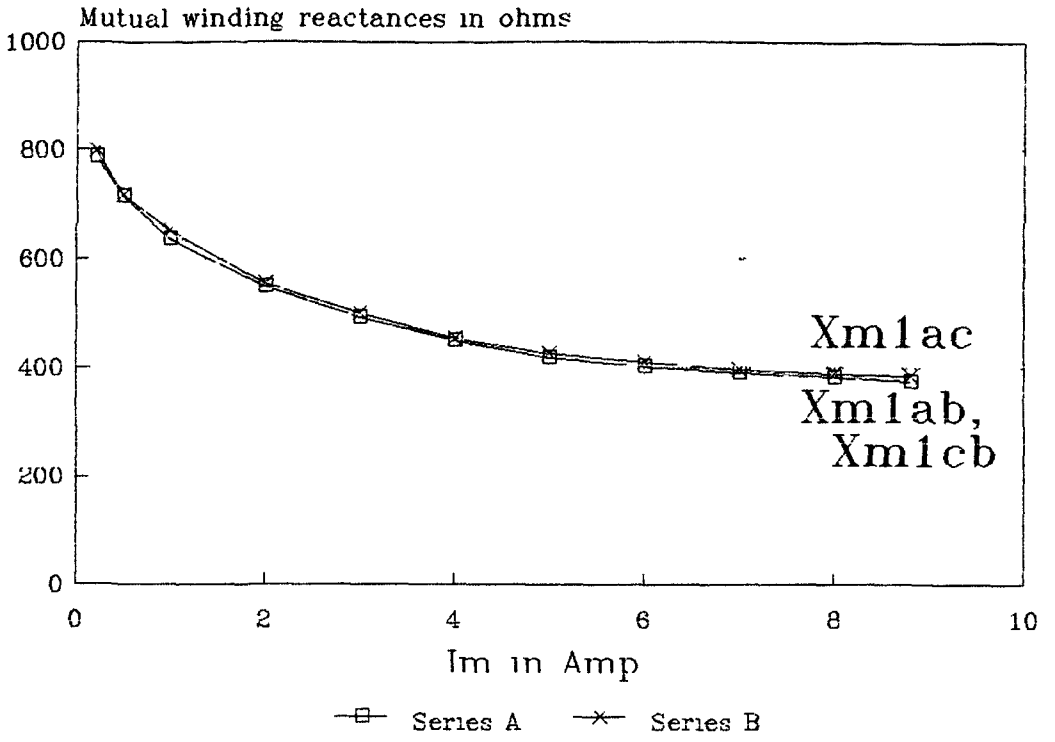

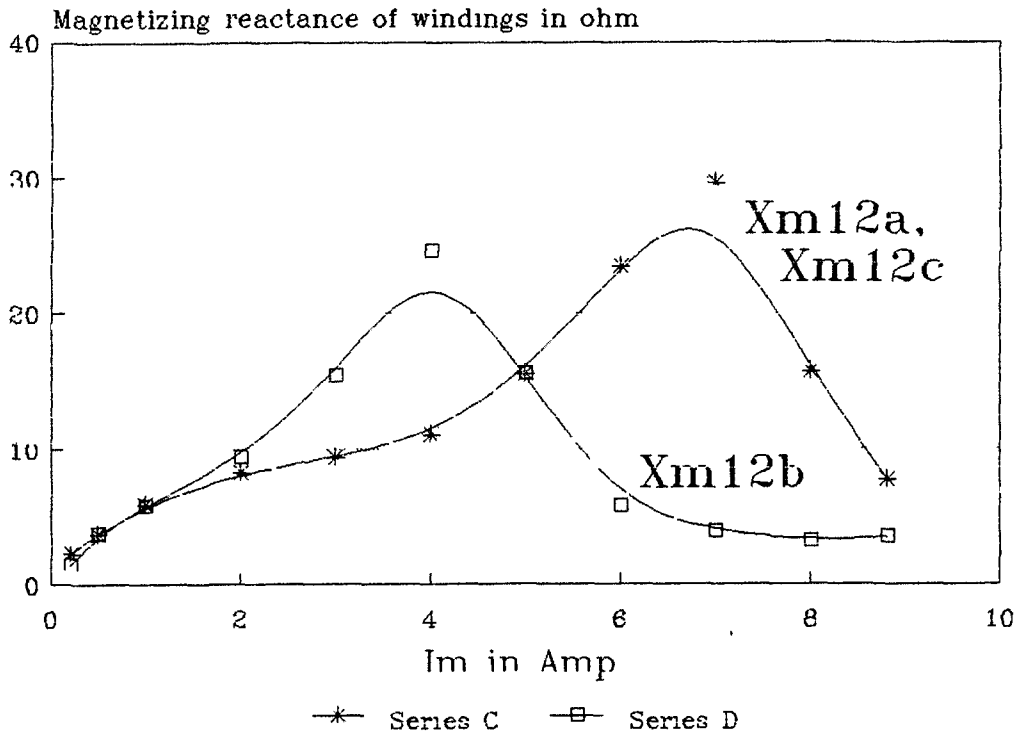

Fig.4.9 Variation of mutual and magnetizing reactances with respect to phase current of different windings of 3-phase transformer.

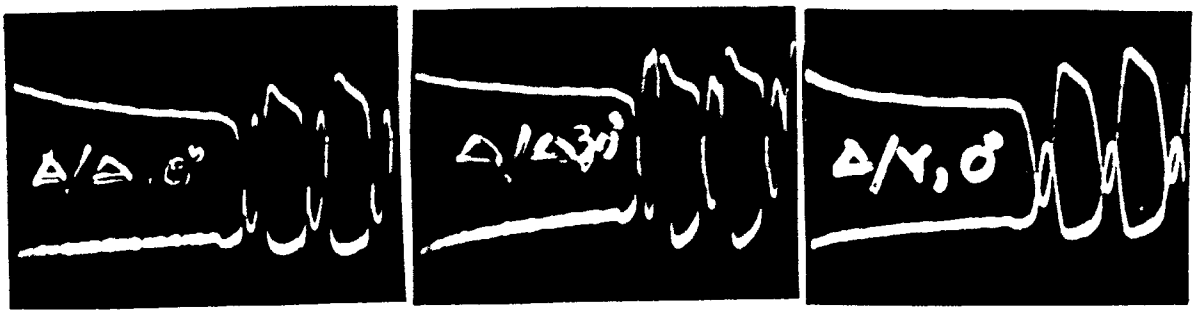

(a) (b) (c)

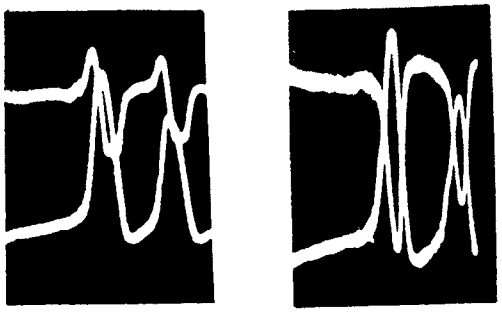

(d) (e)

Fig. 4.10. Photographic records of inrush currents in a 3-phase transformer at different SIs and configurations.

4.4. ICS FOR TESTING OF RELAY

Although the transient current in a transformer persists only for a short while, its large magnitude is sufficient to deceive a differential relay used for the protection of a power transformer. Therefore the normal practice is either to incorporate an arrangement (circuit) to desensitize the percentage-differential relay for about 0.2 second or to use a harmonic-current restraint relay [30]. One of the major drawbacks of the former method is its inability to respond to a fault which may occur during the desensitization period. In the latter case, the harmonic components of the current are separated, rectified and used for restraining purposes. The relay thus, efficiently differentiates between the magnetizing inrush current (rich in harmonics) and the short-circuit current. The obvious disadvantages of this system are its cost, size and the requirement of several auxiliary-transformers in addition to all the drawbacks of the electromagnetic relays.

The off-set nature of the magnetizing current (due to the DC transient component), instead of the the high-order harmonics (as in above mentioned conventional method) can be used to distinguish inrush current from the short-circuit or fault current. The large current peaks (several times the full-load current) of the magnetizing inrush current of a transformer may be either positive or negative depending upon the SI of the applied voltage and residual magnetizing flux, ϕr. Whereas in case of a fault, the large current peaks are positive as well as negative. These characteristics of the two currents (inrush and fault) may be

used to distinguish between the two conditions.

The block diagram of the relay is shown in Fig. 4.11. A low shunt resistance connected to the secondary of the CT converts the current signal into the voltage signal (Fig. 4.12). Two level detectors (for the negative and positive levels) are employed such that each gives a positive output when the voltage level exceeds the set value (corresponding to the peak of the allowable current). The outputs of the level detectors (LD1 and LD2) are connected to the pulse-stretchers and an AND gate. At fault condition both the LDs will have high output as shown in Fig. 4.13. While with the magnetizing inrush condition alone, either one or both the LDs will give a low (logic) output. At the steady-state (no-load or full-load conditions within allowable limit), both the LDs gives zero output as shown in Fig. 4.14.

Two identical active-level detectors are employed. A constant positive DC reference voltage is given to it for the magnitude comparison. An unity-gain inverting-amplifier is employed to enable the second level detector (LD2) to compare the negative level of the voltage signal. A capacitor and a zenor diode is connected at the output of the LDs. To avoid a separate power supply for the integrated circuit gate, a transistorized AND gate circuit using outputs of the LDs, is employed. Complete circuit is shown in Fig. 4.15.

The relay is tested for different θ as the inrush current of a transformer depends upon the SI. The ICS circuit allows a known type of current to start flowing in the primary of a single phase transformer corresponding to the predetermined SI and maintains

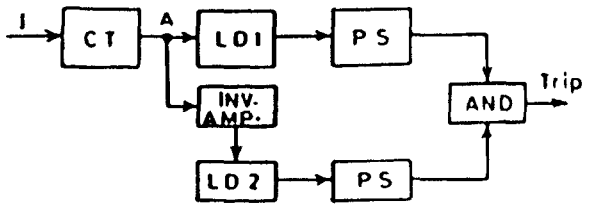

Fig. 4.11 Block diagram of the relay

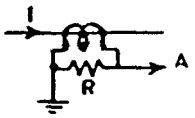

Fig. 4.12 Generation of voltage signal (A).

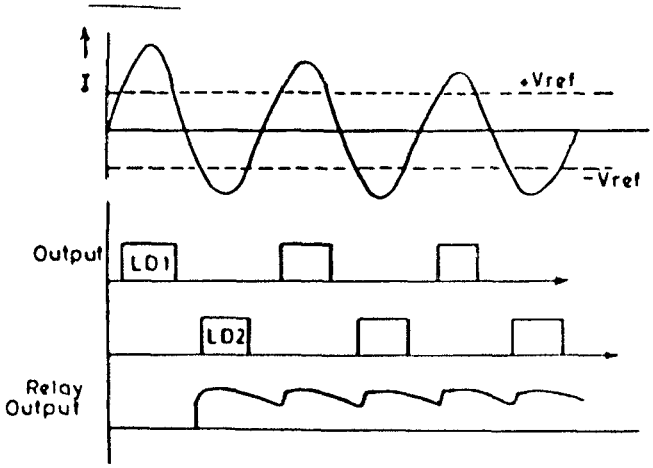

Fig. 4.13 Waveshapes at fault condition

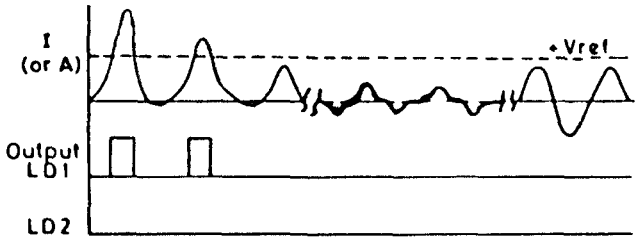

Fig. 4.14 Waveshapes at normal conditions

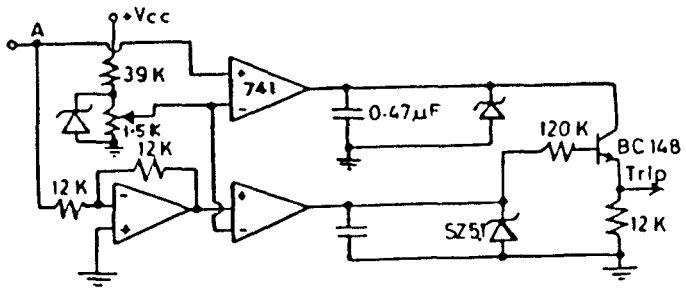

Fig. 4.15 Complete circuit of the relay.

conduction onwards. The complete testing arrangements are shown in Fig. 4.16. The fault current is simulated by connecting low resistance at the secondary side of the transformer. The performance of the relay is recorded with the help of an oscillograph. The photographs are showing the output of the relay and the inrush current (magnetizing only and with fault currents) at dynamic condition. The relay setting is adjusted at 150% (peak) of the full-load current. It is clear from Fig. 4.17 that the relay operates only at fault condition (current exceeds 150% of the full-load) otherwise not.

4.5 ICS FOR ELIMINATION OF INRUSH CURRENT IN TRANSFORMERS

The steady-state magnetizing current of a transformer is about 2-5% of the full load current. But the transient inrush current may be as high as ten times the full-load current and persists only for a short while i.e. for about one-half second [24]. Even then such a large magnitude causes intense localized heating leading to insulation damage, production of excessive mechanical stresses, voltage drop at the consumer's end, blowing of fuses, RFI with the neighboring communication lines and circuits (specially in case of traction transformers), parallel resonance in AC systems and false signals to over-current and differential relays. High induced voltage (1.7 times the normal peak) on the secondary side was found in the transformer of HVDC converter plants [31]. This transient induced voltage (peak) on the secondary side may be some times large enough to damage the circuit components specially the power semiconductor devices in

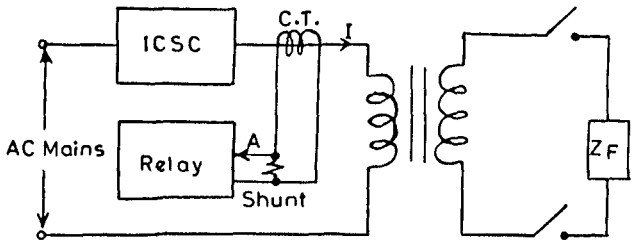

Fig.4.16 Testing arrangements.

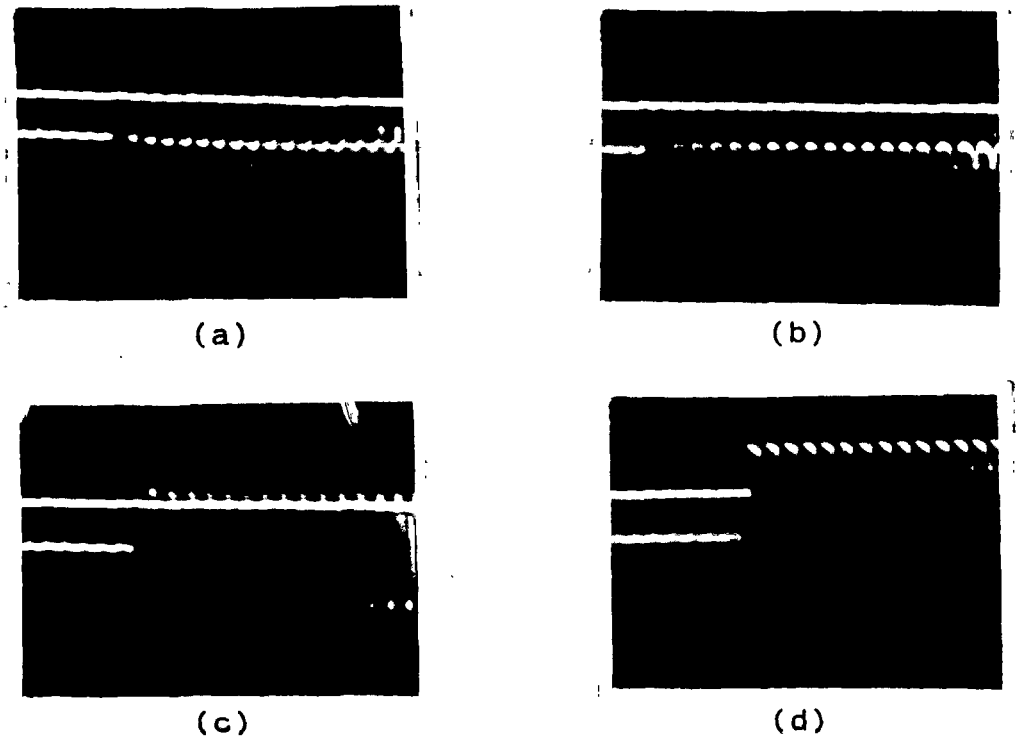

Fig. 4.17. Oscillographic records of switching current and output of relay (upper line) at different SIs. (a) Inrush current with positive and (b) negative offsets. (c) Current at loaded condition. (d) Output of the relay and the fault current.

Fig. 4.18 Inrush current at (a) θ=0 and (b) elimination of inrush current at θ=90 degrees in 1-phase transformer.

converter circuit.

As discussed in previous section, the resistance of the no-load branch of the equivalent circuit of the transformer, is large enough to be neglected as compared to the Xm under saturated condition of the core. The no-load current can therefore be safely taken same as the magnetizing current. Thus the primary winding impedance and Xm constitute a simple RL series circuit.

For RL circuit, if the SI or $\theta=\phi$, then transient current vanishes as discussed earlier. Hence the doubling effect will not take place and the switching current will confined be to its steady-state value only.

4.5.1 Elimination of inrush current in 1-phase transformer

When a faulty traction line is reenergized after removal of the fault and this switching happens to be close to the ZCI, then all the traction transformers of the engines of the stranded trains (in that zone) will draw enormously large amount of current simultaneously as discussed above. Thus causing the circuit-breaker of the other healthy parallel line to trip due to the RFI. This creates problem in smooth movement of the trains. Frequency of occurrence of this 'synthetic fault' is reported to be 2 to 3 times in a month in Aligarh zone of Northern Railways. Since a traction line is a short distance and 1-phase line and thus the line with the transformer constitutes a simple RL series circuit. Thus by reenergizing the line at $\theta=90^{\circ}$ (or 270°) using ICS circuit, the problem of the inrush current and its associated effects can be easily eliminated. This can be done by using the

static switch (thyristor) in parallel with the circuit breaker for initial switching.

The static switch can be realized easily by series and parallel combination of high rating thyristors (triac or SCRs in anti-parallel mode) depending upon the current and voltage requirements. The operating signal should be given simultaneously to the static switch as well as to the circuit breaker (both in parallel). The static switch operates almost instantly (within few micro-seconds depending upon rating of thyristors) which can be later separated out by an isolator as discussed earlier in section 3.2.

Fig.4.18 shows the inrush and normal magnetizing currents for a 1-phase transformer when switched at $\theta = 0^\circ$ and 90° respectively. The magnetizing current is confined to its normal steady-state value.

4.5.2 Elimination of inrush current in 3-phase transformers

Whenever a 3-phase transformer is energized, its one or two phases will be closed to its ZCI at the SI. Thus the choice of the SI control is limited to within 30° only, due to the symmetry of the three phases (Fig. 4.19) unlike the 1-phase system where SI can be varied from 0° to 360°. In a 3-limb, 3-phase, core-type transformer, the switching at points 1 & 2 will cause saturation in two limbs of the phase "A and B" or "A and C" as shown in 4.20(a) and (b) respectively. Where ϕa, ϕb and ϕc are the flux generated in each limb by the currents flowing in the respective windings. All the phases of a 3-phase transformer can be

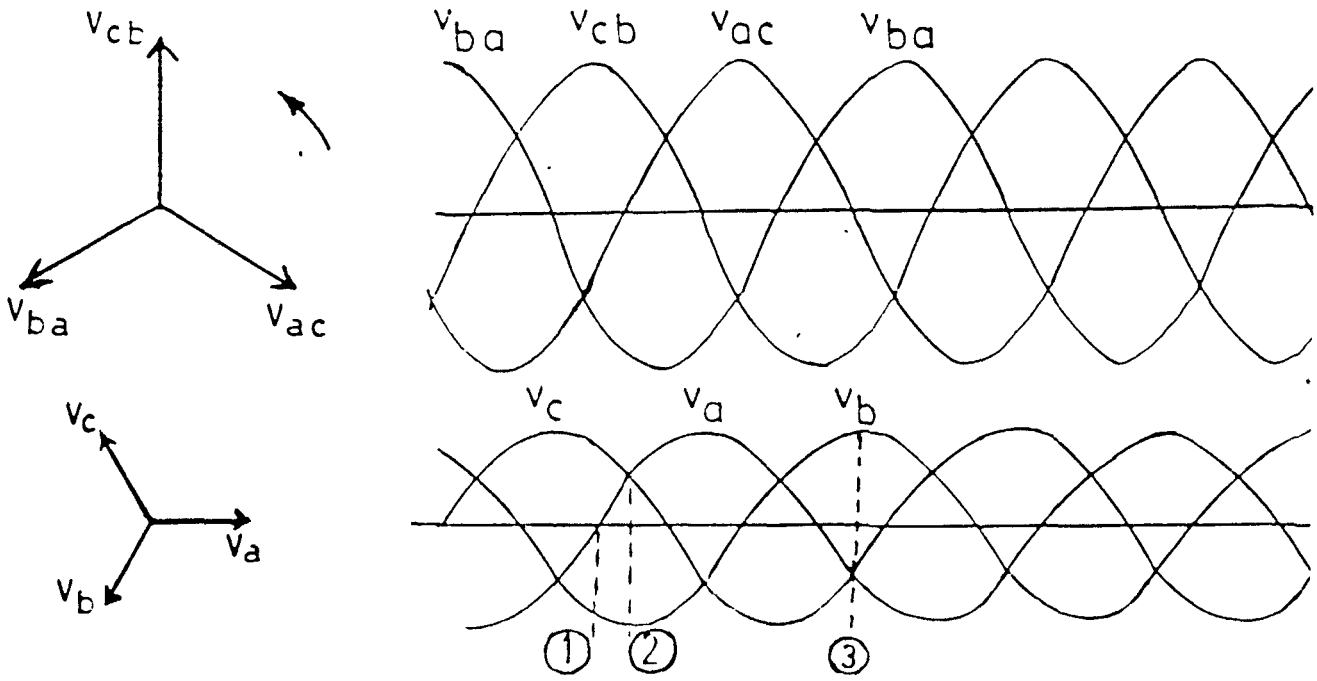

Fig. 4.19. Voltage waveforms at different SIs.

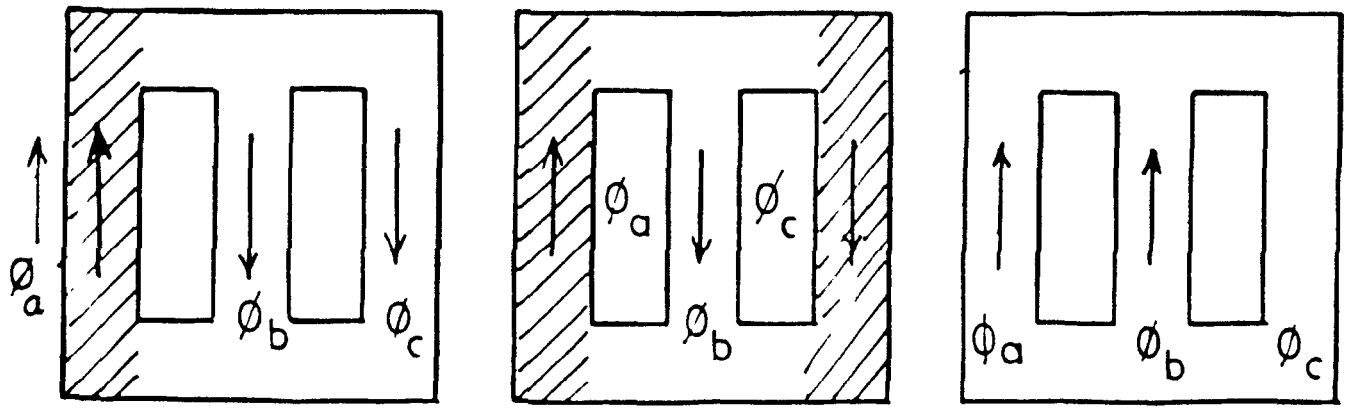

FIG. 4.20 CORE CONDITIONS AT SWITCHING OF TRANSFORMER.

considered, in crude sense, as electrically connected and magnetically isolated. Since an approximate model was used for approximate estimation of inrush current as discussed in previous section [29]. Therefore each phase of the transformer, whether core type or shell type, can be considered as an independent RL circuit.

(a) 3-phase,4-wire system:

By switching each phase of the transformer at the PF angle ($\theta=\phi$) or even at $\theta=90^{o}$, of their respective voltages, the inrush current (due to doubling effect) can be easily eliminated as discussed in section 4.2.2 for ICC of 3-phase independent inductive loads. In that case the switching completes in 1/3 time-period of the applied voltage cycle but the sequence of switching is reversed (A,C,B).

Although the A,B,C switching sequence takes more time (2/3 of cycle) but flux in core of transformer will be reduced at the SIs which is evident from Fig. 4.19 (point 3) and Fig. 4.20(c). Initially when phase A is switched at 90 degree of its phase voltage (B and C open), the transformer behaves as a 1-phase transformer/inductor, no saturation will take place and the switching current is same as the normal steady-state current. However when phase B is switched at 90 degree of its phase voltage (after phase A), both currents hence fluxes in both limbs are of same direction and thus opposing each other. Which reduces magnetizing reactaces both phases and hence over all magnitude of the switching current. Thus the switching angles with reference to phase A are

$$\theta 1=\theta a=90^{0}$$

$$\theta 2=\theta b=120^{0}+90^{0}=210^{0}$$

$$\theta 3=\theta c=240^{0}+90^{0}=330^{0} \qquad (4.3)$$

where θa, θb and θc are SIs of phase A, B and C. Experimental records of the inrush currents were already given in Fig. 4.10, when all phases of a transformer are switched simultaneously in different configurations and at random SIs. Fig. 4.21 shows the elimination of the inrush currents, when the different phases of the same transformer (3-phase, 4-wire system) are switched sequentially in steps by ICS technique as discussed above. Figures 4.21 (a) and (b) show the elimination of inrush current for the switching sequences A,C,B and A,B,C respectively. The switching currents (phase) and Ip, it can be seen, are confined to their normal or steady-state values. The scale of currents in both the cases are kept same for easy comparison.

(b)3-phase, 3-wire system:

In this case, each phase is firmly coupled with another whether it is connected in star-star, star-delta, delta-star or delta-delta combinations. Initially, if only two phases (say C and B) of a 3-phase, 3-wire system is switched-on simultaneously (irrespective of being in star or in delta configuration), the transformer behaves like a 1-phase RL load with line voltage impressed between C and B terminals. For delta configuration, it is like two parallel RL load circuits with same PF and different magnitudes. The total impedance between C and B terminals will be 2/3 of each winding (Z1). Similarly for star configuration, it is

(a)

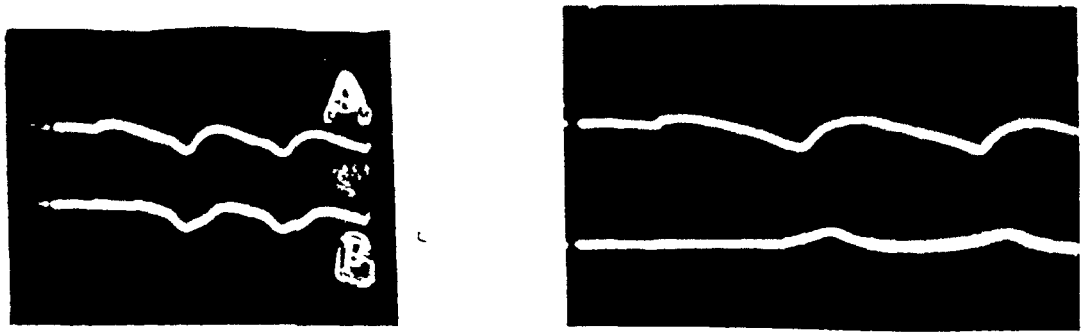

(b)

Fig. 4.21 Elimination of inrush current in 3-phase transformer by ICS. Switching sequence are (a) A,C,B and (b) A,B,C.

like two RL load circuits of same PF connected in series as shown in Fig 4.22. The total impedance will be twice Z1. Thus if the line voltage Vcb is switched at its 90° (or PZI of Va), although the applied (line) voltage magnitude is larger ($\sqrt{3}$ times Va_{rms} or 1.72 Va_{rms}) but it is less than double, no doubling effect hence no saturation will take place (due to $\theta=\phi$ or 90°). The line or phase currents in B and C phases will be equal and opposite, and confined to its steady-state value ($i_c=-i_b$). Thus the net flux in the limb A is zero as shown in Fig. 4.24 i.e. no flux (like residual, Or) will be present at any instant of switching of phase A . Now if phase A is switched at 90° of Va the current hence the flux in that limb will also be confined to its steady-state value and no inrush will take place.

Photographs in Fig 4.10 were already given to show the inrush current of 3-phase transformer in various configurations when all the phases are switched simultaneously. Fig. 4.25 shows the inrush current of the same transformer (as shown in Fig. 4.10 (d) and (e), for 3-phase and 3-wire configurations) is completely eliminated using the technique discussed above. The switching currents are like normal magnetizing currents (confined to their normal steady-state values) when the phase B and C, and phase A of the transformer are switched sequentially at 0° and 90° respectively with Va as reference voltage. Repeated switching at this condition (SIs) is done by ICC technique and it can be seen that the switching currents are confined to their normal (steady-state) values and don't change. The scale of currents in both the cases (maximum and minimum Ip) are kept same for easy comparison.

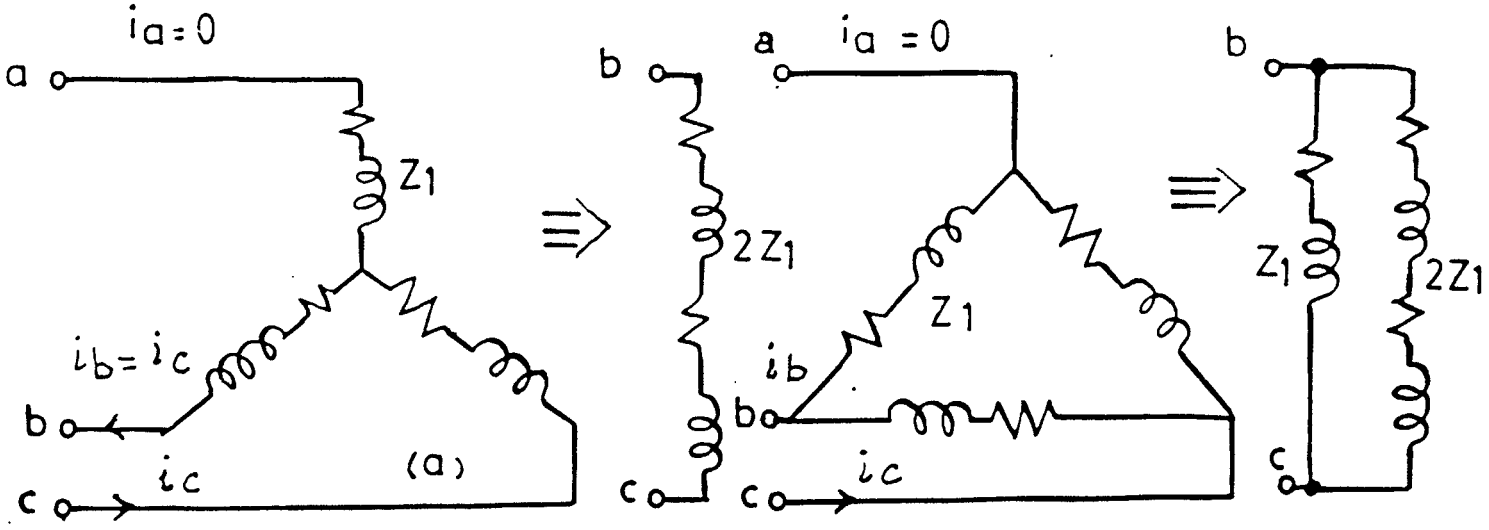

FIG. 4.22 : TRANSFORMER IMPEDANCE AT SWITCHING CONDITION.

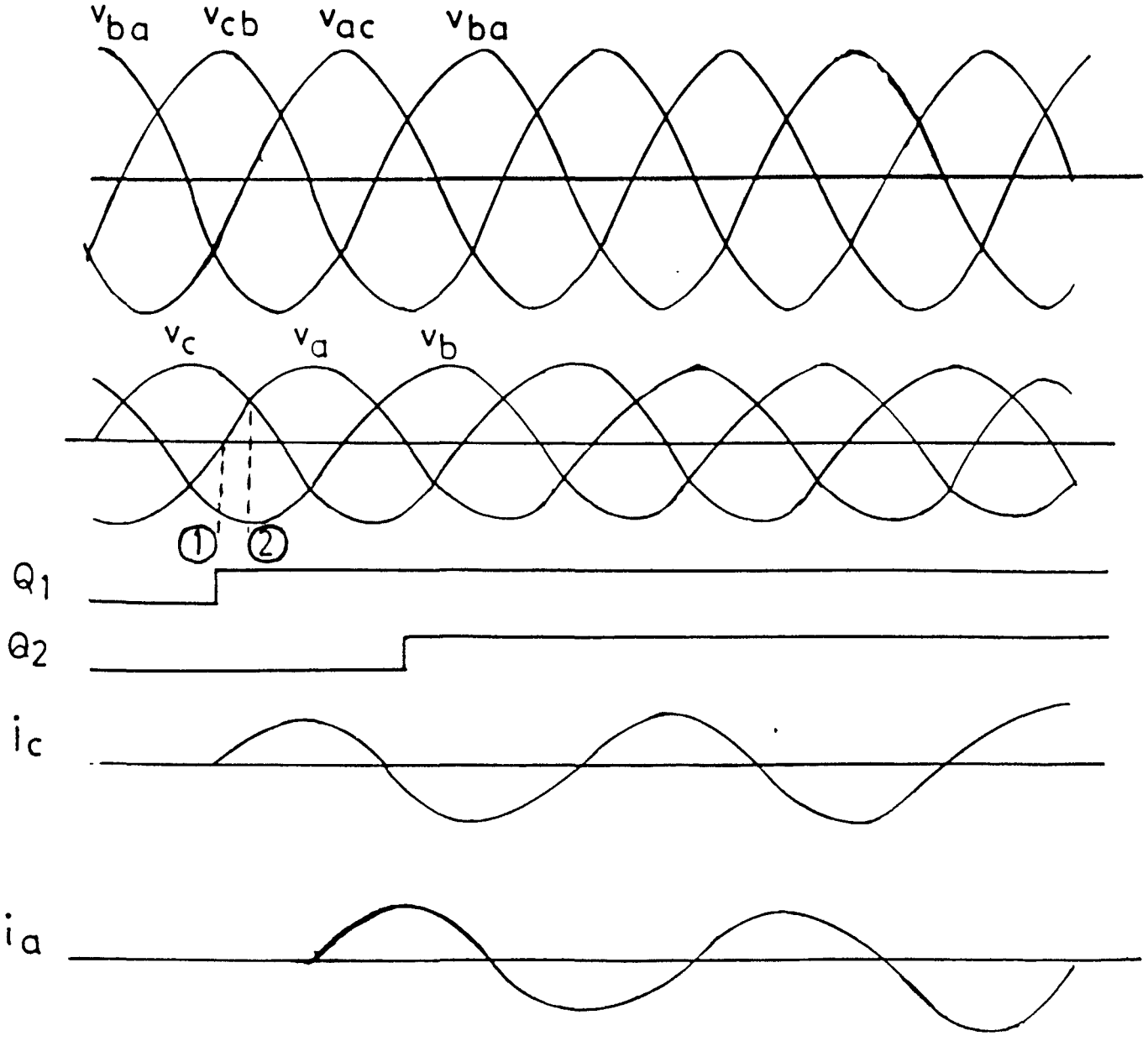

FIG. 4.23 SWITCHING OF THREE PHASE TRANSFORMER.

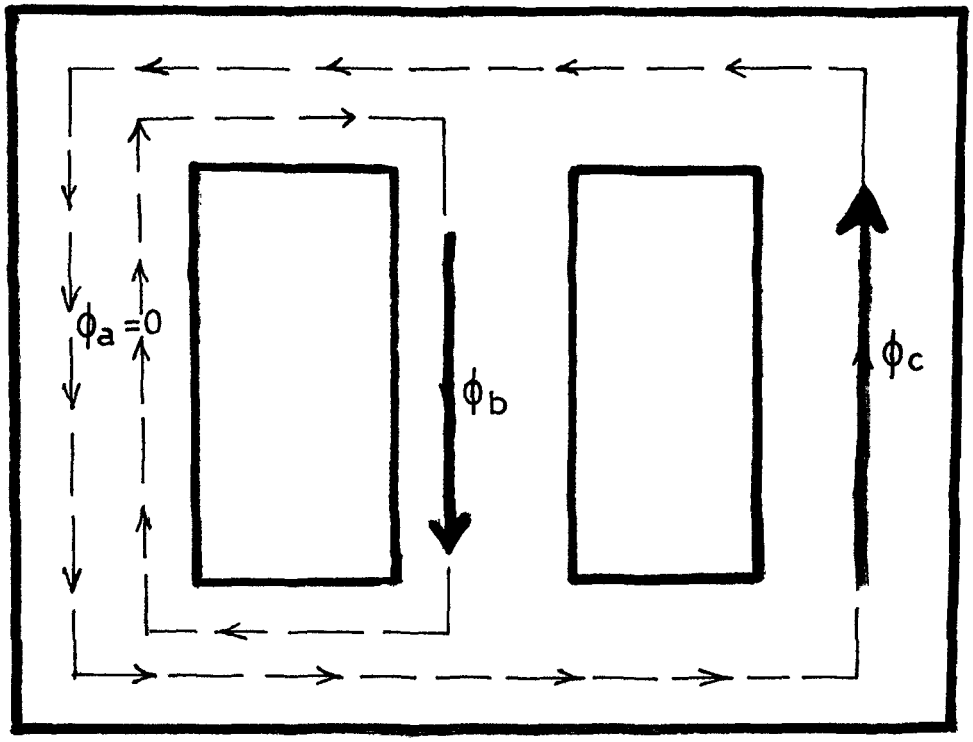

Fig. 4.24 CORE CONDITION AT SWITCHING INSTANT FOR 3-PHASE,3-WIRE ARRANGEMENT.

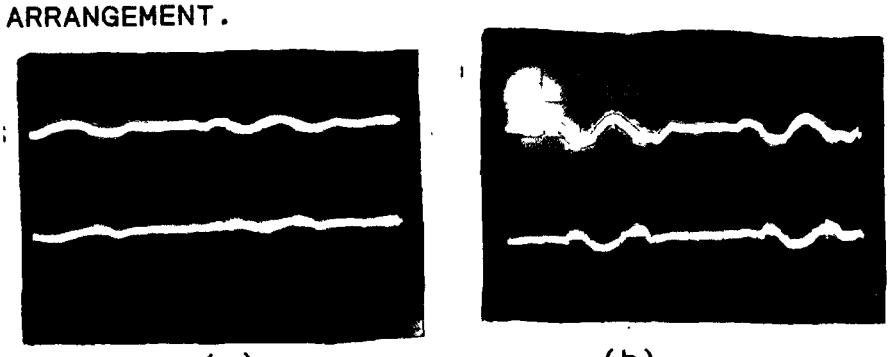

(a) (b)

Fig.4.25 ELIMINATION OF INRUSH CURRENT IN 3-PHASE TRANSFORMER (3-WIRE). (a) STAR-STAR AND (b) DELTA-STAR CONFIGURATIONS.

4.6 ICS FOR INDUCTION MOTORS

The switching current of an induction motor depends upon the stator impedance (including the effect of saturation, if present) and the effective rotor impedance which varies with the variation of speed (slip). The stator as well as rotor windings of an induction motor are basically a RL circuit of low PF. Therefore doubling effect may occur at random switching of the motor i.e. when switching happens to be at or near the ZCI of the applied voltage wave. Hence if the induction motor is subject to repeated switching, it may often draw large switching current from the line due to the doubling effect, in addition to the normal switching current due to rotor at rest or deceleration during off period. Moreover the saturated core (stator as well as rotor) may also aggravate the situation.

4.6.1 Switching current control of 3-phase induction motor

Switching current of a 3-phase induction motor is similar to the inrush current of a 3-phase transformer. Since the flux passes through the air-gap therefore effect of saturation is not so pronouncing and magnetizing current does not increase to several times the full-load current like transformer. However, at the time of starting from rest, induction motor behaves as a transformer at short-circuit condition. The rotor impedance dominates. Since the rotor resistance is very small, the PF of rotor impedance will be low. Normally the effective PF angle, ϕ, at rest or block rotor is about 70° (due to stator leakage winding impedance in series with the parallel branches of

magnetizing and rotor (referred values) impedances of the equivalent circuit [2]. Therefore switching current peak (Ip) increases by 35% in one or two phases for ϕ=70° (unsaturated core or linear circuit condition), when the random switching of the motor happens to be at or near ZCIs of the any phase voltage (as discussed in case of 3-phase transformers and it was already shown in Fig. 2.6). The peak current will be higher for saturated core (stator/rotor) condition.

Thus if motor is subject to repeated switching it will repeatedly draw higher switching current in one or two phases at the time of switching causing disturbances in the line. Switching currents can be thus controlled (reduced) by switching the different phases at different SIs in steps (instead of simultaneous random switching) as it was done for 3-phase transformers. Fig. 4.26 (a) and (b) show the switching currents when all phases of motor are switched simultaneously at running and stationary conditions of rotor respectively.

ICS technique can be thus applied to control/reduce these currents. Initially the line voltage Vcb is switched at its 90° (=0° of Va) followed by the phase voltage Va switched at its 90°. Fig. 4.27 shows the photograph of switching currents of the same motor (at running and stationary conditions) when all the phases are switched in "steps" not simultaneously. Thus the switching currents for both cases are significantly reduced.

4.6.2 Switching current control in 1-phase induction motor

The switching current of a single phase induction motor depends upon the main winding impedance, auxiliary winding

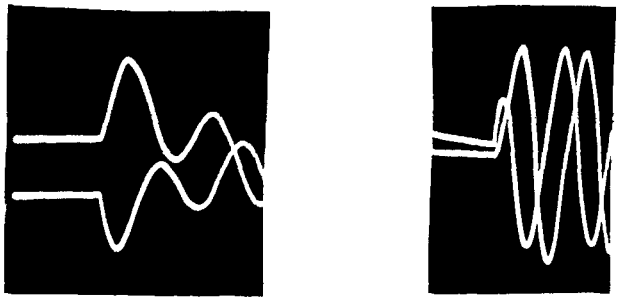

(a) (b)

Fig. 4.26 Switching currents of 3-phase induction motor. At (a) rotating and (b) block rotor conditions.

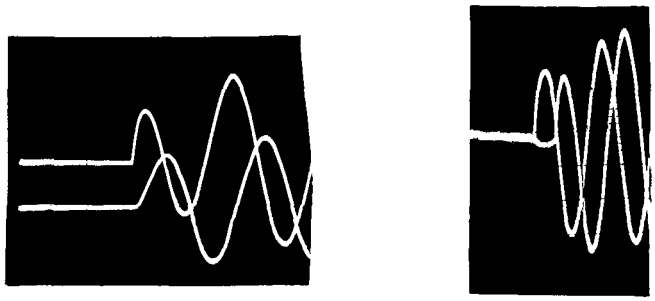

(a) (b)

Fig. 4.27 Reduced switching currents by ICS. At (a) rotating and (b) block rotor conditions.

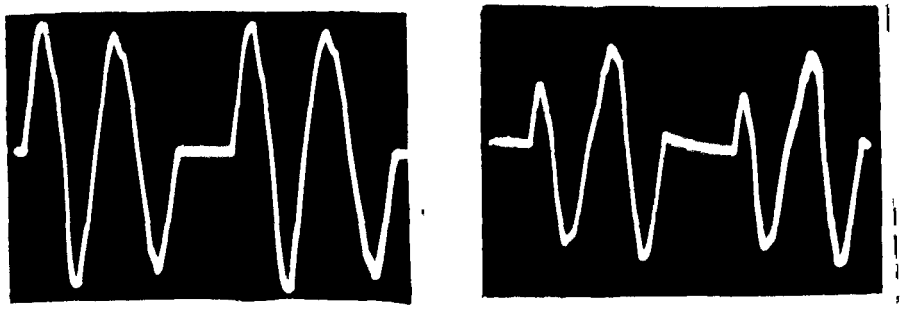

(a) (b)

Fig. 4.28 Switching main winding current of 1-phase induction motor. (a) Maximum at θ=0 and (b) minimum at θ=120 deg. by Icc.

impedance and the effective rotor impedance depending upon the speed (slip). When the motor is made to operate at nearly constant speed, by flywheel arrangement or by ICC of the supply voltage, there is no need of switching the auxiliary winding and no significant change in the rotor impedance takes place. The main winding impedance of the motor is inductive (RL circuit). Thus switching can be done at $\theta=\phi$ or so using ICS circuit to reduce the switching current as shown in Fig. 4.28. However induction motor in this mode has very limited application. Thus switching of the auxiliary (starting) winding is also required.

Since the auxiliary winding circuit is a capacitive under-damped RLC circuit, its switching, with the trapped charge on capacitor (initial condition, Qo), will cause large switching current peaks (Ip) at different SIs, as discussed in detail in chapter 2 (section 2.3.2.). Even with zero initial condition, the switching current peak (Ip) may not be insignificant depending upon the value of the capacitor. Thus ICS technique can be applied to reduce the switching current either by switching

(a) both the windings simultaneously at an appropriate SI depending upon their impedance and effective PF as well as Qo.

(b) auxiliary and main windings sequentially, at different suitable SIs, as it was done for 3-phase transformer.

(a) Simultaneous switching: A suitable SI can be found for adopting the former technique. Since the effective PF angle, ϕ, of 1-phase induction motor is close to 0° (lagging), comprising parallel combination of an inductive RL circuit (main winding) and a capacitive RLC circuit (which behaves as RC circuit). The

value of ϕ depends upon the individual magnitudes and PF angles of both branches. Since the maximum peak current (Ip) with respect to θ, depends upon the Qo or on the initial voltage (polarity as well as magnitude) on the capacitor. Therefore it will be useful to discharge the capacitor before next switching, to make initial condition zero and, to keep Ip low. For this purpose a suitable high value resistance (according to the frequency of repeated switching of the motor) is required to be connected in parallel with the capacitor. Thus a particular SI can be set permanently.

The current response at the time of starting of a 1-phase induction motor (at block rotor condition and with zero initial condition, Y=Qo=0) is computed and shown in Fig. 4.29. The circuit parameters are given in Appendix V. Although the effect of saturation was not considered even then it shows clearly that a suitable SI (here θmin=120°) can be selected for minimum Ip.

(b) Switching in step by ICS: At the time of starting the motor from rest, the PF angle of the main winding, ϕm, due to the parallel branches of magnetizing reactance and effective rotor impedance of the equivalent circuit, is inductive (ϕm= 60° to 70°). Thus the auxiliary winding and the main winding of a 1-phase induction motor can be switched sequentially at θ1=0° and θ2=ϕm (or even 90°) respectively to reduce the switching current.

Experiments were carried out on a 0.5HP, 1-phase induction motor. Fig. 4.30 (a) shows the oscillographic records of the switching current (total line current) when both the windings of motor is switched together randomly at θ=90° with zero initial

FIG. 4.29 Switching current response of 1−phase Ind.Motor at different SIs.

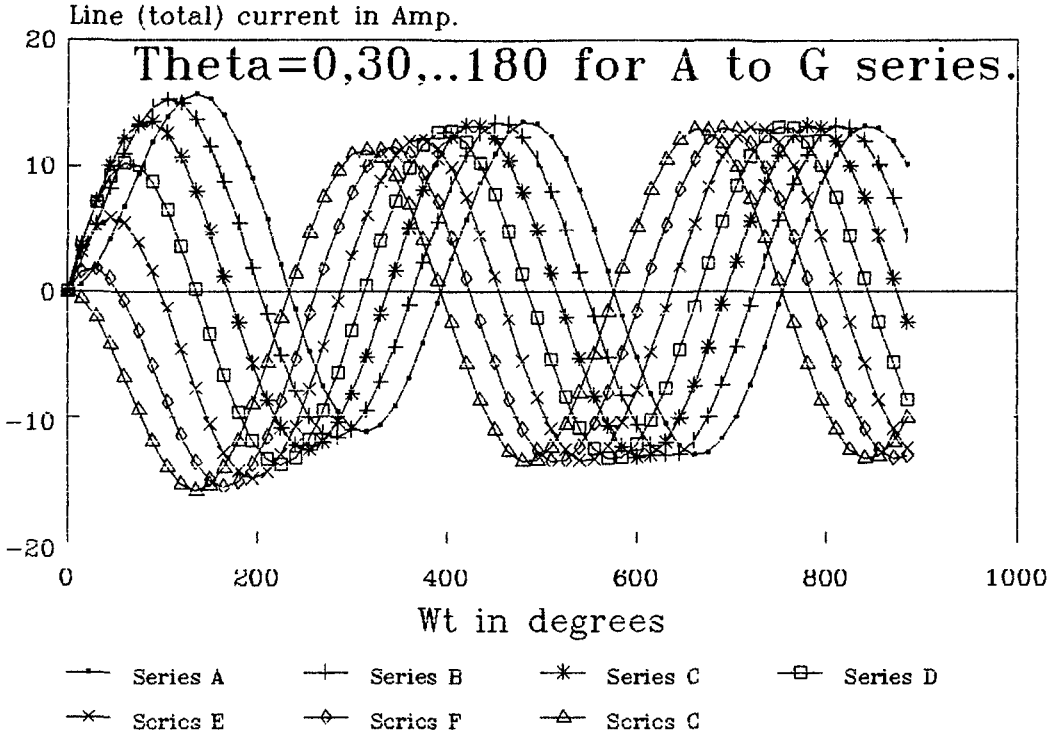

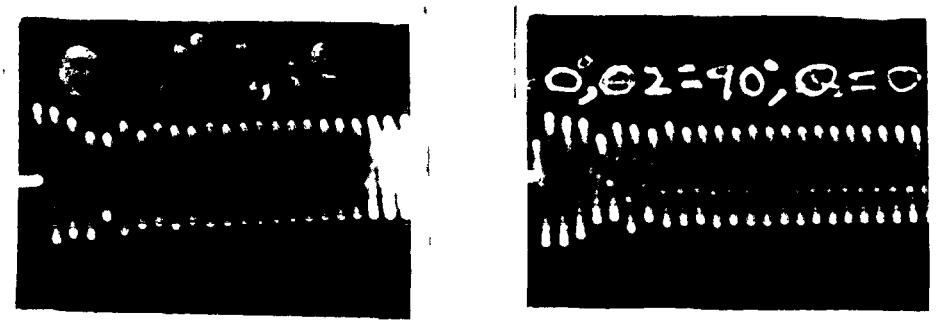

(a) (b)

Fig.4.30 Oscillographic records of switching current (line) of 1-phase induction motor. (a) Randomly at θ=90° with Y=0 and (b) switching in steps by ICS.

condition. While Fig. 4.30(b) refers to that condition when both auxiliary and main windings are switched sequentially (in steps) at $\theta 1=0^{\circ}$ and $\theta 2=90^{\circ}$ respectively. The peak of total line current is significantly reduced.

4.6.3 Speed control of 1-phase induction motor

The speed control of induction motors by ICC is not popular because it causes pulsating torque and random switching during ON period may cause switching to take place closed to ZCI (like ZVS), which causes DC offset or higher current peaks in RL loads. Moreover fine speed control is not possible due to the step voltage variation. The ICC technique employed is normally based on the time-ratio control i.e. by varying the number of ON cycles while keeping the total cycle (ON+OFF) constant [32]. At lower speeds the applied voltage hence the number of ON cycles has to be kept low. Therefore for longer periods (during the OFF cycles) the electrical torque generated is zero causing pulsations on the shaft (torque and speed both).

Here another scheme is proposed to remove these drawbacks by keeping the OFF period fixed and minimum i.e. one cycle (or even half cycle) in addition to the use of ICS circuit. The voltage control is thus possible from 50% to 100%. Thus the controlled voltage available are 50%, 66.67%, 75%, 80%, 83.3%, 85.7%, 87.5%, 88.88% and 90% of the applied voltage for total cycles (OFF+ON) ranging from 2 to 10 respectively and so on. Since torque is approximately proportional to the square of the applied voltage hence speed variation in a large range is possible by this method. Moreover the electrical torque is absent only for small

durations (20 msec. for 50 Hz supply). Thus the pulsation in the torque and speed is not significant due to inertia. It is evident that a very fine speed control is possible in higher range.

Ninety percent electric motors in the world are 1-phase induction motor [2]. Most of them are used in fans, blowers domestic or other low power appliances, where precise speed control is not required. The speed control is achieved either by tap changing of a variable resistance or inductor (regulator) in series or by using phase-controlled switching of thyristor. The resistance causes heating of the surroundings and the power wastage while the inductor decreases PF of the line current. The phase-controlled switching scheme introduces harmonics in the line as well as heating of the core of induction motor that may lead to early insulation breakdown. The speed and voltage at different steps of speed regulator (resistive) of a ceiling fan (230V, 90 Watts, 1.4 m sweep, GEC make) is shown in Fig. 4.31. Since the lower speed corresponds to 56.6% (130V) of the rated voltage (230V). Thus ICC technique can be effectively used for controlling the speed of 1-phase induction motor over wide range.

Speed of a 1-phase induction motor is successfully controlled by ICC method. Fig. 4.32 shows the speed variation with respect to number of ON cycles (with one OFF cycle).

The switching current can be controlled by ICS technique either by switching

(a) both the windings simultaneously at certain SI, or

(b) the main winding only at $\theta=\phi$ or 90°, while keeping the auxiliary winding on.

FIG.4.31 Speed-voltage charact. of fan.

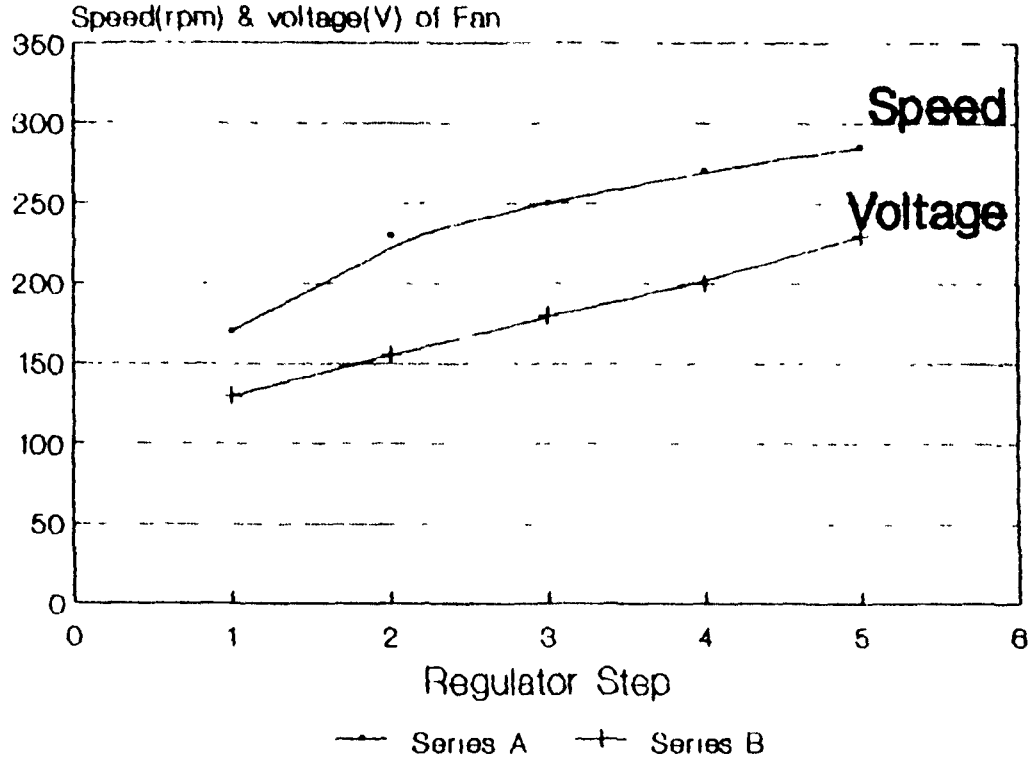

FIG.4.32 Speed variation by ICC.

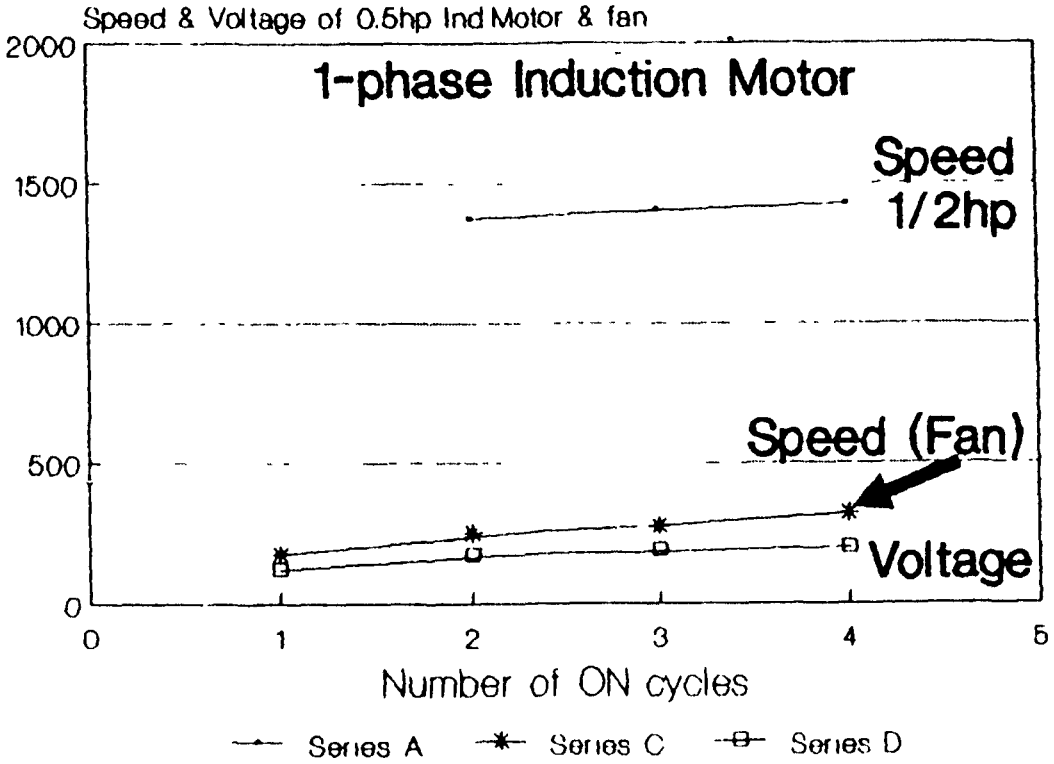

(a) Simultaneous switching: For the former case during the OFF period, the capacitor discharges through the auxiliary as well as main winding (under-damped oscillation). Thus the polarity as well as magnitude of Qo or "Y" at the SI of both the windings will depend upon the trapped charge at the end of ON period as well as the duration of OFF period. Where the polarity of the trapped charge at the end of ON period depends upon whether the auxiliary winding current stops at its positive half-cycle or negative half-cycle. Thus the optimum condition or θmin will vary and depend upon these conditions. Which can be easily found experimentally by varying θ by ICS technique. Fig. 4.33 (a) and (b) show photograph for maximum and minimum auxiliary (upper) and total line currents when switching is done at 150^3 and 120^3 respectively.

(b) Switching main winding only: Fig. 4.34 (a) and (b) show the auxiliary (upper) and main winding currents, when the later control technique is adopted, for $\theta=180^0$ and 30^0 respectively. It is evident from both figures that a suitable SI reduces the peak current.

4.6.2 Speed Control of 3-Phase Induction Motor

Power in any load circuit can be controlled by ICC technique. However to avoid large switching current peaks (higher Ip), ICS is required during each ON period. Since the impedance of a 3-phase induction motor is basically inductive. Therefore ICC technique for inductive or RL loads, as given in section 4.2.2, can be extended easily for controlling the power hence speed of a 3-phase induction motor. It can be achieved either by

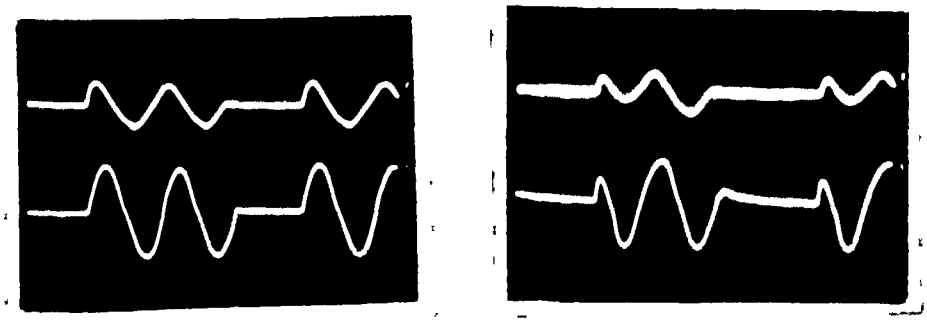

(a) (b)

Fig. 4.33 Auxiliary (upper) and total line currents of 1-phase induction motor under ICC condition at different SIs. (a) θ=120° and (b) θ=150°.

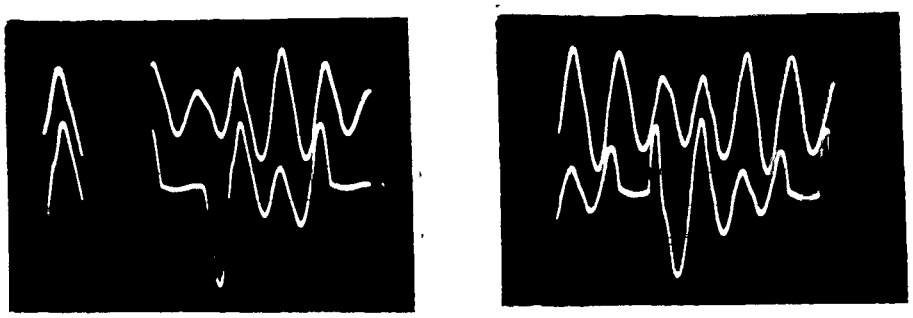

(a) (b)

Fig. 4.34 Auxiliary (upper) and main winding currents of 1-phase induction motor under ICC condition at different SIs. (a) θ=180° and (c) reduced peak at θ=30° .

(a) switching the different phases in steps (as in case of the 3-phase transformer) during the ON period, or

(b) controlling only one phase by the ICC technique while keeping both the remaining phases ON as it was done for 1-phase induction motor.

(a) Switching in steps: The former method causes large pulsation in the torque since the air-gap flux drops to zero during each OFF period. However the pulsation can be reduced by keeping the OFF period to one cycle and varying the total (ON+OFF) period, as discussed in previous section for 1-phase induction motor. Fig. 4.35 shows the photographs of the switching current waveforms for different number of ON cycles when switching is done in step (Vcb at its 90° or 0° of Va, then Va at its 90°).

(b) Switching one phase only: The torque generated by the later technique is more smooth as motor continues to run and generates torque by one line voltage even if one phase is off (during OFF periods of ICC). Thus 3-phase motor behaves as a 1-phase motor, although the generated torque is reduced but it does-not drop to zero, during OFF period. Fig. 4.36 Shows the speed variation for different ON cycles by second method. Fig. 4.37 (a), (b) and (c) show the switching current waveforms when only one phase is controlled by ICC technique at θ=30°, 210° and 120° respectively. It clearly shows, as in previous case, the switching at the controlled instant (θ=120°) reduces the peak current.

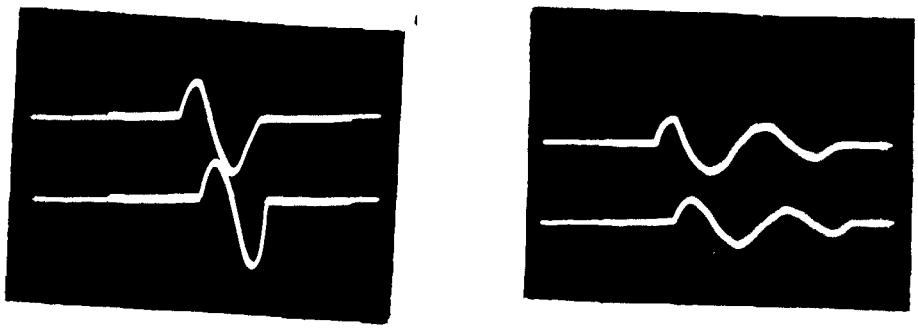

Fig. 4.35 Reduced switching currents of 3-phase induction motor by ICC and ICS (in steps) for different ON cycles.

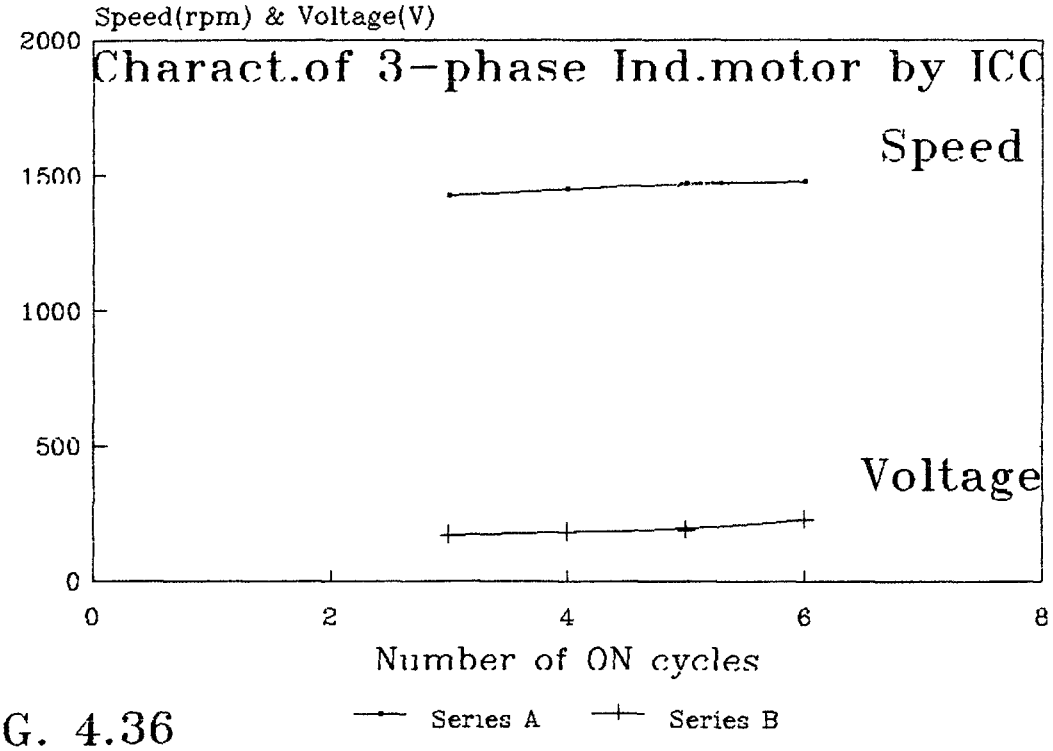

FIG. 4.36

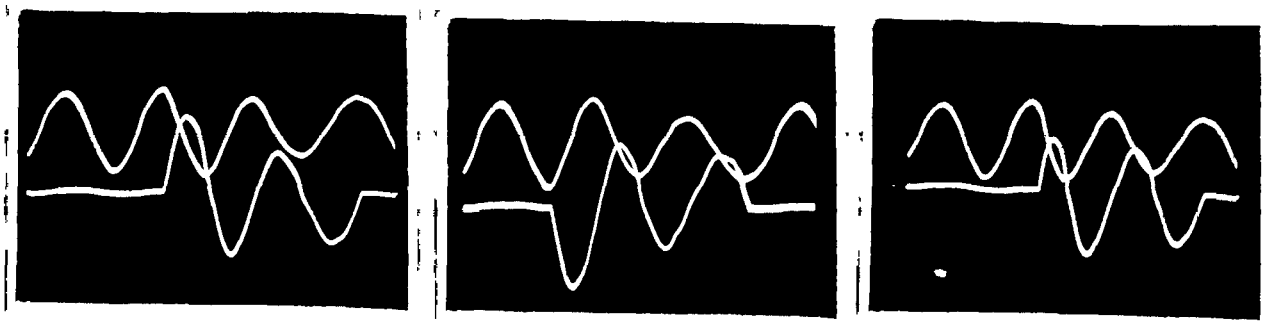

Fig.4.37 Switching currents of 3-phase induction motor by ICC and ICS at different SIs (in phase A only). (a) $\theta=30^{\circ}$, (b) $\theta=210^{\circ}$ and (c) reduced Ip (peak current) at $\theta=120^{\circ}$.

5. CONCLUSION

5.1 CONCLUSION AND FUTURE WORK

It can be now concluded on the basis of previous descriptions that the magnitude (peak) and nature (waves-shapes) of the switching transient current varies over large range depending upon the initial condition and the switching instant of the circuit. The switching transient current studies are generalize and simplified by introducing two factors *Y* and *n*. Thus the switching current level (peak) of all types of the linear AC circuits, can be controlled in between its maximum and minimum values, simply by controlling the SI, at any initial condition. The graphs, showing the peak currents with respect to the whole range of SIs, are given for different types of the circuits at various initial conditions. Equations are also given to find out the correct SIs for minimum and maximum switching currents in the circuit. The minimum value of Ip corresponds to the condition where the transient is either zero or minimum and the maximum value of Ip gives the correct value of the maximum possible switching transient current that may flow into the circuit. The theory presented here are experimentally verified and can be extended easily to non-linear circuits and systems as it is applied here for induction motors and transformers.

Three ICS circuits are designed for controlling the transients in different load circuits. These circuits are found versatile in nature. The MCC is used for transient-free power control in resistive as well as in inductive loads (by combination of ICS and ICC techniques) in addition to its ability to work as controller for converters and choppers. MCC is successfully used as static relay to realize various characteristics of distance protection. Three phase reference sinewave is also generated by MCC that can be used for PWM.

A static relay is designed to distinguish fault current from the inrush current of transformer and it is successfully tested by ICS circuit under dynamic/actual conditions.

By ICS technique, for the first time, inrush current in 1-phase as well as 3-phase transformers are completely eliminated. Which will have enormous utility and applications in power systems. The importance of elimination of inrush current in 1-phase transformers (traction as well as used in converter plants with line filters in HVDC system) is discussed. Its utility in other field could also be sorted out e.g. transformer used in welding etc. [24]. Inrush current in 3-phase, 3-wire system was eliminated more efficiently than in 3-phase 4-wire system. In the former case the switching completes in lesser period (two steps and quarter cycle only). While in later case the switching completes in three steps and the switching currents, although very small, flow in the neutral wire till switching completes in 2/3 cycle. It is shown that the transformers can be switched even repeatedly, without the significant amount of transient current (inrush), by the proposed technique.

By ICS technique the switching current of induction motors (1-phase and 3-phase) also reduces significantly. Instead of simultaneous switch-ing, the switching has to be done in steps as it was done for transformers. A suitable SI is also found for minimum switching current (peak) in case of simultaneous switching of a 1-phase induction motor. Thus the large switching current of saturated motors can be reduced more efficiently.

The speed of 1-phase as well as 3-phase induction motors are controlled by combination of ICS and ICC technique. A minimum OFF cycle (one or half) is proposed to avoid large pulsation. The speed variation is achieved over wide range without significant pulsation in torque and speed. Its utility for 1-phase induction motor (as prime mover of electric fans, coolers and compressors) is established. Thus large power wastage in the rheostatic regulators can be avoided easily by the proposed technique. Which will be certainly a boon to a country like India where the millions of 1-phase induction motors are in use and where power generation is far behind the power demand.

ICS technique can be extended easily for the determination of "decrement factor" of alternator for selection of circuit-breaker of proper MVA rating. Which is normally found by extensive random short-circuiting the alternator [4]. This test can be done in single attempt by ICS technique as it was done for determination of inrush current of transformer. Similarly maximum switching current of any machine can be found in single attempt.

In general ICS technique can be extended to all electrical circuits or systems which are subject to repeated switching and where transient condition has got some significance.

REFERENCES

[1] R. M. Kerchner & G. F. Corcorn, *Alternating Current Circuits,* Toppan Company Ltd. Tokyo, 1960, chapter XIV.

[2] V. Deltoro, *Principles of Electrical Engineering,* New Delhi: Prentice-Hall of India Pvt. Ltd., edition 2, 1975, Chapter V.

[3] E. W. Golding & F. C. Widdis, *Electrical Measurement and Measuring Instruments,* Allahabad: Wheeler publishing, 1956, chapters IX & XVI.

[4] A. T. Starr, *Generation, Transmission and Utilization of Electrical Power,* London: ELBS and Sir Isaac Pitman & Sons Pvt. Ltd., Edition 4, 1957, Chapter VIII.

[5] W. Shepherd, "Steady-state analysis of series resistance-inductance circuit controlled by Silicon controlled rectifiers," IEEE Transactions, Vol. IGA-1, No 4, 1965, pp. 259-264.

[6] W. Shepherd, "Steady-state analysis of single-phase, parallel, resistance-inductance circuits controlled by SCR pairs," IEEE Transactions, Vol. IGA-2, No. 6, 1966, pp. 469-473.

[7] P. J. Gallaghar, T. G. Blant & W. Shepherd, "Power-factor of thyristor-controlled loads with sinusoidal supply voltage and integral-cycle triggering," IEEE Transactions, Vol. IECI-24, Feb. 1977, pp. 92-96.

[8] A. Rahman, S. E. Haque & I. A. Al-Gadhi, "A digital self-compensating method for integral-cycle power control of RL loads," IEEE Trans. Vol. IECI-27, No. 2, May 1980, pp.49-52.

[9] H. M. El-Bolek & S. S. Abl-El-Hamid, "A micro-processor based self adjusting system for integral power control of RL loads, "IEEE Trans. on Industrial Electronics, Vol. IE-37, No. 2, April 1990, pp. 156-159.

[10] S. S. Rao, *Optimization-Theory and applications*, New Delhi: Wiley Eastern Limited, New Delhi, 1979, Chapter II.

[11] V. Rajaraman, *Computer oriented numerical methods*, New Delhi: Prentice-Hall of India Pvt. Ltd., 1988, Chapter III.

[12] F. E. Gentry, F. W. Gutzwiller, N. Holonyak, and E. Von Zastrow, *Semiconductor Controlled Rectifiers*. Englewood Cliffs, N. J.: Prentice-Hall, 1964.

[13] S. C. Gupta, K. Venkatesan & K. Eapen, "A generalized Firing angle controller using phase-locked loop for thyristor control," IEEE Trans. Vol. IECI-28, No.1, Feb.1981,pp.46-49.

[14] V. P. Ramamurthi & B. Ramaswami, "A novel 3-phase reference sinewave generator for PMW inverters", IEEE Trans. on Ind.

Electronics, Vol. IE-29, No. 3, Aug. 1982, pp. 235-240.
[15] L. E. Le & G. J. Berg, "Firing circuit for a three-phase SCR voltage controller," IEEE Trans. Vol. IE-31, No. 4, Nov. 1984, pp.389-390.
[16] S. A. Kumar Bhat, "Novel control scheme for 3-phase zero voltage switching," IEEE Trans. vol. IECI-27, No. 2, May 1980, pp. 81-86.
[17] S. A. K. Bhat, "Some new digital control schemes for three-phase zero-voltage switching," International Journal of Electronics, vol.51, No. 6, 1981, pp. 811-818.
[18] H. M. El-Bolek, "A micro-processor based firing circuit for thyristors working under a three-phase variable frequency supply," IEEE Trans. on Industrial Electronics, Vol. IE-37, No. 2, April 1990, pp. 152-155.
[19] A. R. Von C. Warington, "Protective relaying for long transmission line," AIEE Trans. vol. 52, June 1943, p. 261.
[20] V. G. Paithankar, "Versatile phase comparator based on detection of phase sequence for protective relays," Proc. IEE, vol. 117, No. 8, Aug. 1970, pp. 1703-1704.
[21] N. M. Anil Kumar, "Proposed Distance relay characteristic for E. H. V. line protection," Proc. IEE, vol. 117, No. 10, Oct. 1970, pp. 81-86.
[22] K. P. Basu, G. Mahboob and B. H. Khan, "Distance relay characteristics for protection of series compensated transmission line," Journal of Institution of Engineers (India), vol. 63, Pt. EL4, Feb. 1983, p. 203.
[23] SCR Manual, *General Electric*, Edition 5, 1972, Chapters XI & XII.
[24] T. R. Spect, "Transformer inrush and rectifier transient currents," IEEE Trans. Vol. PAS-88, No. 4, April, 1982, pp. 2695-276.
[25] W. K. Macfaden, R. B. S. Simpson & W. S. Wood, "Methods of predicting transient current patterns in transformers," Proc. IEE, vol. 120, No. 11, 1973, pp. 1393-1396.
[26] Mohibullah & K. P. Basu, "Computerized evaluation of the magnetizing inrush current in transformers," Electric Power System Research, No. 2, 1979, pp. 179-182.
[27] H. L. Nakra & T. H. Barton, "Three phase transformer transients," IEEE Trans. Vol. PAS-93, 1981, pp. 1810-1819.
[28] R. Yacamini & A. Abu-Nasser, "Numerical calculation of inrush current in single phase transformers," Proc. IEE, Vol. 128, Pt. B, No. 6, Nov. 1981, pp. 327-334.
[29] M. A. Rehman & A. Gangopadhyay, "Digital simulation of magnetizing inrush current in three-phase transformer," IEEE Trans. Vol. PWRD-1, No. 4, Oct. 1986, pp. 235-242.
[30] C. R. Mason, *The art and science of protective relaying*, New York: John Wiley & Sons, 1967, Chapter XI.
[31] R. Yacamini, A. Abu-Nasser, "Transformer inrush currents and their associated over-voltages in HVDC schemes," Proc. IEE, Vol. 133, Pt. C, No. 6, Sept. 1986, pp. 353-358.
[32] R. Krishnan, B. Ilango, S. Selvaraj & S. Gunasekran, "Single-phase induction motor speed control with integral cycle switching," IEEE Trans. Vol. IECI-27, No.4, Nov. 1980, pp. 308-311.

LIST OF PAPERS PUBLISHED & PREPARED FROM THESIS

[1] M. Salman Beg, A. Ahmad and M. S. Jamil Asghar, "A digital circuit for instant controlled switching," International Journal of Electronics, vol.57, pp. 693-696, 1984.

[2] M. S. Beg, M. S. Jamil Asghar, "A frequency-invariant phase-difference and power-factor meter," ibid. pp. 767-770, 1984.

[3] M. S. Jamil Asghar, M. Mohibullah and M. S. Beg, "A solid-state relay for transformer switching," ibid., vol. 61, pp. 539-542, 1986.

[4] M. S. Beg, M. Mohibullah and M. S. Jamil Asghar, "A circuit for instant controlled switching," ibid., vol. 59, pp. 525-527, 1985.

[5] M. S. Jamil Asghar, M. S. Beg and M. A. Jani, "Estimation of inrush current in transformers by the dynamic magnetizing reactance measurement," 4th International conference on Instrumentation held at Calcutta on April 18-20,1987.

[6] M. S. Jamil Asghar,B. H. Khan, M. S. Beg and A. Shafey, "A versatile static phase-comparator for distance protection," IEEE Region-8 conference held at Riyadh on March 21-24,1987.

[7] M. S. Beg, B. H. Khan and M. S. Jamil Asghar, "Elimination of inrush current in a transformer, Proc. 4th National Power Systems Conference of India, Banaras, Feb. 15-17, 1986.

[8] M. A. Jani, M. S. Beg, Mohibullah and M. S. Jamil Asghar, "Measurement of dynamic magnetizing reactance of a transformer," 4th All India Seminar on Instrumentation held at Aligarh on Nov. 2-3 1985.

[9] M. S. Jamil Asghar, M. S. Beg, Mohibullah and M. Ayub," Instant controlled switching of transformer," National seminar on recent trends on electric energy systems, IIT Delhi, May 21-23, 1986.

[10] M. S. Jamil Asghar, M. Ayub and M. A. Jani, "A 3-phase frequency invariant power-factor meter," Journal of instrument society of India, vol. 18, No. 2, pp. 110-112, 1988.

[11] M. S. Beg, Mohibullah and M. S. Jamil Asghar," A solid-state 3-step distance relay for UHV/EHV lines," Proc. 9th National Systems Conference (India), Allahabad, Dec. 21-23, 1985.

[12] S. H. Laskar, M. S. Jamil Asghar and M. Nasimuddin, "A frequency invariant phase-angle meter," AMSE Transactions (France), vol. 5, No. 2, 1990, pp.57-64.

[13] M.S.Jamil Asghar, "Switching transient control in circuits," Communicated to IEEE Transactions on Power Electronics.

[14] M.S.Jamil Asghar, "Effifient speed control schemes for speed control of induction motors," to be communicated shortly to IEEE Transactions on Industrial Electronics.

[15] M. S. Jamil Asghar, "Elimination of inrush current of three-phase transformers by instant controlled sequential switching," to be communicated.

APPENDICES

I. Derivation of current response equations with suddenly applied direct voltage:

(a) RL Circuit:

The response equation for an RL circuit with direct voltage, E, and a circulating current, Io, at the switching instant, can be easily derived using Laplace transform [2].

The voltage equation of the circuit is given by

$$L[di(t)/dt]+Ri(t) = E \qquad (A1)$$

Taking Laplace transform,

$$E/s=R.I(s)+L[sI(s)-L.Io] \qquad (A2)$$

or,
$$I(s)=[E/L+sI(s)]/s(s+R/L) \qquad (A3)$$

$$=[E/sR]-[\{E/R-Io\}/(s+R/L)] \qquad (A4)$$

The complete expression for the current is

$$i(t)=E/R-[E/R-Io].e^{-R/Lt} \qquad (A5)$$

(b) RLC circuit with Io & Qo:

Derivation for the current response in RLC circuit with direct voltage input is given in reference [1] for the initial charge at capacitor at the switching instant, Qo only. That can be extended for Qo as well as Io.

The voltage equation of the RLC circuit is given by

$$L[di(t)/dt]+ Ri(t)+ 1/C \int i(t)dt= E \qquad (A6)$$

or, $$[d^2i/dt^2]+(R/L)[di/dt]+i/LC= 0 \quad (A7)$$

The complete solution for the current is

$$i=k1.e^{(-a+b)t}+k2.e^{(-a-b)t} \quad (A8)$$

where

$a=R/2L$ and

$b=\sqrt{\{(R/2L)2-(1/LC)\}}$

Let the initial charge on the capacitor, $\int i.dt = Qo$ and the current $i=Io$ at the switching instant of the circuit ($t=0$), thus from (A8) and (A6) respectively

$$k2=Io-k1 \quad (A9)$$

and $$L[di/dt]_{t=0}+RIo+Qo/C=E \quad (A10)$$

or, $$L[(-a+b)k1+(-a-b)k2]+RIo+Qo/C=E \quad (A11)$$

Thus, putting value of k2 from (A9) in (A11),

$$L[(-a+b)k1+(-a-b)Io-(-a-b)k1)]+RIo+Qo/C=E \quad (A12)$$

or, $$k1=\{E-(Qo/C)+(a+b-R/L)Io\}/2bL \quad (A13)$$

or, $$k1=\{E-(Qo/C)+(-a+b)Io\}/2bL \quad (A14)$$

The transient term in (A8) becomes

$$i=[k1\{e^{(-a+b)t}-e^{(-a-b)t}\}+Io.e^{(-a-b)t} \quad (A15)$$

or, $$i=e^{-at}.[k1\{e^{bt}-e^{-bt}\}+Io.e^{-bt}] \quad (A16)$$

Thus

$$i=[k1.\sinh bt+Io.e^{-bt}]e^{-at} \quad \text{for o/d circuits} \quad (A17)$$

$$i=[k1.\sin Bt+Io.e^{-Bt}]e^{-at} \quad \text{for u/d circuits} \quad (A18)$$

where $B=jb$

II. Derivation of current response equations for RLC circuit with Io, Qo and alternating voltage input:

The voltage equation of the RLC circuit in [1], is given by

$$L[di/dt]+ Ri+ 1/C \int idt=Vm.\sin(wt+\theta) \quad (A19)$$

or, $$[d^2i/dt^2]+(R/L)[di/dt]+i/LC=wVm.\cos(wt+\theta) \quad (A20)$$

The complete expression for the current is

$$i=Im.\sin(wt+\theta-\phi)+c1.e^{(-a+b)t}+c2.e^{(-a-b)t} \quad (A21)$$

Let the initial charge on the capacitor, $\int i.dt = Qo$ and the current $i=Io$ at the switching instant of the circuit ($t=0$), thus from (A21) and (A19) respectively

$$c2=-\{Im.\sin(\theta-\phi)-Io\}-c1 \quad (A22)$$

and $$L[di/dt]_{t=0}+RIo+Qo/C=Vm.\sin\theta \quad (A23)$$

or, $$L[wIm.\cos(\theta-\phi)+(-a+b)c1+(-a-b)c2]+RIo+Qo/C=Vm.\sin\theta \quad (A24)$$

Thus, from (A24) and (A22),

$$c1=Eo/2bL-[Im.\sin(\theta-\phi)-Io]/2 \quad (A25)$$

and $$c2=-Eo/2bL-[Im.\sin(\theta-\phi)-Io]/2 \quad (A26)$$

where

$$Eo=Vm.\sin\theta-wLIm.\cos(\theta-\phi)-Qo/C-R\{Im.\sin(\theta-\phi)+Io\}/2 \quad (A27)$$

The transient term in (A21) becomes

$$[(Eo/bL)(e^{bt}-e^{-bt})/2-\{Im.\sin(\theta-\phi)-Io\}(e^{bt}+e^{-bt})/2]e^{-at} \quad (A28)$$

Thus

$$i=Im.\sin(wt+\theta-\phi)+[(Eo/bL)\sinh bt-\{Im.\sin(\theta-\phi)-Io\}\cosh bt]e^{-at} \quad \text{for o/d circuits} \quad (A29)$$

$$i=Im.\sin(wt+\theta-\phi)+[(Eo.t/L)-\{Im.\sin(\theta-\phi)-Io\}]e^{-at} \quad \text{for c/d circuits} \quad (A30)$$

$$i=Im.\sin(wt+\theta-\phi)+[(Eo/bL)\sin Bt-\{Im.\sin(\theta-\phi)-Io\}\cos Bt]e^{-at} \quad \text{for u/d circuits} \quad (A31)$$

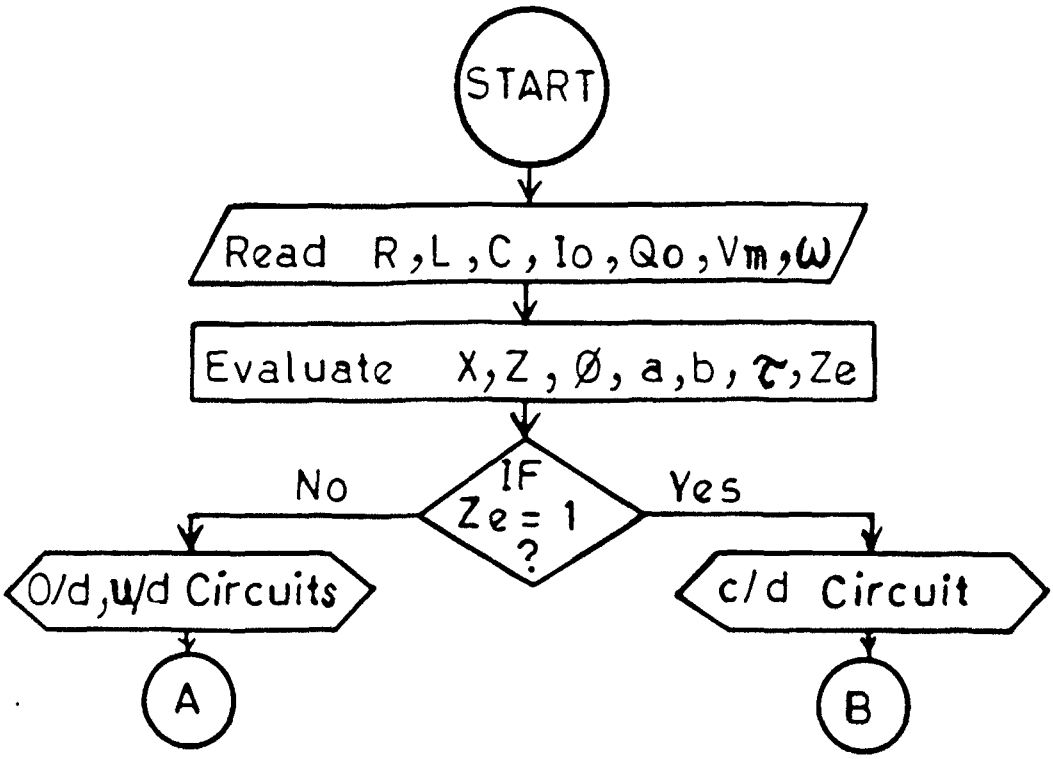
START
Read R, L, C, Io, Qo, Vm, ω
Evaluate X, Z, Ø, a, b, τ, Ze
IF Ze = 1 ?
No
Yes
O/d, ω/d Circuits
c/d Circuit
A
B

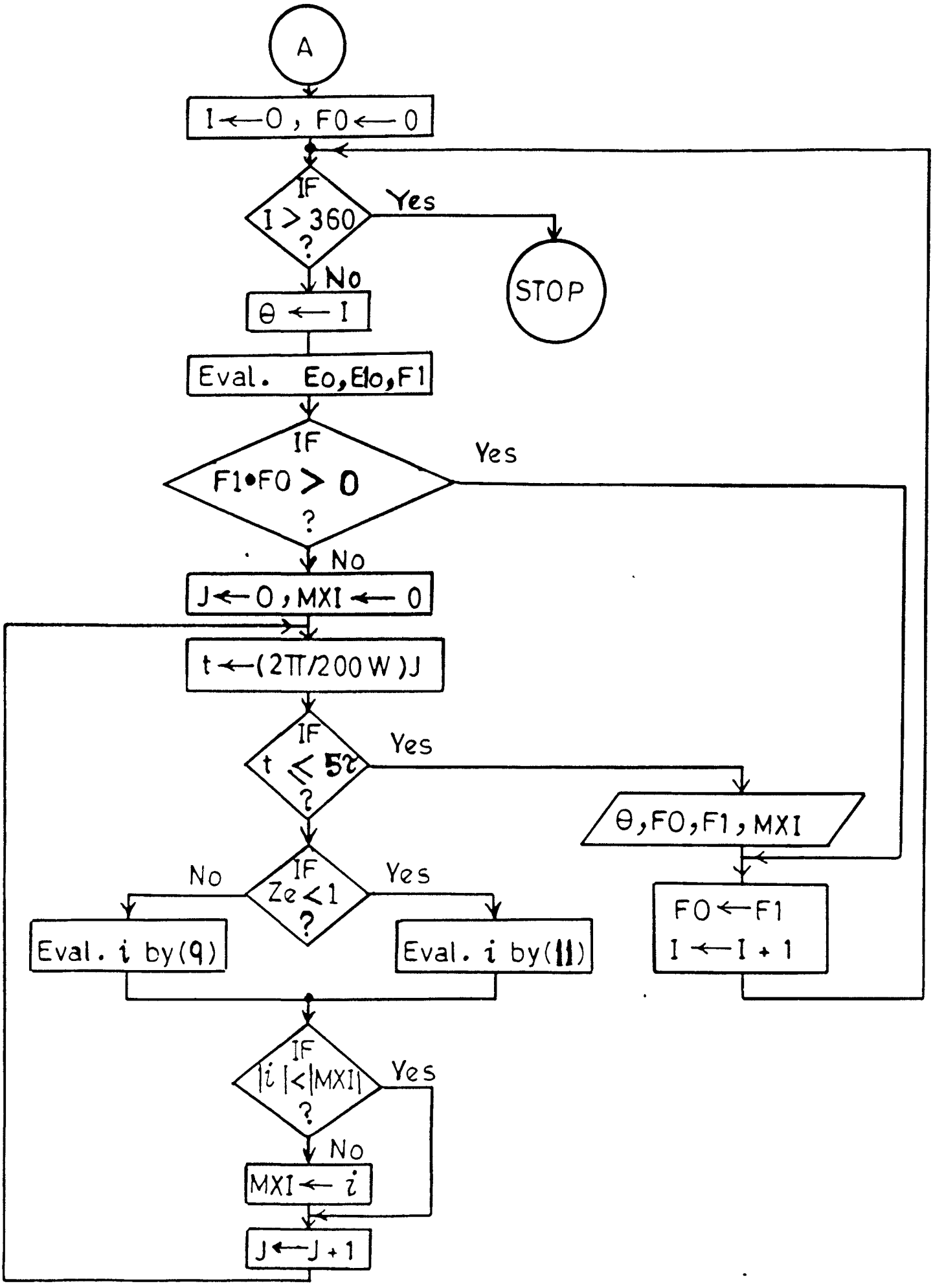
A
I←0 , F0←0
IF I > 360 ?
Yes
STOP
No
θ ← I
Eval. Eo, Elo, F1
IF F1•F0 > 0 ?
Yes
No
J←0 , MXI ← 0
t ←(2π/200W)J
IF t ≤ 5τ ?
Yes
θ, F0, F1, MXI
IF Ze<1 ?
No
Yes
Eval. i by(9)
Eval. i by(11)
F0 ←F1
I ←I + 1
IF |i|<|MXI| ?
Yes
No
MXI ← i
J←J + 1

```
C       File name RLt.FOR and Resultfile is RRLt.
C       For calculation of transient current in RL circuit.
      REAL L,MXI,I,IT
        INTEGER THD,Z,PHID
      OPEN(UNIT=5,FILE='rRL81',STATUS='NEW')
        REWIND 5
        Z=1
       IM=1
        N=0
      PI=(22./7.)
c       give the pf angles for which results are needed.
        DO 33 PHID=80,89,9
        PHI=PHID*PI/180.
        R=Z*COS(PHI)
      X=SQRT(Z*Z-R*R)
        a=R/X
      WRITE(5,3)PHID
3     FORMAT(1X,'PHIdeg=',I4,2X,';Fn. RL1.FOR,Rf. RRL81,TH=0to180')
      DO 33 Jwtdeg=0,1800,30
        DO 99 J=0,7
        THD=30.0*J
        TH=THD*PI/180.
      DI=TH-PHI
        wt=Jwtdeg*pi/180.
      IT=Im*EXP(-a*wt)*(SIN(di)-n)
      I=-IT+IM*SIN(wt+DI)
44      Y=I
        K=J+1
        GOTO(45,46,47,48,49,50,51,52),K
45      Y1=Y
        GOTO 99
46      Y2=Y
        GOTO 99
47      Y3=Y
        GOTO 99
48      Y4=Y
        GOTO 99
49      Y5=Y
        GOTO 99
50      Y6=Y
        GOTO 99
51      Y7=Y
        GOTO 99
52      Y8=Y
99      CONTINUE
        WRITE(5,9)jwtdeg,Y1,Y2,Y3,Y4,Y5,Y6,y7,y8
        WRITE(*,9)jwtdeg,Y1,Y2,Y3,Y4,Y5,Y6,Y7,Y8
9     FORMAT(1X,I6,1X,8(F6.2,1X))
33      CONTINUE
      REWIND 5
        CLOSE(UNIT=5)
      STOP
        END
```

```
C       File name j.FOR for all RLC circuits (u/d&o/d,Xc&Xl,Io&Qo)
      REAL MXI,I,It,n
        INTEGER THD
        character*1 xxc
        PI=(22./7.)
c       Whether capacitive or inductive circuit?
        write(*,*)'write " C " if capacitive circuit'
        READ(*,1)xxc
1       FORMAT(A1)
        write(*,*)'Ze=?','n=?','Y=?',' Program for all RLC circuits'
        READ(*,*)Ze,n,Y
        WRITE(*,*)Ze,n,Y,xxc
      OPEN(UNIT=5,FILE='RJ',STATUS='NEW')
        REWIND 5
        IF(Ze.LT.1.0)THEN
        IF(xxc.EQ.'c'.OR.xxc.EQ.'C')then
C       For under damped circuits
        write(5,3)Ze,n,Y
3      FORMAT(2x,'Ze=',f7.5,1x,'n=',f6.2,1x,'Y=',f6.2,1x,'J.FOR,RJ,
     #,u/d CAPACITIVE circuit')
        ELSE
        write(5,5)Ze,n,Y
5      FORMAT(2x,'Ze=',f7.5,1x,'n=',f6.2,1x,'Y=',f6.2,1x,'J.FOR,RJ,
     #,u/d INDUCTIVE circuit')
        ENDIF
        ELSE
C       For over damped case
        IF(xxc.EQ.'c'.OR.xxc.EQ.'C')then
        write(5,7)Ze,n,Y
7      FORMAT(2x,'Ze=',f7.2,1x,'n=',f6.2,1x,'Y=',f6.2,1x,'J.FOR,RJ,
     #,O/d CAPACITIVE circuit')
        ELSE
        write(5,8)Ze,n,Y
8      FORMAT(2x,'Ze=',f7.2,1x,'n=',f6.2,1x,'Y=',f6.2,1x,'J.FOR,RJ,
     #,O/d INDUCTIVE circuit')
        ENDIF
        ENDIF
C       For each value of THETA calculation starts from here.
        DO 35 THD=0,360,10
        TH=THD*PI/180.
C       For each PHI (20,30,40,50,60,70,80,87 degrees)
        DO 99 J=2,9
        PHID=10.0*J
        IF(J.EQ.9) PHID=87.13
        PHI=PHID*PI/180.
C       Values of R, X, XL & XC are being found.
        Z=1.0
        R=Z*COS(PHI)
        X=Z*SIN(PHI)
        RZe=R/Ze
      X1=(SQRT(X*X+RZe*RZe)-X)*.5
        X2=X+X1
        if(xxc.EQ.'c'.or.xxc.eq.'C')then
      XC=X2
      XL=X1
```

```
        DI=TH+PHI
        else
      XL=X2
      XC=X1
      DI=TH-PHI
        endif
C       Time-period and length of calculation.
        a=R/(2.*XL)
        Tau=1./a
        SPAN=5.*Tau
C       Calculation of different terms.
        BL=0.5*(SQRT(ABS(R*R-4.0*XL*XC)))
        MXI=1.0
        SDI=SIN(DI)
        CDI=COS(DI)
        ED=SIN(TH)-Y*XC-XL*CDI-0.5*R*SDI-0.5*R*n
C       Calculation of i(wt) starts for a particular THETA & PHI
C       Wt varies from 0 to SPAN (5 time-periods).
      DO 83 JWTDEG=0,360000,2
      WT=JWTDEG*PI/180.
       IF(WT.GE.SPAN)GOTO 44
        EAT=EXP(-A*WT)
        BT=BL*wt/XL
        IF(Ze.LT.1.0)THEN
        SBT=SIN(BT)
        CBT=COS(BT)
        ELSE
        SBT=SINH(BT)
        CBT=COSH(BT)
        ENDIF
      It=((ED*SBT/BL)+(n-SDI)*CBT)*eAT
      I=It+SIN(WT+DI)
      IF(ABS(I).LT.ABS(MXI))GOTO 83
      MXI=I
83    CONTINUE
44      YY=ABS(MXI)
C       MXI is Ip, for a particular THETA & PHI.
        K=J-1
        GOTO(45,46,47,48,49,50,51,52),K
45      Y1=YY
        GOTO 99
46      Y2=YY
        GOTO 99
47      Y3=YY
        GOTO 99
48      Y4=YY
        GOTO 99
49      Y5=YY
        GOTO 99
50      Y6=YY
        GOTO 99
51      Y7=YY
        GOTO 99
52      Y8=YY
99      CONTINUE
```

```
C       Values of Ip for various PHIs.
        WRITE(*,9)THD,Y1,Y2,Y3,Y4,Y5,Y6,Y7,Y8
        WRITE(5,9)THD,Y1,Y2,Y3,Y4,Y5,Y6,Y7,Y8
9     FORMAT(1X,I6,1X,8(F6.2,1X))
35      CONTINUE
      REWIND 5
        CLOSE(UNIT=5)
      STOP
        END
```

IV. Generation of values of Xl and Xc from given Ze and ϕ.

At critical damping, critical resistance of the circuit,

$$Rc = 2\sqrt{(L/C)} = 2\sqrt{(Xl.Xc)} \qquad (A32)$$

and damping ratio,

$$Ze = (\text{actual damping})/(\text{critical damping}) = R/\{2\sqrt{(L/C)}\}$$

For particular power-factor, Xl and Xc may assume any value, therefore, to have a generalized solution Ze has to be incorporated. Thus for Xl>Xc,

$$Ze2 = R2/(4Xl.Xc) \leq R2/\{4(X+Xc).Xc\} \qquad (A33)$$

or, $$Xc2+X.Xc+(R/2Ze)2=0 \qquad (A34)$$

is a quadratic equation. Which gives,

$$Xc=[-X+\sqrt{\{X2+(R/Ze)2\}}]/2 \quad \text{and} \quad Xl= X+Xc \qquad (A35)$$

Similarly, for Xc>Xl, the above equations for Xc and Xl will be inter-changed.

V. Rating and parameters of different machines used:

(a)Transformers

Ratings	(a) 1-phase	(b) 3-phase
KVA	2	3
Voltage	230/135,115V	230/115
No-load current	0.95A	1.0A
Full-load current	8.7A	7.53A
PF angle, ϕ at No-load	80°	79.5°

(b) Induction motors:

Ratings	(a) 1-phase	(b) 3-phase
KW	0.37	1.5
Voltage	230V	415V
Rpm	1450	1400
At block rotor:		
PF angle, ϕ	33.25°	60.5°
Impedance of main winding	31.78=10.5+j30Ω	
PF angle, ϕm of main winding	70.75(lagging)	
Impedance of aux. winding	41.76=40+j(60-72)Ω	
PF angle, ϕa of aux. winding	16°(leading)	